BINDING RESPONSES ASSOCIATED WITH SELF-INTERACTING LIGANDS: STUDIES ON THE SELF-ASSOCIATION AND RECEPTOR BINDING OF INSULIN

A thesis submitted for the Degree of

Doctor of Philosophy

of the

Australian National University

by

ALAN EDWARD MARK

July, 1986

The research work described in this thesis was undertaken in the Department of Physical Biochemistry, later known as the Protein Chemistry Group, in the John Curtin School of Medical Research, Australian National University, between March 1983 and July 1986. All experimental results reported in the text were obtained by the author alone, while theoretical considerations in regard to the derivation of binding equations were made in collaboration with both Professor L.W. Nichol and Dr P.D. Jeffrey. The work presented in this thesis has not previously been submitted for a degree of this or any other University.

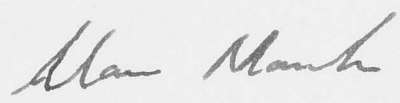

A.E. Mark

ACKNOWLEDGEMENTS

The assistance, advice and encouragement given to me throughout the course of this work by Professor L.W. Nichol and Dr P.D. Jeffrey has been invaluable, both have my deepest gratitude. I am also indebted to the other members of the Department of Physical Biochemistry for their friendship and practical advice. Financial support from the Australian National University and the Commonwealth Department of Education in the form of a Ph.D scholarship is gratefully acknowledged. I also wish to acknowledge the cooperation of the staff from the maternity departments of the Royal Canberra and Calvary Hospitals in supplying the placental tissue. My greatest single debt is, however, to my family and friends without whose constant physical and moral support this thesis could not have come to fruition.

CONTENTS

CHAPTER 1
INTRODUCTION

The interaction between a ligand and an acceptor is a basic event in biological systems. This is exemplified by the fact that ligand-binding forms both the first step and a primary site for control in all enzymic reactions. Examples of other important classes of ligand-acceptor interactions include the binding of oxygen to haemoglobin, the mechanism underlying the uptake of glucose into cells, and the interaction between antibodies and antigens. The obvious biological importance of such interactions has meant that considerable attention has been given to methodology pertinent to the acquisition and analysis of binding data (Nichol and Winzor, 1981; Levitzki, 1978; Wyman, 1964). In relation to this it is important to note that, although ligands are frequently thought of as low molecular weight compounds, interactions between dissimilar macromolecules, such as in blood coagulation or hormone-receptor interaction, are equally important and that, so long as due consideration to non-ideality is given, thermodynamic theory developed in relation to one particular system will be valid for all similar systems.

In any binding experiment the extent of acceptor-ligand interaction may be expressed in terms of the binding function, r, defined as the moles of ligand bound per mole of acceptor. Normally r is plotted as a function of unbound ligand concentration to give what is termed a binding curve. Methods commonly employed to determine the form of the binding curve include equilibrium dialysis, ultrafiltration, frontal chromatography, and sedimentation dialysis (Colwick and Womack, 1969; Blatt, Robinson and Bixler, 1968; Brinkworth, Masters and Winzor, 1975; Nichol and Winzor, 1964). Where partitioning methods are not suitable, as in cases involving interactions between similarly sized macromolecules, radioimmuno- or spectroscopic techniques are used (Hammes, 1981; Desbuquois and Aurbach, 1971).

In order to analyse the results from binding experiments, equations are needed which relate the form of the curve to the molecular basis of the binding response. The

work of Adair (1925) in relation to the form of the oxygen-haemoglobin dissociation curve represents one of the first attempts to formulate such expressions. Adair's approach can be illustrated by considering the binding of a univalent ligand, S, to each of p sites on a single state acceptor, A. In this situation successive equilibria may be described in stoichiometric terms by:

$$AS_{i-1} + S = AS_i; \quad K_i = m_{AS_i}/(m_{AS_{i-1}} m_S); \quad (i=1,2,...,p) \tag{1.1}$$

where K_i is the association constant on a molar scale. By successive substitution it follows that:

$$m_{AS_i} = \left\{ \prod_{l=1}^{l=i} K_l \right\} m_A m_S^i. \tag{1.2}$$

Equation (1.2) may be used to formulate expressions for the total concentrations of ligand and acceptor which, on combination with the general definition of the binding function, r, yields (Nichol and Winzor, 1981):

$$r = \frac{\sum_{i=1}^{i=p} i \left\{ \prod_{l=1}^{l=i} K_l \right\} m_S^i}{1 + \sum_{i=1}^{i=p} \left\{ \prod_{l=1}^{l=i} K_l \right\} m_S^i}. \tag{1.3}$$

This equation, which is of the form originally proposed by Adair (1925), is a ratio of polynomials in m_S. It is independent of m_A and hence the binding curves it describes will be independent of the total acceptor concentration, $\bar{m}_A$. Klotz (1946) effected a considerable simplification of equation (1.3) by noting that, provided the binding sites on the acceptor were equivalent and independent, as might pertain in the case of an oligomeric protein comprised of multiple identical subunits, all stoichiometric equilibrium constants K_i could be related to a single site binding constant, k_A. Klotz showed, using combinatorial theory, that the concentration of any given stoichiometric complex AS_i could thus be written as:

$$m_{AS_i} = C_i^p k_A^i m_A m_S^i; \quad \left\{ \prod_{l=1}^{l=i} K_l \right\} = C_i^p k_A^i \tag{1.4}$$

where C_i^p is the number of combinations of p sites taken i at a time, and furthermore showed that:

$$K_i = (p - i + 1)k_A/i. \tag{1.5}$$

Combination of equations (1.3) and (1.4) yields an expression for r in terms of k_A which, using the binomial theorem, may be readily simplified to give (Nichol and Winzor, 1981):

$$r = \frac{pk_A m_S(1 + k_A m_S)^{p-1}}{(1 + k_A m_S)^p} = \frac{pk_A m_S}{1 + k_A m_S}. \tag{1.6}$$

From equation (1.6) it can be seen that the binding response curve relating to the binding of a monovalent non-interacting ligand to equivalent and independent sites on a single state acceptor will have the form of a rectangular hyperbola. This form of curve can be linearized in many ways; notably by using double-reciprocal, Hill and Scatchard plots (Nichol and Winzor, 1981). Of these, the Scatchard plot (Scatchard, 1949) is possibly the most useful. If equation (1.6) is rearranged in Scatchard format such that:

$$r/m_S = -rk_A + pk_A \tag{1.7}$$

it follows that k_A and p may be obtained from the slope and intercept of a plot of r *versus* r/m_S. Equations (1.4) and (1.5) may then be used to determine both values for K_i and the concentration of each stoichiometric complex.

Deviations from the form of a rectangular hyperbola are common when binding curves are obtained with biological systems. The simplest cause of such deviations is site non-equivalence. It can be readily shown that, when the sites are independent but non-equivalent, r may be expressed simply as a sum of rectangular hyperbolae, giving rise exclusively to Scatchard plots convex to the r axis (Nichol and Winzor, 1981).

Non-linear Scatchard plots can also arise as a result of site interdependence or cooperativity (Koshland, Nemethy and Filmer, 1966). That is, while the sites on an acceptor may be initially equivalent, the affinity of any given site for ligand might

depend upon the occupancy of other sites. Such site interdependence could result from conformational changes in the acceptor associated with ligand binding being translated throughout the acceptor. Charge and steric effects of the bound ligand are two other possibilities. The binding equations relevant to this model, formulated by Koshland and coworkers as ratios of polynomials independent of $\bar{m}_A$, are capable of generating both concave and convex curves in Scatchard format (Koshland and Neet, 1968; Conway and Koshland, 1968; Kirtly and Koshland, 1967). The generality of this approach has led many workers to conclude that a given form of a binding curve must mean either negative or positive cooperativity in Koshland's terms. A major emphasis of this thesis is the critical examination of this interpretation.

An alternative to the Koshland cooperative model was proposed by Monod, Wyman and Changeux (1965). Their model, based on the concept of a pre-existing equilibrium between isomeric acceptor states exhibiting different ligand binding affinities, can also give rise to apparent "positively cooperative" responses. Binding equations derived for this model again take the form of ratios of polynomials independent of $\bar{m}_A$ (Monod, Wyman and Changeux, 1965). The importance of this model is that the form of the binding curve may be regulated by varying the extent of acceptor isomerization. The possibility that this may form the basis of a type of metabolic control has been discussed in detail by Nichol and Winzor (1981). This model may, however, only pertain to a limited number of systems. This is primarily because it exclusively predicts "positively cooperative" responses. A second reason is that for the binding response to deviate significantly from the form of a rectangular hyperbola a very large isomerization constant is required. Thus, fine metabolic control is dependent on the presence of a large pool of inactive receptor.

The acceptor states considered by Monod, Wyman and Changeux need not necessarily be isomeric. Nichol, Jackson and Winzor (1967), and Frieden and Colman (1967) independently noted that acceptor self-interaction could also give rise to non-hyperbolic binding responses. The generalised binding function derived by Nichol, Jackson and Winzor (1967) to describe the case of a ligand, S, binding to a series of polymeric acceptor species coexisting in equilibrium may be written as follows:

$$r = \frac{\sum_{i=1}^{i=n} m_i m_S p_i k_i (1 + k_i m_S)^{p_i - 1}}{\sum_{i=1}^{i=n} i m_i (1 + k_i m_S)^{p_i}} \tag{1.8}$$

where i refers to the polymeric acceptor species [$i = 1$ (monomer), 2 (dimer), ..., n (n-mer)] with m_i, k_i, and p_i, representing respectively, the free molar concentration, the intrinsic binding constant, and the number of sites per mole, for that particular polymer. The form of this expression differs markedly from those discussed previously. It can no longer be expressed as a simple ratio of polynomials with m_S as the sole variable and moreover, in this case, the binding response curves will be dependent upon the concentration of the acceptor. Examples of this type of response are numerous and include the binding of GTP to glutamate dehydrogenase, zinc to α-amylase, and ATP to cytosine triphosphate synthetase (Steiner, 1974; Frieden and Colman, 1967; Tellam, Winzor and Nichol, 1978; Levitzki and Koshland, 1972). Several of these systems have clear regulatory functions (Brown and Reichard, 1969; Beaty and Lane, 1983). This has led to the extensive development of theory pertaining to the determination of the conditions under which particular binding responses would be expected (Nichol, Wills and Winzor, 1979; Baghurst, Nichol and Winzor, 1978).

Although the effects of acceptor self-interaction have been extensively studied, little is known about the implications of ligand self-association. This is despite the fact that many important biological ligands including ATP, cholesterol, prothrombin and insulin are known to self-associate (Heyn and Bretz, 1975; Parker and Bhasker, 1968; Dombrose *et al.*, 1979; Steiner, 1952). The theoretical work that has been conducted to date in this area has been restricted to the analysis of two-state systems with monovalent ligand species (Sculley, Nichol and Winzor, 1981; Nichol, Smith and Ogston, 1969). These studies have, however, demonstrated that ligand self-interaction can lead to complex forms of binding behaviour. For example, the binding of chlorpromazine to brain tubulin, a case in which two critical points are evident in the Scatchard plot, was

effectively modelled by Sculley, Nichol and Winzor (1981) as a two-state ligand system. Many self-associating ligands cannot be approximated so simply. Insulin and lysozyme, for example, two proteins with important physiological roles, both self-associate indefinitely (Jeffrey, Milthorpe and Nichol, 1976; Pekar and Frank, 1972; Wills, Nichol and Siezen, 1980). A prime aim of this thesis is the extension of presently available theory to include these and other complex self-associating systems. Thus, in Chapter 2 the general case of an indefinitely self-associating ligand interacting with a multivalent single-state acceptor is considered. For this initial case the notion of monovalent ligand states is retained.

Once a bivalent ligand species is envisaged, acceptor crosslinking is possible. This has been considered in detail by Flory (1953) and Calvert, Nichol and Sawyer (1979) for cases involving non-interacting ligands. In Chapter 3 the possibility is explored that dimerization of an initially monovalent ligand could give rise to a bivalent species capable of crosslinking the acceptor. The chapter commences with a comprehensive background review of ligand-initiated acceptor associations. A series of three models is then considered. In each case acceptor crosslinking is initiated by either the self-association or isomerization of the ligand. The concept of ligand-induced acceptor association bears on the interactions between several peptide hormones and their respective membrane acceptors. In these cases, following the initial binding event, the acceptors rapidly aggregate (Schlessinger *et al.*, 1978; Conn, Rodgers and McNeil, 1982; King and Cuatrecasas, 1981). While the underlying mechanism of this aggregation is uncertain, evidence suggests that it is an intrinsic property of either the hormone or its receptor (Heffetz and Zick, 1986). As many of the hormones involved strongly self-associate (Greene and Shooter, 1980; Jeffrey, Milthorpe and Nichol, 1976; Swann and Hammes, 1969) the question arises of whether ligand self-association could account not only for the non-hyperbolic binding responses observed in these systems, but also for the phenomenon of receptor aggregation (Buxser, Puma and Johnson, 1985; De Meyts *et al.*, 1973; Desbuquois, 1985). Such a possibility has recently been proposed by Jeffrey (1982) in relation to the binding response of insulin. However, quantitative analysis of

the system was hampered by the lack of appropriate binding theory. Another primary aim of this thesis is the analysis of the role self-association plays in determining the form of the insulin binding response.

A first step in the elucidation of any such behaviour is the acquisition of detailed knowledge in regard to the self-association pattern under investigation; in this case, that of zinc-free insulin. In Chapter 4 information from the existing literature on the X-ray crystal structure of insulin and detailed analyses of sedimentation equilibrium studies are used to support the introduction of a new pattern for the self-association of zinc-free insulin (Nichol *et al.*, 1984). One feature of this association pattern is that certain even-numbered polymeric species might be effectively bivalent toward the insulin receptor.

Chapter 5, the final experimental chapter of the thesis, presents a critical assessment of the implications of the new self-association pattern for *in vitro* and *in vivo* insulin binding studies. The chapter commences with an analysis of the distribution of polymeric insulin species in solution, proper regard being given to the complex nature of the solutions in which binding studies are conducted. The conclusion is drawn that over the range of total insulin concentration used in obtaining binding data, especially that pertaining to *in vitro* studies, the system may be reasonably approximated by a monomer-dimer equilibrium. Binding theory developed in Chapter 3 is then used in order to examine critically models proposed for the binding of insulin to its receptor in relation to binding curves obtained experimentally utilizing solubilized insulin receptors prepared from human placenta.

In summary this thesis has two interconnected themes. The first is the extension of binding theory in the general context of self-associating ligand systems. The specific objectives encompassed in this theme are:

1. to develop binding equations, in closed form, which describe the interaction between a multivalent acceptor and a ligand capable of indefinite self-association in order to show that such a system can give rise to "negatively cooperative" binding responses;

2. to demonstrate the feasibility, at least for a bivalent acceptor, of writing explicit binding equations incorporating both ligand self-interaction and acceptor crosslinking;
3. to establish general criteria for the experimental elucidation of systems involving the binding of self-interacting ligands.

The second theme is concerned with establishing the role ligand self-interaction plays in influencing the binding response in a specific system, namely the interaction between insulin and its membrane receptor. In this part of the work the objectives are:

1. to establish the self-association pattern of zinc-free insulin over wide ranging conditions of temperature, pH and ionic strength;
2. to determine the distribution of polymeric insulin species under the conditions relevant to binding studies;
3. to analyse the results of insulin binding studies, obtained under controlled conditions using solubilized receptors, in the light of equations derived on the basis of particular models.

The binding equations derived in this thesis have primarily been directed toward the analysis of the insulin system. It is hoped, however, that the theoretical developments they represent will be of use not only in further studies on this system but also in a much wider context involving acceptor and ligand systems.

CHAPTER 2

THE BINDING OF AN INDEFINITELY ASSOCIATING LIGAND TO ACCEPTOR: CONSIDERATION OF MONOVALENT LIGAND SPECIES BINDING TO A MULTIVALENT ACCEPTOR

2.1 A REVIEW OF THE BACKGROUND LITERATURE

2.1.1 Two-State Ligand Systems

As pointed out in Chapter 1 several compounds of low molecular weight (termed ligands) are known to self-associate in solution and also to bind to macromolecular acceptors. In 1969 Nichol, Smith and Ogston (1969), in mentioning several such systems, pointed out that a correct analysis of binding results obtained with them required a detailed knowledge of the thermodynamic parameters governing the self-association of the ligand, since the form of the experimental binding curve would be dependent upon the self-association. This may be seen explicitly by reporting the binding equation derived by the earlier workers who considered the following model:

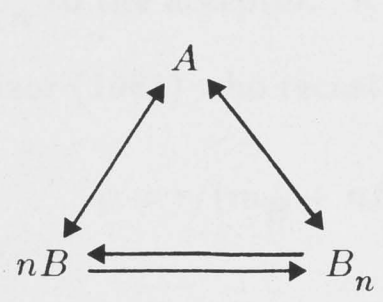

$$; \quad K_n = m_{B_n}/m_B^n \tag{2.1}$$

where the acceptor, A, bears f equivalent and independent sites capable of binding either monomeric ligand B with site binding constant k_A, or (competitively) the polymeric state of the ligand B_n with site binding constant l_A. The molar association constant governing the ligand association is K_n, defined above. With this terminology the relevant binding equation is:

$$r = f(k_A m_B + n l_A K_n m_B^n)/(1 + k_A m_B + l_A K_n m_B^n) \tag{2.2a}$$

where the molar binding function r is defined as the total number of base moles of both forms of ligand bound per mole of acceptor:

$$r = [\bar{m}_B - (m_B + n K_n m_B^n)]/\bar{m}_A \tag{2.2b}$$

$\bar{m}_B$ and $\bar{m}_A$ being the total base molar concentrations of ligand and acceptor, respectively, in solution. Clearly, if a binding function were formulated solely in terms

of the amount of monomeric (or polymeric) ligand bound, the resultant binding equation would be hyperbolic in form; but this would be an unrealistic formulation, since the equilibrium concentration of unbound ligand may only be measured as a sum of both ligand states which necessarily coexist in solution. Accordingly, the definition of r in equation (2.2b) is not only appropriate to the analysis of experimental results, but also correctly reflects the quantity of interest in a biological context where account is required of the total amount of ligand bound in all forms. Such a formulation will be used consistently throughout this work.

It is evident that equation (2.2a) cannot be simplified to describe a rectangular hyperbola except for the special case $n = 1$ (ligand isomerization). Deviations from hyperbolic form for an associating ligand ($n > 1$) were explored by Nichol, Smith and Ogston (1969) using numerical examples for cases involving exclusive binding of either B or B_n to the acceptor. A more rigorous treatment was presented by Sculley, Nichol and Winzor (1981) who recast equation (2.2a) into Scatchard format as follows:

$$\psi = r/(m_B + nK_n m_B^n) \tag{2.3a}$$

$$\psi = \frac{f(k_A m_B + nl_A K_n m_B^n)}{(1 + k_A m_B + l_A K_n m_B^n)(m_B + nK_n m_B^n)} . \tag{2.3b}$$

This permitted differentiation of equation (2.3b) to explore conditions under which the Scatchard plot would deviate from linearity (i.e. the binding curve would deviate from a rectangular hyperbola). These conditions had been formulated previously (Nichol, Wills and Winzor, 1979) as:

$$d^2\psi/dr^2 < 0; \qquad \text{a Scatchard plot concave to the } r\text{-axis} \tag{2.4a}$$

$$d^2\psi/dr^2 > 0; \qquad \text{a Scatchard plot convex to the } r\text{-axis.} \tag{2.4b}$$

A Scatchard plot concave to the r-axis and exhibiting a maximum corresponds to a binding curve (a plot of r *versus* the total free ligand concentration) which is sigmoidal

in form, while a convex Scatchard plot corresponds to a steep hyperbolic binding curve which resembles a "negatively cooperative" response (Baghurst, Nichol and Winzor, 1978). Equation (2.4a) was fulfilled for every value of $n > 1$ when the polymeric state of the ligand (coexisting in equilibrium with the monomeric state) exclusively bound to the acceptor, $k_A = 0$ (Sculley, Nichol, Winzor, 1981), the corresponding sigmoidal binding curve for this case having been illustrated numerically for $n = 2$ by Nichol, Smith and Ogston (1969). In contrast, equation (2.4b) was found to apply, for example, when $n = 2$ and the monomeric state of ligand coexisting in equilibrium with an inactive dimeric state exclusively bound to acceptor, $l_A = 0$, a case also illustrated numerically by Nichol, Smith and Ogston (1969). An example of the latter behaviour is found in binding studies involving single-layer phospholipid vesicles as acceptors and fragment *I* of prothrombin as a dimerizing ligand (Dombrose, Gitel, Zawalich and Jackson, 1979) and arises because the interactive face on fragment *I* is the same for both dimer formation and interaction with the vesicles. Sculley, Nichol and Winzor (1981) made two further points. First, when $n > 2$ and $l_A = 0$, both equations (2.4a) and (2.4b) could be satisfied in particular ranges of m_B and, secondly, when $n > 2$ and $l_A > k_A$, it is possible that the Scatchard plot may exhibit two critical points, a minimum and a maximum. An example of the latter mixed behaviour, provided by the authors, was the preferential binding of the micellar state of chlorpromazine to a single site on monomeric brain tubulin.

It is now evident that the effects of ligand association on binding behaviour have been explored reasonably comprehensively for situations in which only two states of the ligand, both univalent toward acceptor, coexist in equilibrium. There remain, however, two particular areas which require further exploration. The first pertains to a situation where dimerization of the ligand leads to a species bivalent toward the acceptor which may therefore be reversibly crosslinked by a ligand bridge (Nichol, Sculley and Winzor, 1982). Consideration of reversible crosslinking systems is the subject of Chapter 3. The second point which requires elaboration concerns associating ligand systems which are not an equilibrium mixture of only two states. Even in the original examples of

interacting ligand systems provided by Nichol, Smith and Ogston (1969), there appears mention of systems, notably the purines and pyrimidines, which are known to associate indefinitely (Van Holde and Rossetti, 1967). The remainder of this chapter is concerned with such systems and to avoid introducing, at this stage, the potential complication of reversible crosslinking effects, attention is solely directed toward linear "head-to-tail" indefinite association. In this terminology the "head" is viewed as the univalent site which binds to the acceptor so that each polymeric state bears one such site (as does the monomer).

2.1.2 Isodesmic Indefinite Self-Association

This section is concerned with the solution behaviour of a bivalent ligand which undergoes "head-to-tail" association to form an equilibrium mixture of linear-chain polymers according to the reaction, $B_{i-1} + B \rightleftharpoons B_i$ $(i = 2,3,4,...,\infty)$. If it is assumed that the standard free energy change accompanying the addition of each monomeric unit is identical, the indefinite association is termed isodesmic (Van Holde and Rossetti, 1967) and a single stoichiometric equilibrium constant on the molar scale, K_I, suffices to describe the composition of the solution at any given total weight concentration, $\bar{c}$. Thus:

$$K_I = m_i/m_{i-1}m_1 \quad (i = 2,3,...,\infty) \tag{2.5a}$$

$$\bar{c} = M_1m_1 + 2M_1m_2 + 3M_1m_3 + ... + \infty \tag{2.5b}$$

$$\bar{c} = M_1m_1\{1 + 2K_Im_1 + 3K_I^2m_1^2 + ... + \infty\} \tag{2.5c}$$

where the symbol m_i, denotes the molar concentration of species B_i, and M_1 is the molecular weight of the monomer. The infinite sum in equation (2.5c) is of standard form (Dwight, 1961) and thus the open solution may be written in closed form as:

$$\bar{c} = M_1m_1/(1 - K_Im_1)^2; \quad K_Im_i < 1\,. \tag{2.6}$$

Equation (2.6) has been shown to apply to experimental results obtained with a range of

compounds including purines (Van Holde and Rossetti, 1967), lysozyme (Wills, Nichol and Siezen, 1980), glutamate dehydrogenase (Nichol, Siezen and Winzor, 1978) and oxyhaemoglobin (Nichol, Siezen and Winzor, 1979). It is timely to note that the term "ligand", usually referring to a compound of low molecular weight, is a relative one in that macromolecular proteins may be correctly viewed as ligands in situations where they bind to an even larger acceptor species, such as a cell membrane or a phospholipid vesicle.

In a recent paper Kurganov (1984) discussed equation (2.6) by formulating an expression from it for the weight-fraction of species i, as a function of the dimensionless parameter $\alpha = K_I\bar{c}/M_1$. This may be written as:

$$\frac{c_i}{\bar{c}} = \frac{iM_1m_i}{\bar{c}} = \frac{i\{(1 + 2\alpha) - \sqrt{1 + 4\alpha}\}^i}{2^i\alpha^{i+1}} . \qquad (2.7)$$

It may be shown by differentiating equation (2.7), with respect to α, that the weight-fraction of monomer decreases monotonically from a limiting value of unity (as $\alpha \to 0$) and approaches zero (as $\alpha \to \infty$). In contrast the weight-fractions of all polymeric species pass through a maximum value at $\alpha = (i^2 - 1)/4$ and there attain the values of $[4i(i - 1)^{i-1}/(i + 1)^{i+1}]$. It follows that these maxima arise at progressively increasing total concentrations as the value of i increases. This description of the composition of indefinitely associating systems suffices in the present context, but further mention is made in Chapter 4 of indefinite self-associations involving multivalent reactants.

2.2 THE BINDING OF AN INDEFINITELY SELF-ASSOCIATING LIGAND (ISODESMIC) TO A MULTIVALENT ACCEPTOR

The derivation of all binding equations proceeds by first formulating expressions for the total molar concentration of acceptor, $\bar{m}_A$, and for the base molar concentration of ligand bound in all forms, $\bar{m}_B - \sum_{i=1}^{i=\infty} im_i$. The final binding equation is then formulated by forming a ratio of these expressions to define the molar binding function, r, as base moles of ligand bound per mole of acceptor. In other words:

$$r = (\bar{m}_B - \sum_{i=1}^{i=\infty} i m_i)/\bar{m}_A, \tag{2.8}$$

a formulation consistent with equation (2.2b).

2.2.1 The Total Molar Concentration of Acceptor, $\bar{m}_A$

2.2.1.1 The particular case $f = 1$

Consider first a univalent acceptor which binds competitively all states of the ligand, each of which bears one reactive site as a consequence of the linear "head-to-tail" indefinite association of the ligand. Since each molecule of complex contains only one molecule of acceptor, A:

$$\bar{m}_A = m_A + m_{A\text{-}B_1} + m_{A\text{-}B_2} + \ldots + m_{A\text{-}B_\infty} \tag{2.9}$$

where m_A is the concentration of unbound acceptor. It will be assumed that a single site binding constant, k_A, governs the binding of each ligand state to the acceptor independent of the chain length of the attached ligand. Thus:

$$k_A = m_{A\text{-}B_i}/m_A m_{B_i} = m_{A\text{-}i}/m_A m_i \quad (i = 1,2,3,\ldots,\infty). \tag{2.10}$$

Combination of equations (2.5a), (2.9) and (2.10) yields:

$$\bar{m}_A = m_A + k_A m_A m_1 + k_A m_A K_I m_1^2 + k_A m_A K_I^2 m_1^3 + \ldots + \infty \tag{2.11a}$$

which may be summed as a geometric progression with the common ratio $K_I m_1$ as:

$$\bar{m}_A = m_A\{1 + [k_A m_1/(1 - K_I m_1)]\}; \quad K_I m_1 < 1 \tag{2.11b}$$

where it is stressed that m_1 is the molar concentration of monomeric unbound ligand.

2.2.1.2 Generalization to an f-valent acceptor

The first type of complex which needs to be considered is that comprising a single molecule of acceptor bound at any one of the f-sites with a ligand species, whether it be monomer, dimer or any higher polymer. The total constituent concentration of all 1:1 complexes contributing to $\bar{m}_A$ is given by:

$$C_1^f k_A m_A \{ \sum_{i=1}^{i=\infty} m_i \}$$

where the numerical coefficient C_1^f is the number of different ways one molecule of any one of the ligand species may be combined with the f-valent acceptor (Klotz, 1946). The corresponding constituent concentration for 1:2 complexes is:

$$C_2^f k_A^2 m_A \{ \sum_{i=1}^{i=\infty} m_i \}^2$$

which when expanded clearly shows that account has been taken of complexes containing only one type of ligand (as exemplified by the term $C_2^f k_A^2 m_A m_1^2$ referring to acceptor bound at two sites with monomeric ligand) as well as all of those complexes which contain two different states of ligand (illustrated by $2C_2^f k_A^2 m_A m_1 m_2$, the constituent concentration of complexes containing monomer and a dimer of ligand bound at two sites on the acceptor). It follows that:

$$\bar{m}_A = m_A + C_1^f k_A m_A \{ \sum_{i=1}^{i=\infty} m_i \} + C_2^f k_A^2 m_A \{ \sum_{i=1}^{i=\infty} m_i \}^2$$

$$+ \ldots + C_f^f k_A^f m_A \{ \sum_{i=1}^{i=\infty} m_i \}^f \qquad (2.12)$$

where the sum has been taken to account for the concentrations of acceptor complexes with all sites saturated with either a homogeneous population of ligand states or with a heterogeneous population, account having been taken of all possible combinations of ligand states.

It is now noted, from equation (2.5a), that:

$$\sum_{i=1}^{i=\infty} m_i = m_1/(1 - K_I m_1); \quad K_I m_1 < 1 \qquad (2.13)$$

and thus equation (2.12) may be written as:

$$\bar{m}_A = m_A\left\{1 + \sum_{n=1}^{n=f} C_n^f\left[\frac{k_A m_1}{(1 - K_I m_1)}\right]^n\right\} . \qquad (2.14)$$

Equation (2.14) is in the standard form of the binomial theorem (Dwight, 1961) and thus it follows that:

$$\bar{m}_A = m_A\{1 + [k_A m_1/(1 - K_I m_1)]\}^f \qquad (2.15)$$

which becomes equation (2.11b) when $f = 1$, as required.

2.2.1.3 The reacted-site probability approach

Nichol (1981) pointed out that a general framework existed for the derivation of expressions relevant to heterogeneous association of two reactants, which invoked reacted-site probability functions, originally formulated by Flory (1953) and later applied to systems involving multiple equilibria (Singer, 1965; Eisenberg, Josephs and Reisler, 1976; Calvert, Nichol and Sawyer, 1979). It is instructive to examine the applicability of this approach to the formulation of equation (2.15). The molar concentration of unbound acceptor is related to its total concentration by:

$$m_A = \bar{m}_A(1 - P_A)^f \qquad (2.16)$$

where P_A is the probability that any one of the f-sites on A has reacted with a ligand species, P_A ranging from zero to unity. A corresponding function, P_B, exists, which is the probability that a site on any ligand species has reacted with a site on A. It follows that $(1 - P_B)\tilde{\bar{m}}_B$ is the molar concentration of unbound sites on all ligand species where $\tilde{\bar{m}}_B$ is the total molar concentration of sites on ligand both bound and unbound. In other words:

$$\tilde{m}_B = (1\text{-}P_B)\tilde{\bar{m}}_B = m_1 + m_2 + \ldots + \infty = m_1/(1\text{-}K_I m_1); \quad K_I m_1 < 1 \qquad (2.17)$$

where m_1, m_2, etc. are the molar concentrations of unbound monomer, dimer, etc. of ligand, each state bearing one free site. In these terms the site binding constant k_A is defined as the ratio of the concentration of reacted A-sites, $fP_A\bar{m}_A$, to the product of the concentration of unreacted A-sites, $f(1 - P_A)\bar{m}_A$, and the concentration of unreacted ligand sites, $(1 - P_B)\tilde{\bar{m}}_B$. Thus:

$$k_A = P_A/(1 - P_A)(1 - P_B)\tilde{\tilde{m}}_B \,. \tag{2.18}$$

Combination of equation (2.17) and (2.18) gives:

$$P_A = k_A\tilde{m}_B/(1 + k_A\tilde{m}_B);$$

$$1/(1 - P_A) = 1 + [k_A m_1/(1 - K_I m_1)] \,. \tag{2.19}$$

Combination of equation (2.16) and (2.19) gives:

$$\bar{m}_A = m_A\{1 + [k_A m_1/(1 - K_I m_1)]\}^f \,. \tag{2.20}$$

Equation (2.20) is evidently identical with equation (2.15). It may be concluded that the reacted site probability approach provides a ready means of deducing the general formula for an f-valent acceptor without explicit consideration of all complexes present in the equilibrium mixture. It is fair to note, however, that it has been advantageous to consider both types of approach conjointly in that the former, while less direct, does give a proper appreciation of the detailed composition of the equilibrium mixture in terms of the wide variety of complexes present.

2.2.2 The Molar Concentration of Bound Ligand

2.2.2.1 The particular case $f = 1$

An expression for the molar concentration of bound ligand is found by summing the molar concentrations of all complexes with due account for the stoichiometry of each ligand state bound to the single site on the acceptor. Thus, with the use of equation (2.6):

$$\bar{m}_B - \sum_{i=1}^{i=\infty} i m_i = \bar{m}_B - m_1/(1 - K_I m_1)^2$$

$$= m_{A\text{-}B_1} + 2m_{A\text{-}B_2} + 3m_{A\text{-}B_3} + \ldots + \infty. \tag{2.21}$$

The lower part of equation (2.21) becomes $k_A m_A m_1\{1 + 2K_I m_1 + 3K_I^2 m_1^2 + \ldots + \infty\}$ which may be readily summed to yield $k_A m_A m_1/(1 - K_I m_1)^2$. Thus the required expression is given by:

$$\bar{m}_B - m_1/(1 - K_I m_1)^2 = k_A m_A m_1/(1 - K_I m_1)^2 \tag{2.22}$$

with $K_I m_1 < 1$, m_1 as before being the molar concentration of unbound monomeric ligand. This particular solution will provide a check on the general solution for an f-valent acceptor which will be derived by the more direct reacted-site probability function approach.

2.2.2.2 Generalization to an *f*-valent acceptor

The statement of conservation that the concentration of A-sites that are bound with ligand must equal the concentration of ligand sites that have reacted is given by:

$$f P_A \bar{m}_A = P_B \tilde{\bar{m}}_B. \tag{2.23}$$

An expression for P_A in terms of the concentrations of unbound ligand sites is given in equation (2.19). While the corresponding expression for P_B is seen from equation (2.17) to be: $P_B = (\tilde{\bar{m}}_B - \tilde{m}_B)/\tilde{\bar{m}}_B$. It follows that:

$$\tilde{\bar{m}}_B - \tilde{m}_B = f k_A \tilde{m}_B \bar{m}_A / (1 + k_A \tilde{m}_B) \; . \tag{2.24}$$

It is now required to express $\tilde{\bar{m}}_B$ and $\tilde{m}_B$, referring to concentrations of sites, in terms of $\bar{m}_B$, the total base molar concentration of ligand, and m_1, the concentration of unbound monomeric ligand in the equilibrium mixture. One relevant expression is given by equation (2.17), where it is seen that $\tilde{m}_B = m_1/(1 - K_I m_1)$. The other pertinent relationship follows by noting that in the absence of acceptor:

$$\tilde{\bar{m}}_B = m_B + m_{B_2} + m_{B_3} + \ldots + \infty = m_1/(1 - K_I m_1) \tag{2.25a}$$

$$\bar{m}_B = m_B + 2m_{B_2} + 3m_{B_3} + \ldots + \infty = m_1/(1 - K_I m_1)^2 \tag{2.25b}$$

$$\tilde{\bar{m}}_B = \bar{m}_B(1 - K_I m_1) \; . \tag{2.25c}$$

These expressions all require that the common ratio $K_I m_1 < 1$ and it is noted that equation (2.25c) is in fact valid regardless of whether acceptor is present or not since it refers to the total concentration of ligand and to the total concentration of reactive sites irrespective of whether or not the ligand is bound to acceptor. Substituting these equations for $\tilde{m}_B$ and $\tilde{\bar{m}}_B$ into equation (2.24), together with the expression for $\bar{m}_A$ given by equation (2.20), yields, on division by $(1 - K_I m_1)$:

$$\bar{m}_B - \frac{m_1}{(1 - K_I m_1)^2} = \frac{f k_A m_1 m_A \{1 + [k_A m_1/(1 - K_I m_1)]\}^{f-1}}{(1 - K_I m_1)^2} . \qquad (2.26)$$

The left-hand side of equation (2.26) gives the base molar concentration of bound ligand and the right-hand side simplifies to that of equation (2.22) when $f = 1$, as required. In this connection it is noted that equation (2.26), the generalized form for an f-valent acceptor, cannot be readily induced from the particular solution given in equation (2.22).

2.2.3 The Binding Equation

Combination of equation (2.8), the definition of the binding function, r, equation (2.20), the expression for the total molar concentration of acceptor, and equation (2.26), the relationship for the base molar concentration of bound ligand, yields:

$$r = f k_A m_1/(1 - K_I m_1)^2 \{1 + [k_A m_1/(1 - K_I m_1)]\} . \qquad (2.27)$$

Two arrangements of this basic binding equation are useful. The first is suggested by the fact that while equation (2.27) is written in terms of the concentration of unbound ligand, m_1, an experimenter may only determine the total molar concentration of all forms of unbound ligand, termed m_L. It is evident from equation (2.21) that:

$$m_L = \sum_{i=1}^{i=\infty} i m_i = m_1/(1 - K_I m_1)^2 . \qquad (2.28)$$

The solution of equation (2.28) expressed as a quadratic is (provided $K_I \neq 0$):

$$m_1 = [(1 + 2K_I m_L) - \sqrt{1 + 4K_I m_L}]/2K_I^2 m_L, \qquad (2.29)$$

the negative root being selected on the basis that $K_I m_1 < 1$. Substitution of equations (2.28) and (2.29) into equation (2.27) yields when $K_I \neq 0$:

$$r = \frac{2 f k_A K_I m_L}{2K_I + k_A(\sqrt{1 + 4K_I m_L} - 1)} . \qquad (2.30)$$

The second rearrangement is aimed at comparing the form of the binding curve

described by equation (2.30) with that which would be obtained if no self-association of the ligand was operative. This is achieved by writing equation (2.30) as:

$$r = fk_A m_L/(1 + k_A m_L) + \psi \tag{2.31a}$$

$$\psi = \frac{fk_A^2 m_L(1 + 2K_I m_L - \sqrt{1 + 4K_I m_L})}{(1 + k_A m_L)[2K_I + k_A(\sqrt{1 + 4K_I m_L} - 1)]} . \tag{2.31b}$$

The first term in equation (2.31a) describes a hyperbolic relationship between r and m_L and may be viewed as a reference term describing the binding of univalent monomeric ligand to the f-valent acceptor: it would be the only term present if $K_I = 0$ and $m_L = m_1$. The second term in equation (2.31a), ψ, is necessarily positive since from equation (2.29) the numerator of equation (2.31b) is positive ($m_1 > 0$) and the denominator is also positive ($\sqrt{1 + 4K_I m_L} > 1$). Thus, it may be immediately concluded that the values of r, in the case of self-association of the ligand, are greater than those of the reference curve at all values of m_L.

It is also possible to use equation (2.31) to examine the limiting value of r as the ligand concentration approaches infinity. By expanding the square root terms in equation (2.31b) it may be shown that:

$$\lim_{m_L \to \infty} \quad r = f + f\sqrt{K_I m_L} = \infty . \tag{2.32}$$

It is seen from this formulation that if $K_I = 0$ (i.e. the ligand does not self-associate) the limiting value of r would be f, corresponding to saturation of the acceptor and consistent with the conclusion reached by Klotz (1946). For an indefinitely self-associating ligand system, however, at very large ligand concentrations indefinitely long chains of ligand would occupy each acceptor site and thus the value of r, expressed in terms of the number of base moles of ligand bound, would indeed tend to infinity as correctly predicted by equation (2.32).

2.2.4 The Form of the Binding Curve and Numerical Examples

Figure 2.1 presents numerical examples of binding curves calculated using equation (2.30) for systems in which ligand indefinitely self-associates, each state binding via one site to an f-valent acceptor. In these calculations a single value for the site-binding constant, $k_A = 500\ M^{-1}$, was arbitrarily selected which corresponds to a standard free energy change of -3.6 kcal $mole^{-1}$. The following points merit comment in relation to Figure 2.1. First, ordinate values have been plotted as r/f to emphasize that the valency of the acceptor is merely a scaling factor, the numerical value of which does not alter the basic form of the binding curve. Secondly, it is stressed that for each value of K_I examined (corresponding to a particular system) the binding curve is independent of acceptor concentration: this significant point is also evident in equations (2.27), (2.30) and (2.31) where the term m_A, evident in the precursor equations (2.20) and (2.26), has cancelled. Thirdly, consistent with the observation that $\psi > 0$ in equation (2.31), it is evident that all binding curves in Figures 2.1 lie above the rectangular hyperbolic reference curve (---). Fourthly, it is evident that as the value of the indefinite self-association constant, K_I, increases values of r/f at any given value of m_L progressively increase. This is consistent with the concept that all states of the ligand are bound to the acceptor in the equilibrium mixture, including long chains whose relative molar concentrations increase with K_I. For intrinsically the same reason all solid curves in Figure 2.1 exhibit no limiting value of r/f, a point discussed earlier in relation to equation (2.32).

While it is evident from Figure 2.1 that binding curves associated with a self-interacting ligand do deviate from the form of a rectangular hyperbola, the nature of this deviation is better seen by constructing corresponding Scatchard plots of r/fm_L *versus* r/f, where again the valency of acceptor has been incorporated as a scaling factor in both ordinate and abscissa values. Such curves are shown in Figure 2.2, together with the linear Scatchard plot (---) corresponding to the rectangular hyperbolic curve in Figure 2.1. Clearly, all curves for which $K_I > 0$ are convex to the abscissa, with no defined limiting value of r/f. Thus, each convex plot has the abscissa as an asymptote

Figure 2.1: Binding curves constructed numerically using equation (2.30) to show the effect of varying the magnitude of the equilibrium constant, K_I, governing the isodesmic self-association of a ligand, each state of which bears one site capable of interaction with an f-valent acceptor. The value of the site-binding constant, k_A, governing each acceptor-ligand interaction was given the value 500 M^{-1}. The abscissa, m_L, is the equilibrium concentration of all forms of unbound ligand and the ordinate is the binding function, r, defined in the same terms and divided by the scaling factor f, the number of binding sites on the acceptor. The broken curve was computed using the first term of equation (2.31a) and is a reference curve which pertains when the ligand does not self-associate.

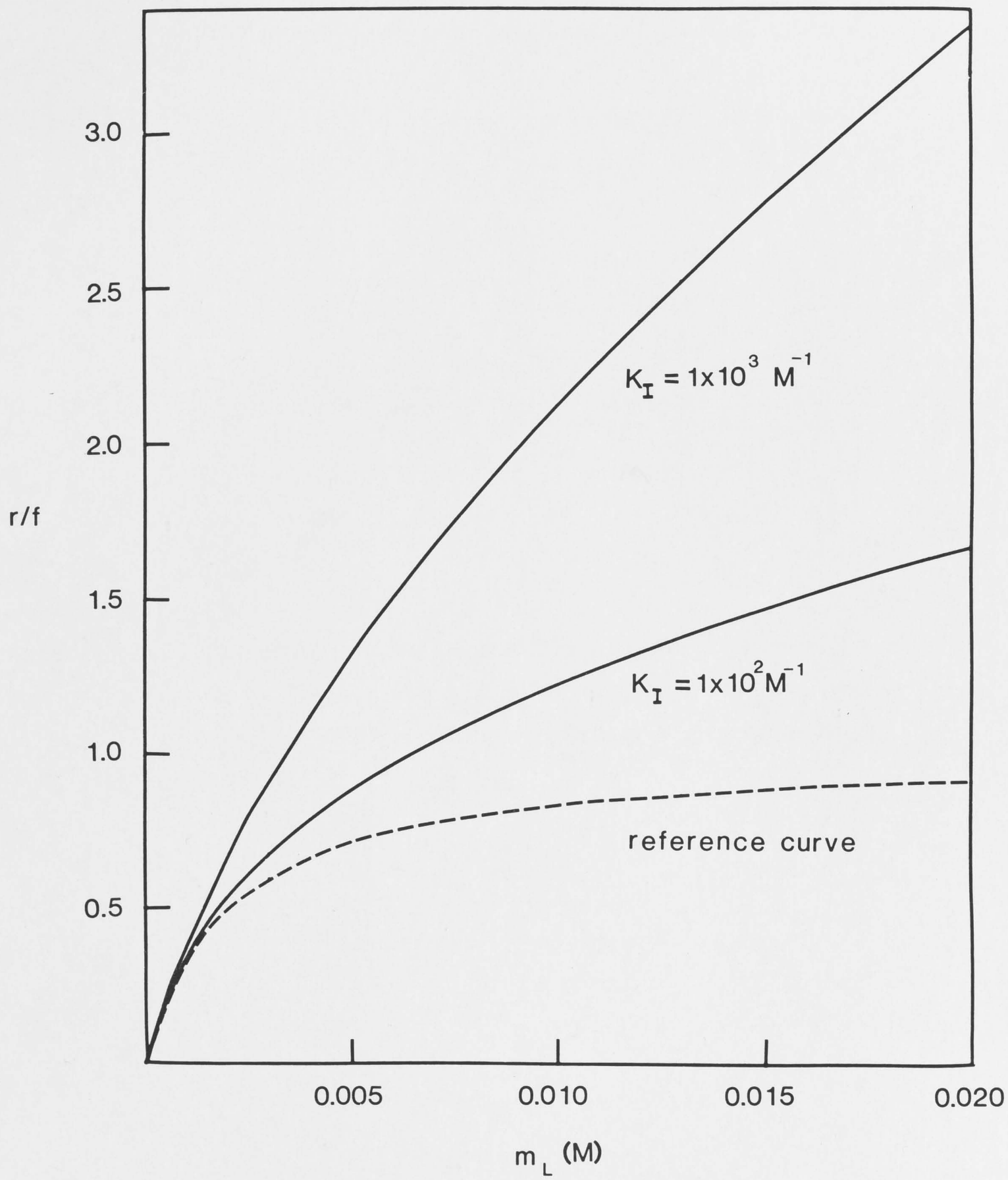
3.0
2.5
2.0
r/f
1.5
1.0
0.5
$K_I = 1x10^3\ M^{-1}$
$K_I = 1x10^2 M^{-1}$
reference curve
0.005
0.010
0.015
0.020
m_L (M)

Figure 2.2: Numerical examples of Scatchard plots corresponding to the binding curves shown in Figure 2.1. The broken line, which is seen to be the limiting tangent of all curves, also corresponds to the broken curve in Figure 2.1.

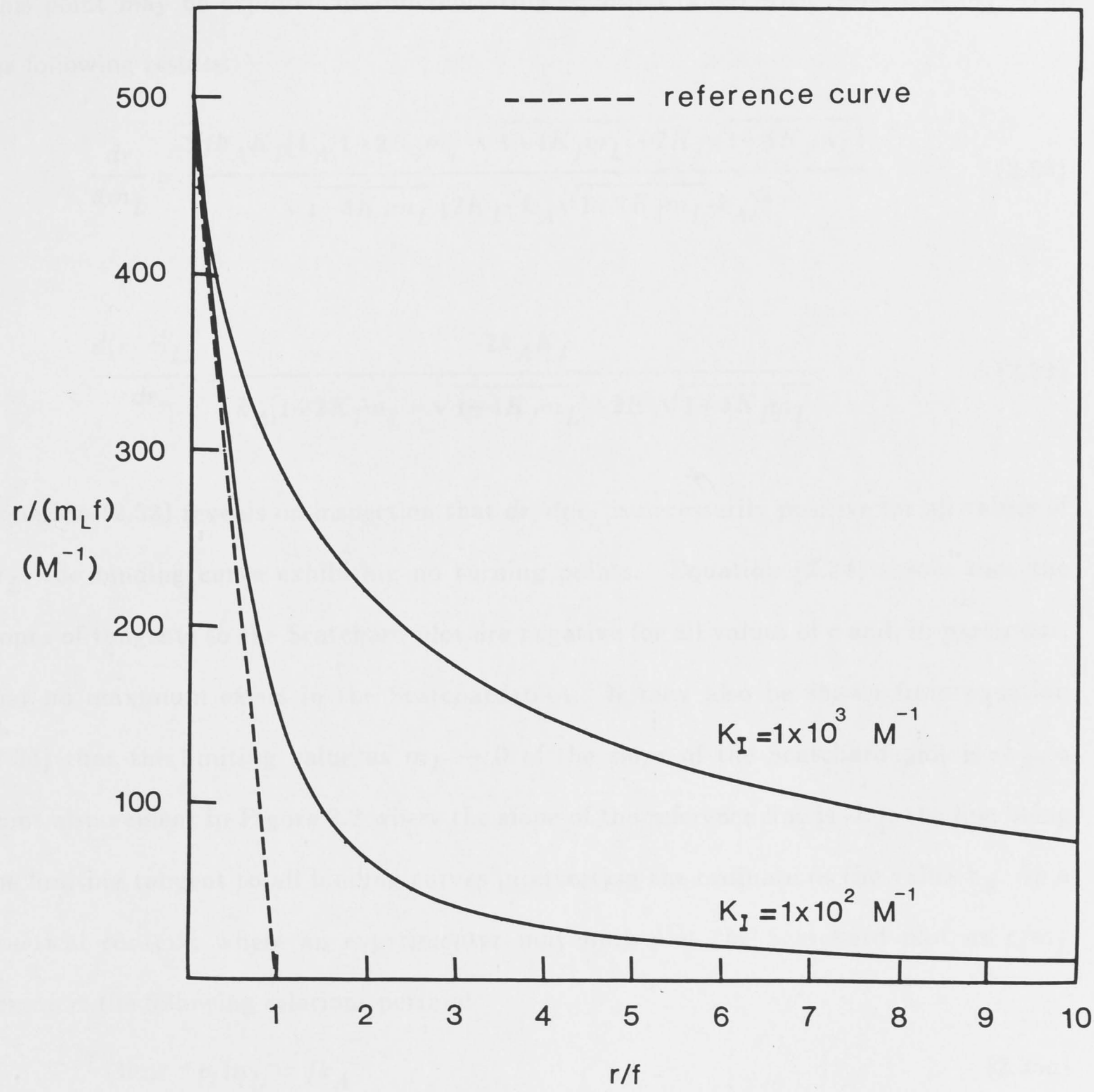
500
400
300
200
100
r/(m_L f)
(M^-1)
reference curve
K_I =1x10^3 M^-1
K_I =1x10^2 M^-1
1
2
3
4
5
6
7
8
9
10
r/f

consistent with equation (2.32). The interesting question emerges whether this form of Scatchard plot pertains regardless of the values of k_A and K_I appropriate to the system. This point may be explored by differentiating equation (2.30) with respect to m_L with the following results:

$$\frac{dr}{dm_L} = \frac{2fk_AK_I\{k_A[1+2K_Im_L-\sqrt{1+4K_Im_L}]+2K_I\sqrt{1+4K_Im_L}\}}{\sqrt{1+4K_Im_L}\,(2K_I+k_A\sqrt{1+4K_Im_L}-k_A)^2} \tag{2.33}$$

$$\frac{d(r/m_L)}{dr} = \frac{-2k_AK_I}{k_A[1+2K_Im_L - \sqrt{1+4K_Im_L}]+2K_I\sqrt{1+4K_Im_L}}\,. \tag{2.34}$$

Equation (2.33) reveals on inspection that dr/dm_L is necessarily positive for all values of m_L, the binding curve exhibiting no turning points. Equation (2.34) shows that the slopes of tangents to the Scatchard plot are negative for all values of r and, in particular, that no maximum exists in the Scatchard plot. It may also be shown from equation (2.34) that the limiting value as $m_L \rightarrow 0$ of the slope of the Scatchard plot is $-k_A$, a point also evident in Figure 2.2 where the slope of the reference line is $-k_A$, the line being the limiting tangent to all binding curves intersecting the ordinate at the value k_A. In a practical context, where an experimenter may only plot the Scatchard plot as r/m_L *versus* r, the following relations pertain:

$$\lim_{m_L \rightarrow 0} \quad r/m_L = fk_A \tag{2.35a}$$

$$\lim_{m_L \rightarrow 0} \quad d(r/m_L)/dr = -k_A \tag{2.35b}$$

from which it is possible to obtain first estimates of both f and k_A from the slope and ordinate intercept of the limiting tangent. Differentiation of equation (2.34) with respect to r reveals that the sign of the second derivative $d^2(r/m_L)/d(r)^2$, is determined by the sign of: $2K_I[k_A(\sqrt{1+4K_Im_L}-1)+2K_I]/\sqrt{1+4K_Im_L}$. This term is evidently always positive and thus from equation (2.4b) it has been proven that Scatchard plots are convex to the abscissa for all values of f, k_A and K_I, as illustrated in Figure 2.2.

2.3 THE COMPOSITION OF THE SOLUTION

In an equilibrium mixture comprising an f-valent acceptor and a ligand which indefinitely self-associates such that each ligand state bears one binding site, the weight concentration of unbound ligand may be written as:

$$\bar{c}(unbound) = M_1 m_1 + 2M_1 K_I m_1^2 + \ldots + iM_1 K_I^{(i-1)} m_1^i + \ldots + \infty \qquad (2.36a)$$

$$= M_1 m_1 / (1 - K_I m_1)^2 \, . \qquad (2.36b)$$

Thus, the weight-fraction of the i-th ligand species (unbound) is given by:

$$\frac{c_i(unbound)}{\bar{c}(unbound)} = i(K_I m_1)^{(i-1)}(1 - K_I m_1)^2 \, . \qquad (2.37)$$

On noting that $m_1 = (1 + 2\alpha - \sqrt{1 + 4\alpha})/2K_I\alpha$, where $\alpha = K_I\bar{c}(unbound)/M_1$, it may be shown that equation (2.37) is identical to equation (2.7), which we have seen has been discussed by Kurganov (1984) in terms of the attainment of maximal values of the weight-fractions of all species except monomer. Reference to equation (2.26) permits a similar expression to be written for the weight-fractions of ligand species bound to the acceptor since the right-hand side of that equation may be expanded as a series, the i-th term of which is given by:

$$c_i(bound) = iM_1 f k_A m_A K_I^{(i-1)} m_1^i \{1 + [k_A m_1/(1 - K_I m_1)]\}^{f-1}. \qquad (2.38)$$

The total weight-concentration of ligand bound is seen from equation (2.26) to be:

$$\bar{c}(bound) = \frac{M_1 f k_A m_A m_1 \{1 + [k_A m_1/(1 - K_I m_1)]\}^{f-1}}{(1 - K_I m_1)^2} \, . \qquad (2.39)$$

The ratio of equations (2.38) and (2.39) gives:

$$\frac{c_i(bound)}{\bar{c}(bound)} = i(K_I m_1)^{(i-1)}(1 - K_I m_1)^2 \, . \qquad (2.40)$$

Comparison of equation (2.37), and (2.40) reveals that the weight-fractions of all ligand species (including monomer) are identical in the bound and unbound states. It follows in relation to bound ligand states that, provided $i > 1$, the weight-fractions must pass through a maximum as the total ligand concentration increases, the concentration at which this maximum is attained increasing with the value of i. Thus, the composition of bound ligand states exactly parallels that described by Kurganov (1984) in relation to unbound ligand states. This is not to say that the composition of ligand free in solution and bound to acceptor is identical with that which pertained before acceptor was added. Clearly, addition of acceptor reduces the total concentration of ligand free in solution and hence unbound monomeric ligand (and hence bound monomeric ligand) is favoured on a weight-fraction basis.

2.4 GENERAL DISCUSSION

A major development in this chapter has been the extension of binding theory to obtain a closed solution which quantitatively describes the binding of an indefinitely self-associating ligand to an f-valent acceptor in cases where each ligand state bears one binding site. It should be noted that the equations developed not only permit comment on the composition of the solution in terms of a comparison of bound and unbound ligand states, as in the preceding section; but also provide a means of specifying the exact composition of a system characterized by the constants f, k_A and K_I, for any given initial mixing composition of $\bar{m}_A$ and $\bar{m}_B$. Explicitly, equations (2.20) and (2.26) may be solved simultaneously by eliminating m_A between them, to find corresponding values of m_1 and m_A. The molar concentration of every unbound ligand species may then be calculated using the relation $m_i = K_I^{(i-1)} m_1^i$ $(i = 2,3,...,\infty)$. The molar concentration of the stoichiometric complexes A - B_i may be evaluated from equation (2.38) by dividing by iM_1, noting that the concentration of any such given stoichiometric complex is the sum of the concentrations of all constituent species which have this overall stoichiometry. An example is provided by the stoichiometric complex A - B_3 which is to be viewed as comprising a combination of three monomeric units

bound to three separate acceptor sites (in all combinations among the *f*-sites), a dimer and a monomer bound at two acceptor sites, in all combinations, and a trimer bound to one acceptor site, with again every such arrangement between the *f*-sites being considered.

In an experimental situation where the aim is to evaluate the thermodynamic interaction parameters f, k_A and K_I, it is recommended that studies be performed on the ligand in the absence of acceptor to establish the operation of an indefinite self-association and, if it is isodesmic, the value of K_I. Chapter 4 will outline in some detail the way in which sedimentation equilibrium analysis may be used for this purpose. It is then suggested that binding results be obtained and plotted in Scatchard format so that the limiting tangent as $m_L \rightarrow 0$ may be used to obtain first estimates of f and k_A as suggested by equations (2.35a) and (2.35b). Refinement of these values may then proceed by curve fitting all binding results to the binding equation given in equation (2.30).

Another point which has emerged in the chapter which merits further discussion is the convex nature of Scatchard plots. This form has been shown to pertain for all values of the interaction parameters governing the system under consideration and has been illustrated numerically in Figure 2.2. There seems little doubt that many workers attribute such curvilinearity to the mechanistic operation of negatively cooperative allosteric effects (Koshland and Neet, 1968). Thus, the binding sites on the acceptor are considered to be initially equivalent, with binding of ligand to one or more of the sites inducing a conformational change in the acceptor which perturbs other sites in a way which decreases the extent of ligand association to them. It is now evident that it is unwise to attribute a convex Scatchard plot arbitrarily to the operation of negative cooperativity without first exploring other possibilities. This point is emphasized in Table 2.1 which summarizes certain molecular bases giving rise to this form of Scatchard plot. The first entry refers to negative cooperativity and shows the binding equation as a ratio of polynomials written in terms of site-binding constants pertaining to the mutually interactive binding sites (Nichol and Winzor, 1981). The second entry gives a

Table 2.1: A summary of systems and related binding equations which give rise to Scatchard plots convex to the abscissa.

System	Binding Equation	Reference
Equivalent and dependent binding sites on a single acceptor state: negative cooperativity	$r = \dfrac{2k_1 m_B + 2k_1 k_2 m_B^2}{1 + 2k_1 m_B + k_1 k_2 m_B^2}; \quad k_1 > k_2$	Levitzki and Koshland (1972); Koshland, Nemethy and Filmer (1966)
Non-equivalent and independent binding sites on a single acceptor state	$r = \sum_{j=1}^{j=F} \dfrac{f_j k_j m_B}{1 + k_j m_B}$	Blake and Peacocke (1968)
Two state acceptor, $nM \rightleftharpoons P$, with ligand B binding to one site on P	$r = \dfrac{k_P m_P m_B}{m_M + n m_P (1 + k_P m_B)}$	Tellam, Winzor and Nichol (1978); Baghurst, Nichol and Winzor (1978)
Single acceptor state exclusively binding the monomer of an associating ligand, $2B \rightleftharpoons B_2$	$r = \dfrac{f k_A m_B}{1 + k_A m_B}$	Nichol, Smith and Ogston 1969); Dombrose *et al.* (1979)
Single acceptor state binding all states of an isodesmically associating ligand each state bearing one site	$r = \dfrac{2f k_A K_I m_L}{2K_I + k_A(\sqrt{1 + 4K_I m_L} - 1)}$	Present work

binding equation which is the sum of terms individually describing rectangular hyperbolic responses. It pertains when an acceptor possesses F classes of binding sites each class being constituted of f_j equivalent sites associated with a site binding constant k_j, which differs between the classes. It is noted that the same form of equation arises when the same ligand binds two or more acceptor states which are not in equilibrium, an example being the binding of α-D-methylglucopyranoside to a mixture of different states of concanavalin-A (McKenzie and Sawyer, 1973). Moreover, in the same vein, it is possible that closely adjacent binding sites on certain acceptors may become effectively non-equivalent due to, for example, marked electrostatic repulsion between ligand molecules occupying adjacent sites. The third entry of Table 2.1 refers to a system in which acceptor, rather than ligand, self-associates with the ligand binding exclusively to the polymeric state of the acceptor with a site binding constant k_p. The cited binding equation is a particular form of the general binding equation formulated by Nichol, Jackson and Winzor (1967) and shows that binding curves for such systems will exhibit acceptor concentration-dependence as observed experimentally in the binding of Zn(II) to one site on the dimeric form of α-amylase, which exists in equilibrium with the monomeric state even in the absence of the ligand (Tellam, Winzor and Nichol, 1978). Such acceptor concentration-dependence is not predicted for any other type of system summarized in Table 2.1 and, as we have seen, nor is it a property of binding responses obtained when the ligand indefinitely self-associates. The final entries in Table 2.1 repeat, for completeness, equations (2.2a) and (2.30). The former refers to a dimerizing ligand in which monomer binds exclusively to the f-valent acceptor ($l_A = 0$). In this connection, it is stressed that the convex Scatchard plot associated with such a system is one of r/m_L *versus* r, where r is given by equation (2.2a) and $m_L = m_B + 2k_2 m_B^2$. Consistency is noted between the preferential binding of monomer of a two-state ligand system and the same form of curve observed in Figure 2.2 to which equation (2.30) applies. Thus, a ligand indefinitely self-associating by a "head-to-tail" mechanism creates a situation where binding sites are not conserved on self-association, but rather a potential binding site is lost with each successive addition of monomer to form higher polymers.

With the entries in Table 2.1 in mind, it can be said that the interpretation of a convex Scatchard plot should not proceed without an understanding of the association behaviour (or otherwise) of the acceptor and of the ligand, studied separately. Moreover, it is desirable also to establish whether binding curves exhibit acceptor concentration-dependence, or not. If it is shown that the ligand undergoes an indefinite "head-to-tail" self-association, as does lysozyme (Wills, Nichol and Siezen, 1980), the equations developed in this chapter, which add to those presented in Table 2.1, will be of direct relevance. However, the theoretical developments in this chapter have not been formulated primarily for this purpose; but rather they form a necessary introduction to the consideration of other types of interacting ligand systems. Explicitly, if one removes the restriction that each state of the ligand bears only one binding site for acceptor, a situation arises where crosslinking of acceptor molecules via ligand bridges is possible. This is the subject of the next chapter, where it will be seen that systems in addition to those summarized in Table 2.1 exist which may give rise to convex Scatchard plots.

CHAPTER 3

BINDING THEORY PERTAINING TO THE REVERSIBLE CROSSLINKING OF ACCEPTORS BY LIGAND BRIDGES

3.1 INTRODUCTION

The simplest case of the reversible crosslinking of acceptor molecules initiated by the addition of a ligand arises when a single state of a univalent acceptor interacts with a non-self-associating bivalent ligand according to the equilibria $A+B \rightleftharpoons A\text{-}B$; $A\text{-}B+A \rightleftharpoons A\text{-}B\text{-}A$, as exemplified by the interaction of human mercaptalbumin, A, and mercuric chloride, B (Edelhoch *et al.*, 1953). Nichol and Winzor (1976a) formulated the binding equation for such a system and established with it three basic properties of the binding response. The first was that the form of the Scatchard plot was convex to the r-axis, $d^2(r/m_B)/d(r)^2 > 0$. The second established that for a given system a family of binding curves would arise, each obtained at a fixed but different value of the acceptor concentration and intersecting at a common point ($r = 0.5$, $m_B = 1/2k_A$). The third property was that the concentration of the crosslinked complex, $A\text{-}B\text{-}A$, attained a maximal value when $r = 0.5$, the species favoured as $m_B \rightarrow \infty$ being the $A\text{-}B$ complex; increased ligand concentration perturbs the equilibria therefore effectively counteracting the formation of crosslinked complexes.

The notion that a binding equation could be formulated for crosslinking systems was extended by Calvert, Nichol and Sawyer (1979) in their consideration of the interaction between a bivalent ligand and an f-valent acceptor ($f > 1$). In this case an infinite array of complexes, A_iB_j, is formed comprising linear chains, and three dimensional networks, of alternating acceptor and ligand molecules. The authors restricted consideration to systems where a single site-binding constant, k_A, defined in terms of reacted-site probability functions (Goldberg, 1952; 1953; Flory, 1953; Singer, 1965), sufficed to describe all interactions and obtained the following binding equation, where $\alpha = 2k_Am_B$:

$$r = [f\alpha/(1 + \alpha)] + \psi \qquad (3.1a)$$

$$\psi = \frac{(1 - \alpha^2)}{4k_A\bar{m}_A\alpha}\left\{1 + \frac{2fk_A\bar{m}_A\alpha}{(1+\alpha)^2} - \left[1 + \frac{4fk_A\bar{m}_A\alpha}{(1+\alpha)^2}\right]^{1/2}\right\}. \qquad (3.1b)$$

The forms of binding curves predicted on the basis of equation (3.1) are markedly similar to those predicted earlier by Nichol and Winzor (1976a) in that Scatchard plots are convex to the r-axis, exhibiting acceptor concentration-dependence and intersecting at the common point ($r = f/2$, $m_B = 1/2k_A$). At this point $\psi = 0$ and the overall extent of reaction was shown to be maximal as were the concentrations of those complexes for which $j/i = f/2$. Indeed, it was shown that at a fixed acceptor concentration the concentrations of all A_iB_j complexes pass through a maximum as the concentration of ligand is increased, except for the fully-saturated complex AB_f which alone exists as $m_B \rightarrow \infty$. In contrast to the behaviour of the system when $f = 1$, it was shown for the infinitely crosslinking case that gelation may arise if the overall extent of reaction exceeds the value $1/(f\text{-}1)$, established by Flory (1953) as the criterion for gelation. It also follows that gelation is not possible in systems where $f = 2$, the case of a bivalent acceptor being linked by a bivalent ligand to form an equilibrium mixture of linear chain polymers.

While equation (3.1) may well not be directly applicable to studies on the interactions between f-valent antigens and bivalent antibodies (Heidelberger and Kendall, 1935) due to the assumptions that reactants are homogeneous and only one site-binding constant prevails, assumptions which were discussed by Palmiter and Aladjem (1963), it seems generally agreed that the simplified derivation does suffice to reveal the basic properties of such systems, including the commonly observed precipitation effect when the concentration of one reactant is held fixed and the other is varied (Nichol, Sculley and Winzor, 1982). The latter workers extended their considerations to a system in which the ligand self-associated according to the two-state dimerization, $2B \rightleftharpoons B_2$. They assumed (somewhat unrealistically) that the monomer, B, did not bind to the f-valent acceptor, but that the dimer, B_2, was bivalent toward it,

such that the dimer became the ligand bridge in the infinite array of acceptor-ligand complexes which existed in equilibrium with unbound acceptor, ligand monomer and ligand dimer. This formulation was primarily used by the authors to discuss unusual precipitation effects which might arise on dilution of the system with solvent and which had found experimental manifestation in a particular immunological system (Brown and Rodkey, 1979). The pertinent point to this work is that a system had been visualized where the self-association of the ligand, as discussed in Chapter 2, was directly related to a crosslinking of the acceptor. It is noted that while Nichol, Sculley and Winzor (1982) did discuss the limiting value of the binding function, $r = (\bar{m}_B - m_B - 2m_{B_2})/\bar{m}_A$, they did not provide any information on the forms of binding curves characteristic of this type of system.

The purpose of this chapter is to extend further the crosslinking concepts introduced above with the ultimate intention of illustrating how ligand self-association may be coupled with crosslinking of acceptor in affecting the form of the binding response. In common with the work of Nichol, Sculley and Winzor (1982), the development will be in terms of a two-state ligand system, $2B \rightleftharpoons B_2$, but the assumption that binding sites are created on dimerization will not be made in that competitive binding of univalent monomer and bivalent dimer to the acceptor will be considered. At the outset it is observed that the formulation of the binding equation has only been possible for the situation where the acceptor is bivalent, $f = 2$. Nevertheless, even in this case extensive formation of linear chain polymers is possible, a situation that may well pertain to the crosslinking of certain receptor sites on membrane surfaces. Certainly, this treatment with $f = 2$ avoids the complications of the formation of three-dimensional networks and of the possible onset of gelation or precipitant effects. Before this work is presented, it is helpful to form a comparative basis by discussing the crosslinking of a bivalent acceptor by a ligand which does not dimerize. Evidently, this preliminary theory will bear relation to that given by Calvert, Nichol and Sawyer (1979), but will differ from it in that two site-binding constants will be considered, and a contrast will be made between systems in which a single ligand molecule alternates

between acceptor molecules in polymer chains and those where only acceptor complexed with ligand may interact. As will be seen the essential difference between these cases is one involving the stoichiometry of complexes in the equilibrium mixture, an aspect which has not hitherto been discussed in this work, but which leads to profound differences in the forms of binding curves, a point first made in relation to a univalent acceptor by Nichol and Winzor (1976a).

3.2 INTERACTIONS OF NON-ASSOCIATING LIGANDS WITH BIVALENT ACCEPTORS

3.2.1 Bridging of Acceptors by a Single Ligand Molecule

In this section a bivalent ligand, B, is considered where the binding sites interacting with the bivalent acceptor, A, are non-equivalent and independent such that two site-binding constants, k_1 and k_2, are needed to describe the equilibria. The array of complexes, A_iB_j, which form in the equilibrium mixture may be written in stoichiometric terms as:

$$\begin{array}{llll} i = 1; & A, & AB, & AB_2 \\ i = 2; & A_2B, & A_2B_2, & A_2B_3 \\ i = 3; & A_3B_2, & A_3B_3, & A_3B_4 \\ . & . & . & . \\ . & . & . & . \\ . & . & . & . \\ \infty & \infty & \infty & \infty \end{array} \qquad (3.2)$$

where $i = 1,2,\ldots,\infty$ and for each i, $j = (i\text{-}1),\ i,\ (i+1)$.

It may be shown by induction that the molar concentrations of these stoichiometric complexes may be written as:

$$m_{A_iB_{i\text{-}1}} = (4k_1k_2m_B)^{i\text{-}1}m_A^i \qquad (3.3a)$$

$$m_{A_iB_i} = 2(k_1m_B + k_2m_B)(4k_1k_2m_B)^{i\text{-}1}m_A^i \qquad (3.3b)$$

$$m_{A_iB_{i+1}} = (k_1 m_B + k_2 m_B)^2 (4k_1 k_2 m_B)^{i-1} m_A^i. \tag{3.3c}$$

In this formulation, the origin of the numerical coefficient, 4, which appears as a constituent term in each expression, may be exemplified with the complex A_2B which may be viewed as one in which ligand is fully saturated with the bivalent acceptor in each of four possible arrangements. The total molar concentration of acceptor, $\bar{m}_A$, is given by:

$$\bar{m}_A = \sum_{i=1}^{i=\infty} i(m_{A_iB_{i-1}} + m_{A_iB_i} + m_{A_iB_{i+1}}). \tag{3.4}$$

Therefore, combination of equations (3.3) and (3.4) yields,

$$\begin{aligned} \bar{m}_A = \sum_{i=1}^{i=\infty} i(4k_1 k_2 m_B)^{i-1} m_A^i [1 + 2(k_1 m_B + k_2 m_B) \\ + (k_1 m_B + k_2 m_B)^2] \\ = m_A [1 + (k_1 + k_2) m_B]^2 / (1 - 4k_1 k_2 m_A m_B)^2 \end{aligned} \tag{3.5}$$

with the common ratio, $4k_1 k_2 m_A m_B < 1$.

The total molar concentration of ligand, $\bar{m}_B$, is given by:

$$\bar{m}_B = m_B + \sum_{i=1}^{i=\infty} [(i\text{-}1) m_{A_iB_{i-1}} + i m_{A_iB_i} + (i+1) m_{A_iB_{i+1}}] \tag{3.6}$$

which on combination with equation (3.3) yields on extensive re-arrangement:

$$\begin{aligned} \bar{m}_B = m_B \{1 + 2m_A(k_1 + k_2) + 4k_1 k_2 m_A^2 \\ + 2(k_1 - k_2)^2 m_A m_B (1 - 2k_1 k_2 m_A m_B)\} / (1 - 4k_1 k_2 m_A m_B)^2. \end{aligned} \tag{3.7}$$

A check on equations (3.5) and (3.7) may be made by placing $k_1 = k_2 = k_A$, the special case considered by Calvert, Nichol and Sawyer (1979) involving the crosslinking of acceptor by a bivalent ligand involving only one site-binding constant. Equations (3.5) and (3.7) become respectively:

$$\bar{m}_A = m_A (1 + 2k_A m_B)^2 / (1 - 4k_A^2 m_A m_B)^2; \quad 4k_A^2 m_A m_B < 1 \tag{3.8a}$$

$$\bar{m}_B = m_B(1 + 2k_A m_A)^2/(1 - 4k_A^2 m_A m_B)^2; \quad 4k_A^2 m_A m_B < 1 \tag{3.8b}$$

which are equations (15a) and (15b) of Calvert, Nichol and Sawyer (1979) with the required symmetry. It also follows from equation (3.7) that:

$$\bar{m}_B - m_B = \frac{m_B m_A[2(k_1+k_2)+4k_1k_2m_A+2m_B(k_1+k_2)^2(1-2k_1k_2m_Am_B)]}{(1-4k_1k_2m_Am_B)^2} \tag{3.9}$$

Thus, the binding equation may be written, using equations (3.5) and (3.9) as:

$$r = \frac{m_B[2(k_1+k_2)+4k_1k_2m_A+2m_B(k_1+k_2)^2(1-2k_1k_2m_Am_B)]}{[1+(k_1+k_2)m_B]^2}. \tag{3.10}$$

Alternatively equation (3.10) may be written as:

$$r = 2(k_1 + k_2)m_B/[1 + (k_1 + k_2)m_B] + \psi \tag{3.11a}$$

$$\psi = 4k_1k_2m_Am_B[1 - (k_1 + k_2)m_B]/[1 + (k_1 + k_2)m_B] \tag{3.11b}$$

where the first term in equation (3.11a) is of rectangular hyperbolic form and describes a reference curve which specifically eliminates effects due to the crosslinking of acceptor. It is evident from equation (3.11b) that, when $m_B = 1/(k_1 + k_2)$, $\psi = 0$ and $r = 1$. This describes the point of intersection of the family of binding curves which exhibit acceptor concentration-dependence as is evident from equation (3.11b). Thus there is complete analogy between equation (3.11) and equation (3.1), and indeed the former becomes the latter, as we have seen, by placing $k_1 = k_2 = k_A$. Thus, it may be concluded that the crosslinking of a bivalent acceptor by ligand bridges results in Scatchard plots convex to the abscissa regardless of whether the sites on the ligand are equivalent or non-equivalent.

A special case arises in this context where the ligand (initially possessing one binding site for bivalent acceptor) on binding to the acceptor with site-binding constant, k_1, undergoes a conformational change which exposes a second site capable of crosslinking with site-binding constant, k_2. The same array of stoichiometric complexes as shown in equation (3.2) arises but the molar concentrations of these complexes must now be written as:

$$m_{A_iB_{i-1}} = k_2^{i-1} m_A^i (k_1 m_B)^{i-1} \tag{3.12a}$$

$$m_{A_iB_i} = 2k_2^{i-1} m_A^i (k_1 m_B)^i \tag{3.12b}$$

$$m_{A_iB_{i+1}} = k_2^{i-1} m_A^i (k_1 m_B)^{i+1}. \tag{3.12c}$$

In this connection it is noted, for example, in relation to the complex AB, that there is no term of the type $2k_2 m_A m_B$ and thus the formulation differs from that given in equation (3.3). Nevertheless, by following entirely analogous reasoning it may be shown that:

$$\bar{m}_A = m_A(1+k_1 m_B)^2/(1-k_1 k_2 m_A m_B)^2; \quad k_1 k_2 m_A m_B < 1 \tag{3.13}$$

and

$$r = \frac{2k_1 m_B}{1 + k_1 m_B} + \frac{k_1 k_2 m_A m_B(1 - k_1 m_B)}{1 + k_1 m_B}. \tag{3.14}$$

It is noted that equations (3.13) and (3.14) again become the corresponding expressions presented by Calvert, Nichol and Sawyer (1979) when $k_1 = k_2 = 2k_A$, as required. Moreover, acceptor concentration-dependence is predicted by this simultaneous set of equations, the family of curves intersecting at the point ($r = 1$, $m_B = 1/k_1$). Before discussing the binding equation further it is advantageous to first express m_A in terms of the experimentally determinable parameter $\bar{m}_A$. This may be achieved by re-arranging equation (3.13) as:

$$k_2 m_A = \frac{(1 + k_1 m_B)^2 + 2k_1 m_B k_2 \bar{m}_A - (1 + k_1 m_B)\sqrt{\Delta}}{2k_1^2 m_B^2 k_2 \bar{m}_A} \tag{3.15a}$$

$$\Delta = (1 + k_1 m_B)^2 + 4k_1 k_2 \bar{m}_A m_B. \tag{3.15b}$$

It may be readily shown, by combination of equations (3.14) and (3.15), that the binding function, r, may be expressed solely in terms of the two dimensionless parameters $k_1 m_B$ and $k_2 \bar{m}_A$. Indeed, Figure 3.1a presents numerical examples of binding curves plotted in dimensionless format as r *versus* $k_1 m_B$ for selected values of $k_2 \bar{m}_A$, with Figure 3.1b showing the corresponding Scatchard plots. The forms of both sets of curves are entirely

Figure 3.1: The binding of a non-associating univalent ligand, B, to a bivalent acceptor, A, where a conformational change of the bound ligand results in exposure of a second binding site, which is capable of crosslinking a second acceptor molecule. The equilibrium mixture comprises unbound reactants and an infinite array of chains of alternating A and B units.

(a) Plots of the binding function, r, *versus* the dimensionless parameter, $k_1 m_B$, the product of the site-binding constant, k_1, governing acceptor-ligand interaction prior to the conformational change, and the molar concentration of unbound ligand. The curves were calculated using equations (3.14) and (3.15) with the following values of the dimensionless product, $k_2 \bar{m}_A$, where k_2 is the site-binding constant appropriate to the site exposed on ligand binding and $\bar{m}_A$ is the total acceptor concentration: $k_2 \bar{m}_A = 5$, (— —), $k_2 \bar{m}_A = 1$, (----). The solid curve was calculated using the first term of equation (3.14) and is a reference curve which excludes effects due to the crosslinking of the acceptor.

(b) Scatchard plots corresponding to the binding curves shown in (a).

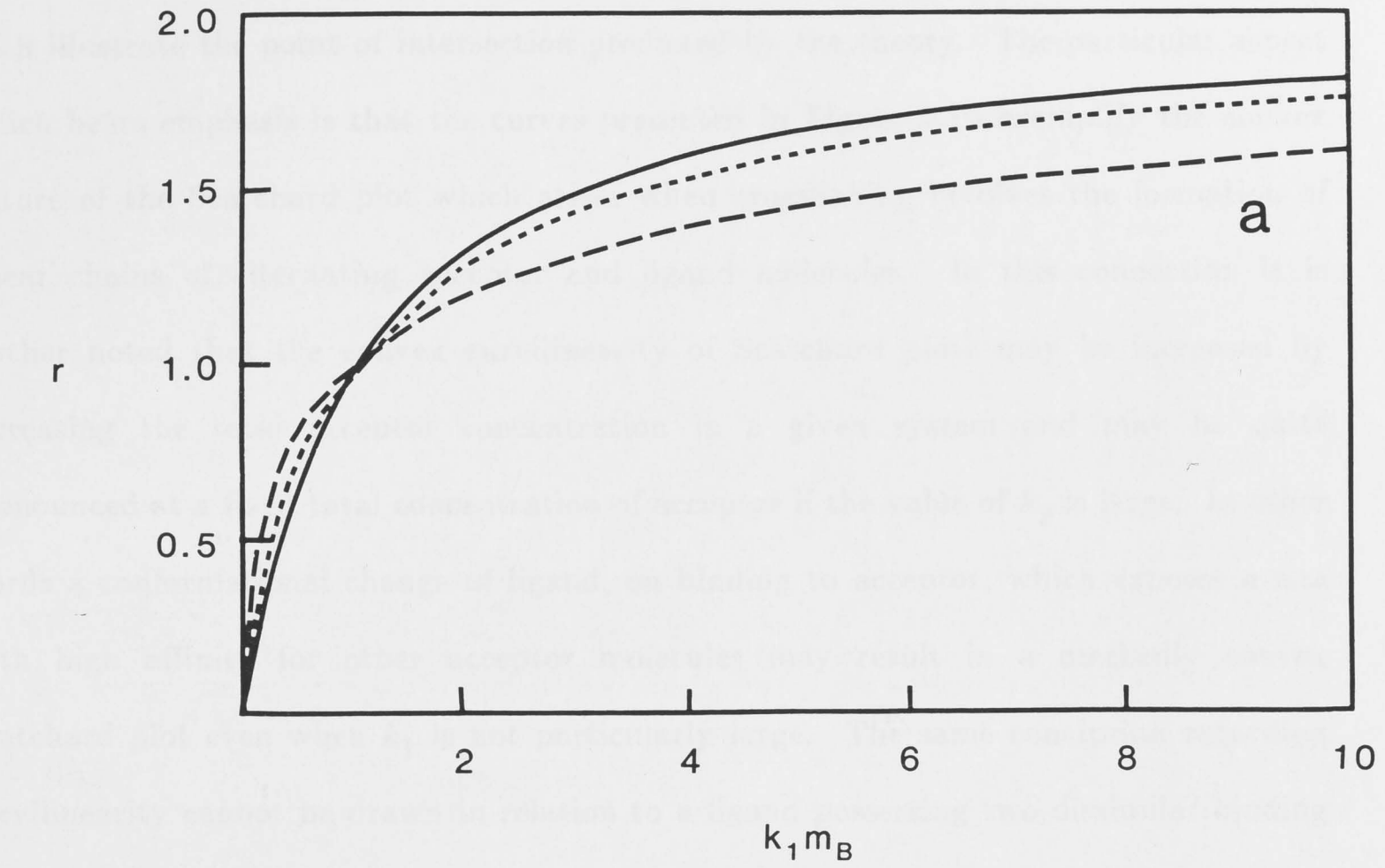
2.0
1.5
1.0
0.5
r
a
2
4
6
8
10
$k_1 m_B$

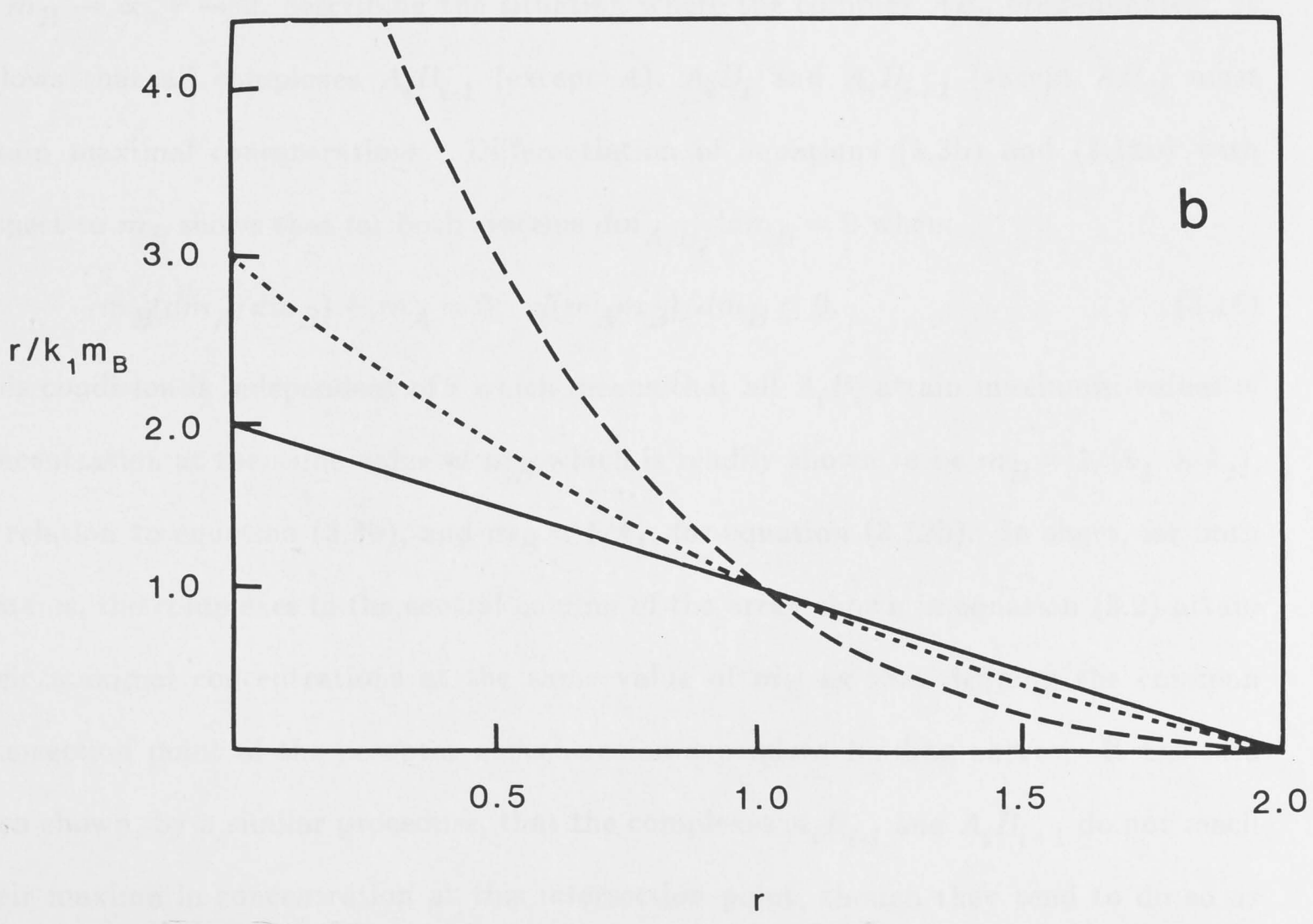
4.0
3.0
2.0
1.0
$r/k_1 m_B$
b
0.5
1.0
1.5
2.0
r

similar to the numerical examples presented by Calvert, Nichol and Sawyer (1979) and both illustrate the point of intersection predicted by the theory. The particular aspect which bears emphasis is that the curves presented in Figure 3.1b exemplify the convex nature of the Scatchard plot which arises when crosslinking involves the formation of linear chains of alternating acceptor and ligand molecules. In this connection it is further noted that the convex curvilinearity of Scatchard plots may be increased by increasing the total acceptor concentration in a given system and may be quite pronounced at a fixed total concentration of acceptor if the value of k_2 is large. In other words a conformational change of ligand, on binding to acceptor, which exposes a site with high affinity for other acceptor molecules may result in a markedly convex Scatchard plot even when k_1 is not particularly large. The same conclusion regarding curvilinearity cannot be drawn in relation to a ligand possessing two dissimilar binding sites prior to complex formation unless $k_1 \approx k_2$ and both are large.

As a final point in this section comment is made on the composition of the solution as the concentration of ligand increases. It follows from equation (3.11) and (3.14) that as $m_B \to \infty$, $r \to 2$, describing the situation where the complex AB_2 predominates. It follows that all complexes $A_iB_{i\text{-}1}$ (except A), A_iB_i and A_iB_{i+1} (except AB_2) must attain maximal concentrations. Differentiation of equations (3.3b) and (3.12b) with respect to m_B shows that for both systems $dm_{A_iB_i}/dm_B = 0$ when:

$$m_B(dm_A/dm_B) + m_A = 0; \quad d(m_A m_B)/dm_B = 0. \tag{3.16}$$

This condition is independent of i which means that all A_iB_i attain maximum values of concentration at the same value of m_B which is readily shown to be $m_B = 1/(k_1 + k_2)$, in relation to equation (3.3b), and $m_B = 1/k_1$, for equation (3.12b). In short, for both systems, the complexes in the central column of the array shown in equation (3.2) attain their maximal concentrations at the same value of m_B as that defining the common intersection point of the acceptor concentration-dependent binding curves. It has also been shown, by a similar procedure, that the complexes $A_iB_{i\text{-}1}$ and A_iB_{i+1} do not reach their maxima in concentration at this intersection point, though they tend to do so as the value of i increases. This supports the conclusion drawn by Calvert, Nichol and

Sawyer (1979) that the overall extent of crosslinking in systems where acceptors are bridged by a single ligand molecule arises concurrently with the intersection of the binding curves.

3.2.2 Association of Acceptor-Ligand Complexes

It is timely to note that convex Scatchard plots do not always arise when linear-chain formation is initiated by ligand binding to acceptor. This statement may be elaborated by the consideration of a system involving a bivalent acceptor and a univalent ligand where the stoichiometry of the complexes A_iB_j, is defined by $i = 1,2,3,...,\infty$ and $j = (2i\text{-}2)$, $(2i\text{-}1)$ and $2i$. The stoichiometric complexes are as follows:

$$\begin{array}{llll} i=1; & A, & AB, & AB_2 \\ i=2; & A_2B_2, & A_2B_3, & A_2B_4 \\ i=3; & A_3B_4, & A_3B_5, & A_3B_6 \\ \cdot & \cdot & \cdot & \cdot \\ \cdot & \cdot & \cdot & \cdot \\ \cdot & \cdot & \cdot & \cdot \\ \infty & \infty & \infty & \infty. \end{array} \qquad (3.17)$$

The formation of A_2B_2 may be visualized as involving an interaction between domains on either the acceptor or the ligand molecule in an AB complex made possible by a charge neutralization effect or a conformational change inherent only in the formation of the AB complex. In these terms self-interaction of neither A nor B is possible, but dimerization of AB may occur. The first column of complexes in equation (3.17) specifies the core complexes by such association, those in the two remaining columns delineating complexes arising from progressive saturation of a core complex with ligand.

The thermodynamic description of the system requires the introduction of two site-binding constants, k_1 governing the acceptor-ligand interactions and k_2 describing linear chain growth in the formation of the core complexes. It may be shown by induction that molar concentrations of the stoichiometric complexes, given by equation (3.17), may be written as:

$$m_{A_iB_{2i-2}} = k_2^{(i-1)} m_A^i (k_1 m_B)^{2i-2} \tag{3.18a}$$

$$m_{A_iB_{2i-1}} = 2k_2^{(i-1)} m_A^i (k_1 m_B)^{2i-1} \tag{3.18b}$$

$$m_{A_iB_{2i}} = k_2^{(i-1)} m_A^i (k_1 m_B)^{2i}. \tag{3.18c}$$

The total molar concentration of acceptor, $\bar{m}_A$, is given by:

$$\bar{m}_A = \sum_{i=1}^{i=\infty} i\{m_{A_iB_{2i-2}} + m_{A_iB_{2i-1}} + m_{A_iB_{2i}}\} \tag{3.19}$$

which becomes, with the use of equation (3.18):

$$\bar{m}_A = \frac{m_A(1+k_1 m_B)^2}{[1-k_2 m_A (k_1 m_B)^2]^2}\,; \quad k_2 m_A (k_1 m_B)^2 < 1. \tag{3.20}$$

The corresponding summations to find the concentration of bound ligand $\bar{m}_B - m_B$, are more complicated in that they involve series of the types $1 + 3x + 5x^2 + 7x^3 + \ldots + \infty$ and $1 + 2x + 3x^2 + \ldots + \infty$, where $x = k_2 m_A (k_1 m_B)^2$, but a closed solution is possible and is given by:

$$\bar{m}_B - m_B = \frac{2k_1 m_A m_B[1+k_1 m_B+k_2 m_A (k_1 m_B)^2]+2k_2 m_A^2 (k_1 m_B)^2}{[1-k_2 m_A (k_1 m_B)^2]^2}. \tag{3.21}$$

Combination of equation (3.20) and (3.21) yields:

$$r = 2k_1 m_B/(1 + k_1 m_B) + \psi \tag{3.22a}$$

$$\psi = 2k_2 m_A (k_1 m_B)^2/(1 + k_1 m_B). \tag{3.22b}$$

It is noted that the limiting value of r is 2 as $m \to \infty$ since in this limit $m_A \to 0$. In contrast to the previous case, however, all complexes in the fourth column of equation (3.17) have the stoichiometry $j/i = 2$. This implies that as concentration of the ligand increases the single complex AB_2 does not predominate alone but rather all saturated complexes, including those comprising long chains, are favoured. This basic difference in compositional behaviour of the solution is reflected in the binding curves which, for

different concentrations of acceptor must lie above the reference rectangular hyperbola since $\psi > 0$ for all values of m_B. In particular, no intersection of the binding curves is possible.

The forms of the binding curves, for this case, are best explored in terms of the Scatchard plot. The relevant equation was formed from equation (3.22), with m_A being substituted by its solution in terms of $\bar{m}_A$ obtained by expressing equation (3.20) as a quadratic, and is given by:

$$\frac{r}{m_B} = \frac{1+k_1m_B+2k_2\bar{m}_A(k_1m_B)^2-\sqrt{(1+k_1m_B)^2+4k_2\bar{m}_A(k_1m_B)^2}}{k_2\bar{m}_A(k_1m_B)^2m_B}. \qquad (3.23)$$

It has been shown by differentiating equation (3.23) with respect to m_B that $d(r/m_B)/dm_B$ [and hence $d(r/m_B)/dr$] equals zero when:

$$k_2\bar{m}_A(1 + 4k_2\bar{m}_A)(k_1m_B)^2 + 2k_1m_B(5k_2\bar{m}_A + 1) - 3(k_2\bar{m}_A - 1) = 0. \qquad (3.24)$$

By Descartes' rule of sign, one positive root (a value for k_1m_B) exists provided $3(k_2\bar{m}_A - 1) > 0$. Thus, provided $k_2\bar{m}_A > 1$, the Scatchard plot will exhibit a turning point (in fact a maximum). When $k_2\bar{m}_A < 1$, the Scatchard plot remains concave to the r-axis but does not exhibit a maximum, a situation determined by Baghurst, Nichol and Winzor (1978) to be outside the domain of sigmoidality of the binding curves. Figure 3.2a presents numerical examples of binding curves calculated using equation (3.23) for a range of values of the dimensionless parameter $k_2\bar{m}_A$ with Figure 3.2b showing the corresponding Scatchard plots, both for the domain $k_2\bar{m}_A > 1$ and $k_2\bar{m}_A < 1$. The marked contrast between the concave plots shown in Figure 3.2b and the convex plots in Figure 3.1b leaves little doubt that an experimenter may distinguish between the two cases of ligand-initiated association. An example is provided by the binding of Ca(II) to fragment I, the NH_2-terminal, 156 residues, of bovine prothrombin which bears a high net negative charge. It has been shown by sedimentation velocity studies that Ca(II) initiates the association of fragment I, the weight-fraction of dimer progressively increasing with Ca(II) concentration (Prendergast and Mann, 1977; Jackson *et al.*,

Figure 3.2: The binding characteristics of a system in which the association of a bivalent acceptor, A, governed by the site binding constant, k_2, is initiated by the binding of a non-associating univalent ligand, B, to the acceptor, described by the site binding constant, k_1. The stoichiometry of the complexes A_iB_j, formed is given in equation (3.17), where it is noted that all complexes in the last column are defined by $j/i = 2$, thereby excluding the possibility that acceptor-ligand links will be effectively broken by increasing the ligand concentration.

(a) Binding curves calculated using equation (3.23) with $k_2\bar{m}_A = 10$ (— - —), 1.0 (— —), 0.5 (- - - -). The solid reference curve was calculated employing the first term in equation (3.22a).

(b) Plots in Scatchard format corresponding to the binding curves shown in (a). In contrast to Figure 3.1b the plots are concave to the r-axis with no point of intersection.

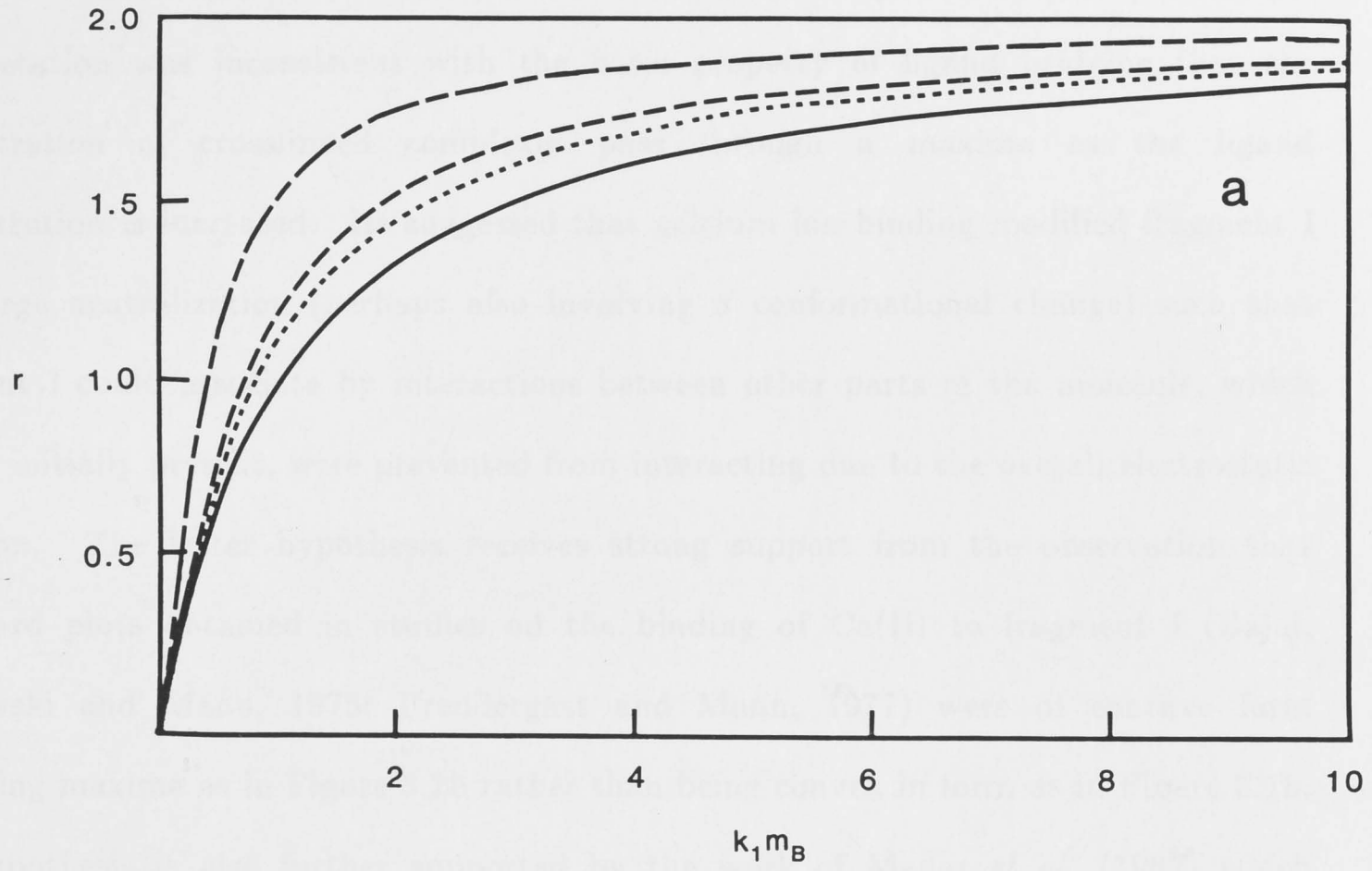
2.0
1.5
1.0
0.5
r
a
2
4
6
8
10
$k_1 m_B$

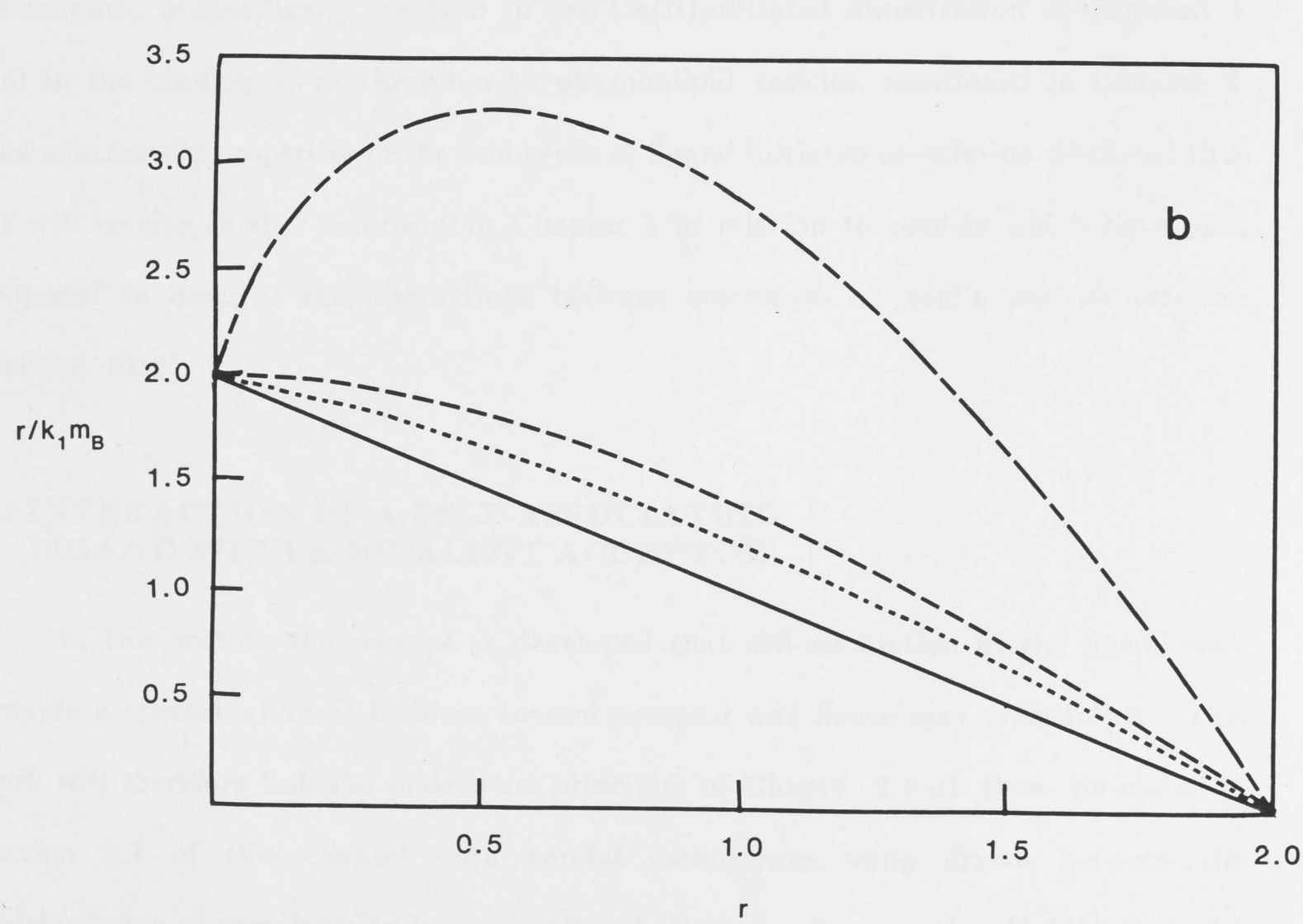
3.5
3.0
2.5
2.0
1.5
1.0
0.5
$r/k_1 m_B$
b
0.5
1.0
1.5
2.0
r

1979). One interpretation given to these results was that the calcium ions formed a bridge between fragment I molecules, but it was noted by Nichol (1980) that this interpretation was inconsistent with the basic property of ligand bridging that the concentration of crosslinked complexes pass through a maxima as the ligand concentration is increased. He suggested that calcium ion binding modified fragment I by charge neutralization (perhaps also involving a conformational change) such that fragment I could associate by interactions between other parts of the molecule, which though initially present, were prevented from interacting due to the overall electrostatic repulsion. The latter hypothesis receives strong support from the observation that Scatchard plots obtained in studies on the binding of Ca(II) to fragment I (Bajaj, Butkowski and Mann, 1975; Prendergast and Mann, 1977) were of concave form exhibiting maxima as in Figure 3.2b rather than being convex in form as in Figure 3.1b. The hypothesis is also further supported by the work of Madar *et al.* (1982) which suggests that a hydrophobic region of prothrombin, containing at least the NH_2-terminal 39-residues, is specifically involved in the Ca(II)-initiated dimerization of fragment I, and in the binding of prothrombin to phospholipid vesicles, mentioned in Chapter 2. The contrasting properties of the two types of ligand-initiated association discussed thus far will receive further comment in Chapter 5 in relation to models which have been proposed to describe the interactions between complexes of insulin and its receptor (Jeffrey, 1982).

3.3 INTERACTION OF A SELF-ASSOCIATING LIGAND WITH A BIVALENT ACCEPTOR

In this section the concept is developed that self-association of the ligand may provide a species which is bivalent toward acceptor and hence may crosslink it. This work will therefore link the underlying principles of Chapter 2 with those presented in Section 2.1 of this chapter with careful comparison being drawn between the stoichiometry of complexes to be proposed and those given in equation (3.17). Consider a ligand which undergoes the dimerization reaction $2B \rightleftharpoons B_2$, governed by an

association constant K_2. The monomeric ligand, B, is univalent toward the bivalent acceptor, A, interactions between them being governed by the site-binding constant, k_1. The ligand dimer, B_2, is bivalent with all interactions between it and the bivalent acceptor governed by the single site binding constant, k_2. The stoichiometric complexes, A_iB_j, which form may be written in the following array:

$$\begin{array}{llllll}
i=1; & A, & AB, & AB_2, & AB_3, & AB_4 \\
i=2; & A_2B_2, & A_2B_3, & A_2B_4, & A_2B_5, & A_2B_6 \\
i=3; & A_3B_4, & A_3B_5, & A_3B_6, & A_3B_7, & A_3B_8 \\
. & . & . & . & . & . \\
. & . & . & . & . & . \\
. & . & . & . & . & . \\
\infty & \infty & \infty & \infty & \infty & \infty
\end{array} \tag{3.25}$$

from which it is apparent that $i = 1,2,3,...,\infty$ and for each i, $j = (2i\text{-}2)$, $(2i\text{-}1)$, $2i$, $(2i+1)$, $(2i+2)$. The first column of complexes in equation (3.25) are the crosslinked core complexes identical in stoichiometry to those proposed in equation (3.17): in the present context they are viewed as linear chains of alternating acceptor and dimeric ligand molecules and indeed it is possible to view the core complexes in equation (3.17) in the same way even though in the latter case the linkage between ligand molecules would arise only after the ligand had bound to acceptor. Of course, the expression for the equilibrium concentrations of the stoichiometric complexes is independent of the pathway by which they are formed and thus consistent with equation (3.18a) we may write:

$$m_{A_iB_{2i\text{-}2}} = K_2^{(i-1)} m_A^i (2k_2 m_B)^{2i-2}. \tag{3.26a}$$

The remaining complexes in the array given in equation (3.25) arise from the progressive saturation of the available sites on the core complexes by, B, B_2 and a combination of both. For example the stoichiometric complex AB_2 is comprised of BAB, B_2A and AB_2 and the A_2B_4 complex has as constituents BAB_2AB, B_2AB_2A and AB_2AB_2. By induction the molar concentration of these complexes may be written as:

$$m_{A_iB_{2i\text{-}1}} = 2k_1 m_B K_2^{(i-1)} m_A^i (2k_2 m_B)^{2i-2} \tag{3.26b}$$

$$m_{A_iB_{2i}} = (k_1^2 + 4K_2k_2) m_B^2 K_2^{(i-1)} m_A^i (2k_2 m_B)^{2i-2} \tag{3.26c}$$

$$m_{A_iB_{2i+1}} = 4k_1k_2K_2m_B^3K_2^{(i-1)}m_A^i(2k_2m_B)^{2i-2} \tag{3.26d}$$

$$m_{A_iB_{2i+2}} = 4k_2^2K_2^2m_B^4K_2^{(i-1)}m_A^i(2k_2m_B)^{2i-2}. \tag{3.26e}$$

It follows from equation (3.26) that:

$$\bar{m}_A = m_A(1 + k_1m_B + 2k_2K_2m_B^2)^2 \sum_{i=1}^{i=\infty} i(4k_2^2\, m_AK_2m_B^2)^{i-1} \tag{3.27}$$

and thus:

$$\bar{m}_A = m_A(1 + k_1m_B + 2k_2K_2m_B^2)^2/(1 - 4k_2^2m_AK_2m_B^2)^2;$$

$$4k_2^2\, m_AK_2m_B^2 < 1. \tag{3.28}$$

The total base molar concentration of ligand bound is given by:

$$\bar{m}_B - m_B - 2K_2m_B^2 = \sum_{i=1}^{i=\infty} \{(2i-2)m_{A_iB_{2i-2}} + (2i-1)m_{A_iB_{2i-1}}$$

$$+ 2im_{A_iB_{2i}} + (2i+1)m_{A_iB_{2i+1}}$$

$$+ (2i+2)m_{A_iB_{2i+2}}\} \tag{3.29a}$$

which on substitution of equation (3.26) and collection yields:

$$\bar{m}_B - m_B - 2K_2m_B^2 = 2m_A(1+k_1m_B+2k_2K_2m_B^2)\left[\frac{2k_2K_2m_B^2 - 1}{1 - 4k_2^2m_AK_2m_B^2}\right.$$

$$\left. + \frac{1 + k_1m_B+2k_2K_2m_B^2}{(1 - 4k_2^2m_AK_2m_B^2)^2}\right]. \tag{3.29b}$$

Division of equation (3.29b) by equation (3.28) gives on re-arrangement:

$$r = 2(k_1m_B + 4k_2K_2m_B^2)/(1+k_1m_B + 2k_2K_2m_B^2) + \psi \tag{3.30a}$$

$$\psi = 8k_2^2K_2m_Am_B^2(1-2k_2K_2m_B^2)/(1 + k_1m_B + 2k_2K_2m_B^2). \tag{3.30b}$$

The first term of equation (3.30a) describes the competitive binding of monomeric and dimeric ligand to a bivalent acceptor excluding effects due to the crosslinking of the

acceptor. This reference equation is equation (2.2a) with $f = 2$, $n = 2$, $k_A = k_1$ and $l_A = 2k_2$. Scatchard plots calculated using this reference equation may take various forms which are illustrated in Figure 3.3.

It may be readily shown, by differentiation, that no maximum arises in the Scatchard plot of the reference curve when $2k_2 \leqslant k_1$ or when $2k_2 > k_1$ and $k_1 \geqslant \sqrt{K_2^2 + 4k_2K_2} - K_2$. The solid curve and the broken curve (----) conform, respectively, to these conditions and illustrate a Scatchard plot which is convex to the r-axis and one which, while concave, lies outside the domain of sigmoidality of the corresponding binding curve. When $2k_2 > k_1$ and $k_1 < \sqrt{K_2^2 + 4k_2K_2} - K_2$ it has been shown, by the differentiation procedure, that a maximum must arise in the Scatchard plot as illustrated by the uppermost reference curve (— —) in Figure 3.3, which corresponds to a sigmoidal binding curve. It is now possible to compare these reference curves with Scatchard plots calculated on the basis of both terms in equation (3.30a) and thereby examine the behaviour introduced due to the crosslinking of the acceptor by the divalent dimeric ligand. It suffices to consider two extremes. In Figure 3.4a the effect of crosslinking on a convex reference Scatchard plot (——) is shown, the introduction of a maximum at relatively low values of r with the retention of convex form at higher values of r being clearly apparent, especially at higher concentrations of total acceptor. In Figure 3.4b the situation is examined where the reference curve exhibits a maximum corresponding to the conditions that $2k_2 > k_1$ and $k_1 < \sqrt{K_2^2 + 4k_2K_2} - K_2$. Crosslinking of the acceptor has the effect of accentuating the maximum apparent at relatively low values of r and of conveying convexity on the remaining part of the curve, evident in the region of larger values of r. The overall effect of crosslinking apparent in both Figures 3.4a and 3.4b is then to give a composite of the effects apparent in Figures 3.1b and 3.2b. In qualitative terms this may be understood by recalling that the complexes in equation (3.25) with $j = (2i\text{-}2)$, $(2i\text{-}1)$ and $2i$ are identical with those shown in equation (3.17) and are likely to predominate at low values of r where the Scatchard plots, emphasizing this type of stoichiometry, exhibit maxima. At larger values of r, the complexes in equations (3.25) with $j = (2i+1)$ and

Figure 3.3: The competitive binding to a bivalent acceptor, A, of a univalent ligand monomer, B (site-binding constant, k_1), and bivalent ligand dimer, B_2 (site-binding constant, k_2), in the situation where no crosslinking of acceptor molecules arises. K_2 denotes the association constant governing the dimerization of the ligand. All Scatchard plots were calculated on the basis of the first term of equation (3.30a) and with the following values of interaction parameters chosen to exemplify the domains, cited in parentheses, required for complete examination of possible binding responses: (——), $k_1 = 1\ M^{-1}$, $k_2 = 0.05\ M^{-1}$, $K_2 = 2\ M^{-1}$ $[2k_2 < k_1]$; (- - - - -), $k_1 = 1\ M^{-1}$, $k_2 = 0.6\ M^{-1}$, $K_2 = 2\ M^{-1}$ $[\sqrt{K_2^2 + 4k_2K_2} - K_2 \leq k_1 < 2k_2]$; (— —), $k_1 = 1\ M^{-1}$, $k_2 = 1\ M^{-1}$, $K_2 = 2\ M^{-1}$ $[2k_2 > k_1$ and $k_1 < \sqrt{K_2^2 + 4k_2K_2} - K_2]$.

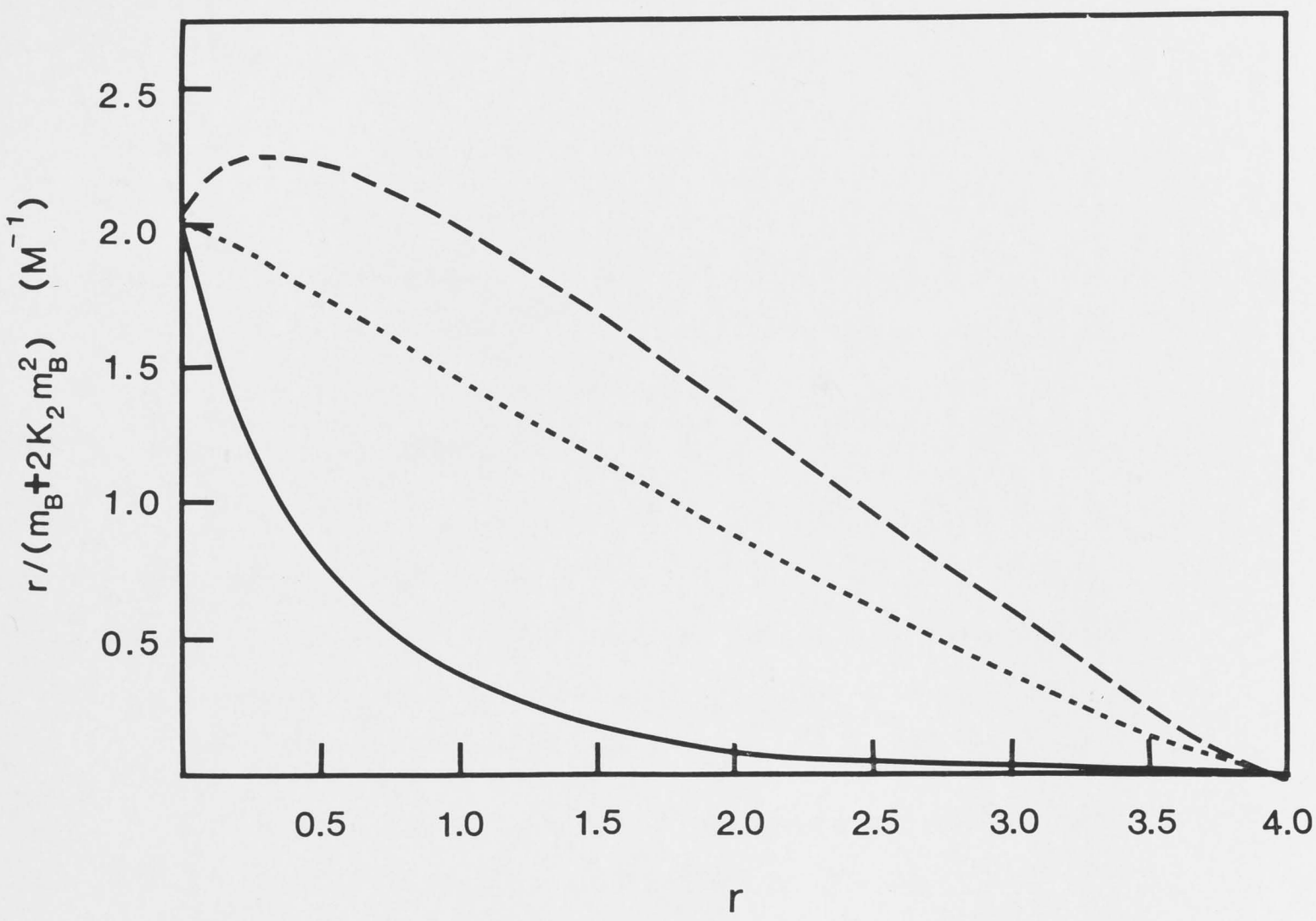
2.5
2.0
1.5
1.0
0.5
r/(m_B+2K_2m_B^2) (M^-1)
0.5
1.0
1.5
2.0
2.5
3.0
3.5
4.0
r

Figure 3.4: Scatchard plots for the system described in the caption to Figure 3.3 involving the competitive binding of the two states of a dimerizing ligand to a bivalent acceptor, but including the effects arising from crosslinking of the acceptor by the bivalent dimer to form complexes specified in equation (3.25).

(a) The solid curve is a reference curve reproduced from Figure 3.3 with $k_1 = 1\ M^{-1}$, $k_2 = 0.05\ M^{-1}$, $K_2 = 2\ M^{-1}$. Other curves were calculated employing the same parameters in the complete equation (3.30a) with the following values of the total acceptor concentration, $\bar{m}_A$, appropriate to the simultaneous equation (3.30b): (—-—), 1×10^3 M; (— —), 5×10^2 M; (-----) 2×10^2 M.

(b) Similar calculations employing the interaction parameters $k_1 = 1\ M^{-1}$, $k_2 = 1\ M^{-1}$, $K_2 = 2\ M^{-1}$ appropriate to the domain $2k_2 > k_1$ and $k_1 < \sqrt{K_2^2 + 4k_2K_2} - K_2$. The solid curve reproduces the uppermost curve in Figure 3.3, other curves being simulated with the following values of $\bar{m}_A$: (—-—), 10 M; (— —), 5 M; (-----), 2 M.

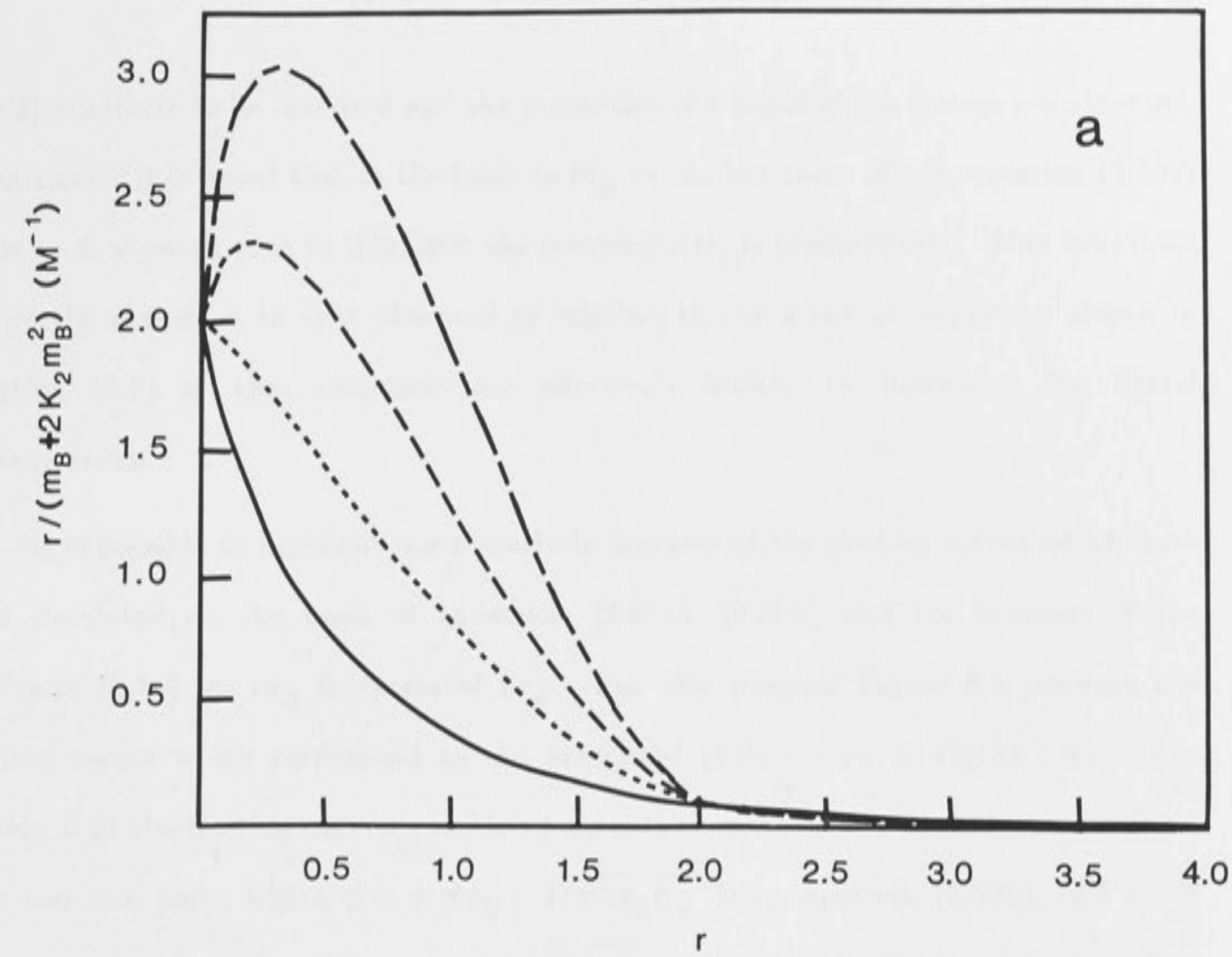
a
3.0
2.5
2.0
1.5
1.0
0.5
r/(m_B+2K_2m_B^2) (M^-1)
0.5
1.0
1.5
2.0
2.5
3.0
3.5
4.0
r

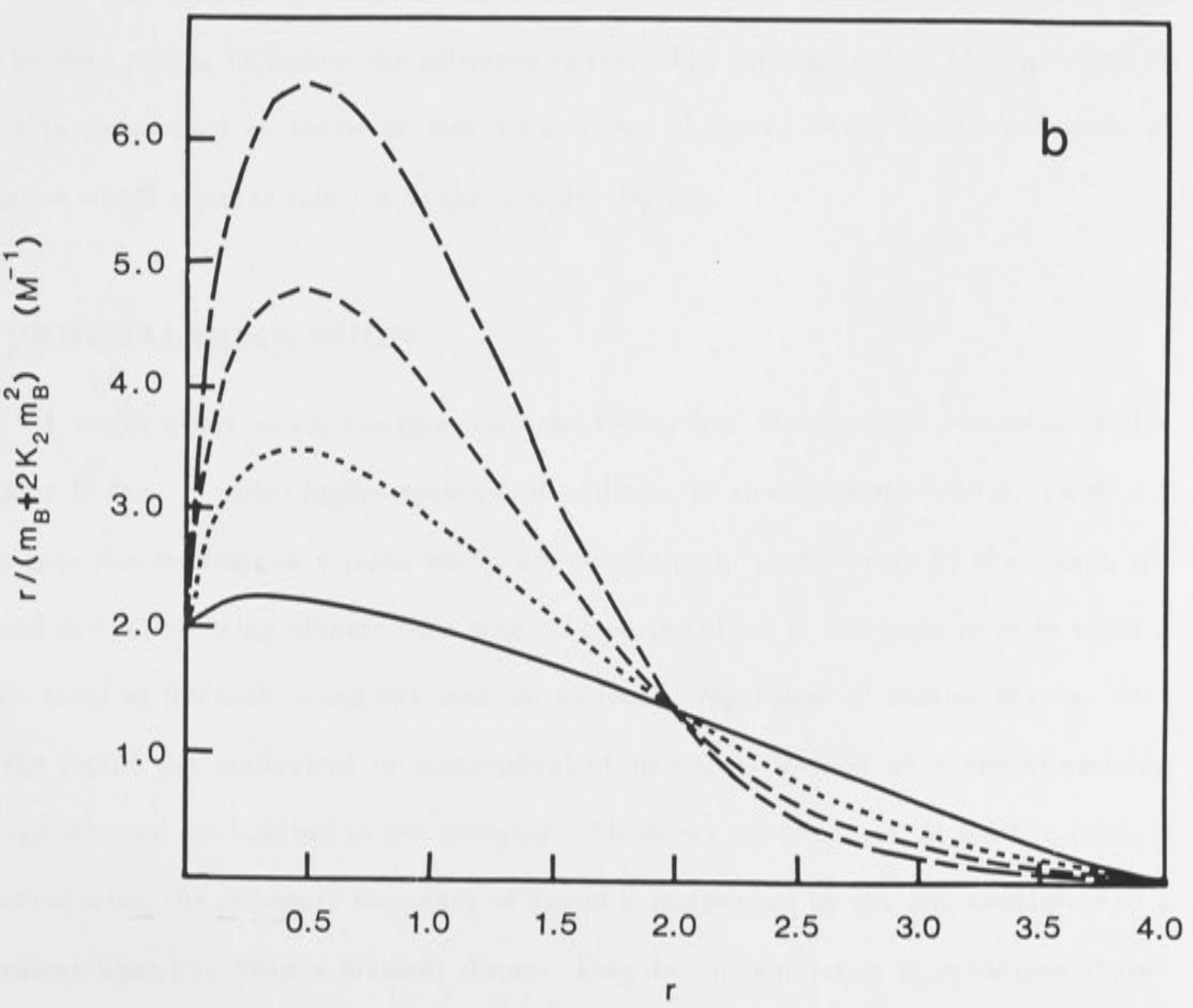
b
6.0
5.0
4.0
3.0
2.0
1.0
r/(m_B+2K_2m_B^2) (M^-1)
0.5
1.0
1.5
2.0
2.5
3.0
3.5
4.0
r

$(2i+2)$ are likely to be favoured and the properties of a crosslinking system are observed. In particular it is noted that in the limit as $m_B \rightarrow \infty$, the value of r in equation (3.30a) tends to 4, showing that in this limit the complex AB_4 is predominant. This behaviour is directly analogous to that observed in relation to the array of complexes shown in equation (3.2) in that crosslinks are effectively broken by increasing the ligand concentration.

It is possible to highlight more precisely features of the binding curves which have been simulated on the basis of equations (3.30a), (3.30b) and the solution of the quadratic (3.28) for m_A in terms of $\bar{m}_A$. For this purpose Figure 3.5 presents the binding curves which correspond to the Scatchard plots shown in Figure 3.4b. It is evident that the binding curves, exhibiting acceptor concentration dependence, intersect at a common point where $\psi = 0$, $m_B = 1/\sqrt{2k_2K_2}$ [from equation (3.30b)] and $r = 2$ [from equation (3.30a)]. When $m_B < 1/\sqrt{2k_2K_2}$ and, thus, $(1 - 2k_2K_2m_B^2) > 0$, values of ψ are necessarily positive for all values of m_B and the binding curve is seen to lie above the reference curve. Beyond the intersection point, ψ is necessarily negative and the binding curves lie below the reference curve. The limiting value, as $m_B \rightarrow \infty$, of $r = 4$ is understood in terms of four base moles of ligand being bound per mole of acceptor which arises in relation to the complex B_2AB_2.

3.4 GENERAL DISCUSSION

A major point which emerges from the theoretical development presented in this chapter is that acceptor-ligand systems in addition to those summarized in Table 2.1 may give rise to Scatchard plots which are wholly or in part convex to the r-axis, the second derivative being greater than zero. Thus, the effect is now seen to arise when a single bivalent molecule crosslinks acceptor molecules regardless of whether the two sites on the ligand are equivalent or non-equivalent or one is formed by a conformational change inherent on binding to the acceptor. Moreover convex form, at least in part, is observed when the necessary bivalency of ligand is introduced by the self-association of a univalent ligand to form a bivalent dimer. Despite this similarity of behaviour shared

Figure 3.5: The acceptor concentration-dependence of binding curves obtained with a system involving the crosslinking of bivalent acceptor by a bivalent dimeric ligand existing in equilibrium with monovalent monomeric ligand, which also binds to the acceptor. The numerical examples were derived from the data used to construct Figure 3.4b, where the values of the relevant interaction parameters have been cited.

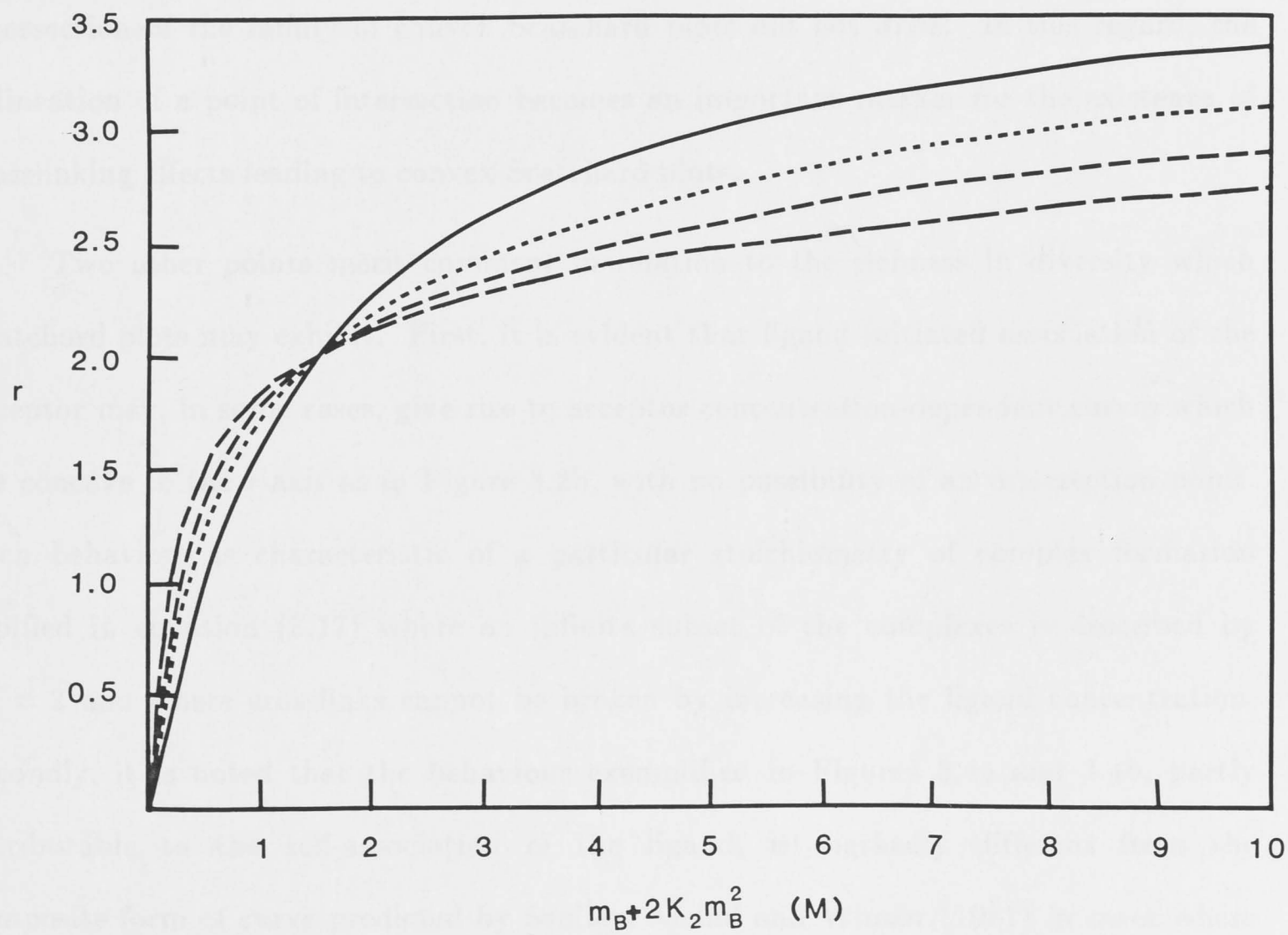
3.5
3.0
2.5
2.0
1.5
1.0
0.5
r
1
2
3
4
5
6
7
8
9
10
$m_B+2K_2m_B^2$ (M)

by crosslinking systems and those given in Table 2.1 there are marked distinguishing characteristics which may be useful to an experimenter concerned with the elucidation of the molecular basis of the binding response. Notable in this regard is the acceptor concentration-dependence exhibited by the crosslinking systems and illustrated in Figures 3.1a, 1b, 4a, 4b, 5. The only system in Table 2.1 which exhibited this type of behaviour was that involving the preferential binding of a non-associating ligand to the dimeric state of the acceptor (Tellam, Winzor and Nichol, 1978), and in that instance intersection of the family of convex Scatchard plots did not arise. In this regard, the delineation of a point of intersection becomes an important marker for the existence of crosslinking effects leading to convex Scatchard plots.

Two other points merit comment in relation to the richness in diversity which Scatchard plots may exhibit. First, it is evident that ligand initiated association of the acceptor may, in some cases, give rise to acceptor concentration-dependent curves which are concave to the r-axis as in Figure 3.2b, with no possibility of an intersection point. Such behaviour is characteristic of a particular stoichiometry of complex formation typified in equation (3.17) where an infinite subset of the complexes is described by $j/i = 2$ and where crosslinks cannot be broken by increasing the ligand concentration. Secondly, it is noted that the behaviour exemplified in Figures 3.4a and 3.4b, partly attributable to the self-association of the ligand, is markedly different from the composite form of curve predicted by Sculley, Nichol and Winzor (1981) in cases where the polymer of the ligand bound preferentially (but competitively with the monomer) to the acceptor. In the latter case, pertinent to the binding of chlorpromazine (a micellar system) to brain tubulin (Hinman and Cann, 1976), the Scatchard plot exhibited a minimum, at low values of r, followed by a maximum, behaviour which could not be confused with that exhibited by the crosslinking system on which Figures 3.4a and 3.4b are based. In this connection it is emphasized that Sculley, Nichol and Winzor (1981) while considering a self-associating ligand, as in the present work, did not contemplate the possibility that the polymeric ligand species might act as a crosslinking agent for the acceptor.

The potential utility of the theory developed is further extended by noting that all binding equations in this chapter, equations (3.11, 14, 22 and 30), have been deliberately written as the sum of two terms, the first being a reference term which describes ligand binding devoid of any effect attributable to ligand-initiated association of the acceptor. The purpose of this, in addition to permitting a ready discussion of the second term, ψ, was to render the formulation potentially more useful in relation to ligand membrane-receptor binding. Since the theory has been written in general thermodynamic terms, essentially in terms of equilibrium constants and hence changes in standard free energy, it applies equally to such systems, albeit that heterogeneous equilibria are involved. It is acknowledged, however, that association of membrane bound receptors initiated by ligand binding may well be a time-dependent event requiring diffusional motion of the receptor in the membrane matrix. With this in mind, and with reservations regarding the time scales and simplifications involved, it might not be unreasonable to suggest that the first term of the binding equations might reflect the equilibrium situation pertinent to an early stage of binding with receptors regarded as effectively immobile. The full binding equations would then reflect the equilibrium situation after sufficient time had elapsed to permit diffusion and linkage of the receptors.

It is believed that the contributions in Chapters 2 and 3 have extended binding theory relevant to situations where the ligand undergoes self-association. However, not all possibilities have been encompassed. Thus, in addition to "head-to-tail" association (Chapter 2) and "tail-to-tail" dimerization (Chapter 3), other ligand association patterns may well arise in practice. This point is elaborated further in the next chapter where it is shown that the indefinite self-association of zinc-free insulin leads to a situation where several of the polymeric species are potentially bivalent toward the acceptor.

CHAPTER 4

THE ASSOCIATION PATTERN OF ZINC-FREE INSULIN: A SEDIMENTATION EQUILIBRIUM STUDY

4.1 INTRODUCTION AND THEORY

In Chapter 2 it has been seen that a mathematical description of an indefinitely self-associating system governed by a single association constant may be formulated in closed form. Such mathematical descriptions are also used in the analysis of experimental results to delineate the type of association pattern appropriate to a system under investigation. Since it is a primary aim of this chapter to discuss in detail the association behaviour of insulin, it is timely to summarize the form of the mathematical expressions appropriate to this investigation. It will emerge that two basic types of formulation are useful. The first describes the composition of the solution of the associating single solute at any given total concentration in terms of the concentration of monomer and the equilibrium constant(s) governing the equilibria. The second expresses the weight-average molecular weight of the system in the same terms. The introductory section commences with a summary of relations which have been established by others; but later, as will be seen, new formulations are required to obtain the set required to interpret the sedimentation equilibrium results to be presented on insulin.

4.1.1 Mathematical Description of Different Types of Self-Association Patterns

The self-association of a monomer, P_1, may be represented by the general scheme:

$$\begin{aligned} P_1 + P_1 &\rightleftharpoons P_2 \\ P_{i-1} + P_1 &\rightleftharpoons P_i \\ P_{n-1} + P_1 &\rightleftharpoons P_n. \end{aligned} \tag{4.1}$$

If it is assumed that the system is thermodynamically ideal the association equilibrium constants governing the system are simply given by:

$$K_i = \frac{m_i}{m_{i-1} m_1} \tag{4.2}$$

where m_i is the molar concentration of species P_i and $K_1 = 1$ by definition. The concentration of species P_i is thus formulated in terms of the concentration of monomer, m_1, as:

$$m_i = \left\{ \prod_{l=1}^{l=i} K_l \right\} m_1^i. \tag{4.3}$$

The total weight concentration of protein $\bar{c}$ (g/litre) is then given by:

$$\bar{c} = \sum_i c_i = M_1 \sum_i i \left\{ \prod_{l=1}^{l=i} K_l \right\} m_1^i \tag{4.4}$$

where M_1 is the molecular weight of the monomer P_1.

4.1.1.1 **Definite associations**

Where the value of n in equation (4.1) is finite so that a limited series of polymers coexist in solution, the association is termed definite or discrete. For this type of system, it is always possible to utilize equation (4.4) directly to describe the relationship between total weight concentration and the molar concentration of monomer. An example is provided by the solution behaviour of the genetic variant β-lactoglobulin A at pH 4.65. Both Gilbert and Gilbert (1973) and Winzor, Tellam, and Nichol (1977) have analysed the reaction boundary observed in sedimentation velocity experiments with this system in terms of the equilibrium coexistence of monomer, dimer, trimer and tetramer: the termination of the association at tetramer ($n = 4$) is almost certainly due in this instance to the formation of a closed structure with tetrahedral symmetry. In these terms equation (4.4) is written in closed form as:

$$\bar{c} = M_1 m_1 (1 + 2K_2 m_1 + 3K_2 K_3 m_1^2 + 4K_2 K_3 K_4 m_1^3) \tag{4.5}$$

and it is noted for the β-lactoglobulin A system that the magnitudes of K_2, K_3 and K_4 differ. The corresponding expression for the weight-average molecular weight, $\overline{M}_w$, may be readily derived by combining equation (4.3) with the general definition of $\overline{M}_w$,

$$\overline{M}_w = \sum_{i=1}^{i=n} M_i c_i \Big/ \sum_{i=1}^{i=n} c_i \tag{4.6}$$

for the β-lactoglobulin system this is

$$\frac{\overline{M}_w}{M_1} = \frac{M_1 m_1 (1 + 4K_2 m_1 + 9K_2 K_3 m_1^2 + 16K_2 K_3 K_4 m_1^3)}{\bar{c}} \tag{4.7}$$

where $(\overline{M}_w/M_1)$ is termed the reduced weight-average molecular weight. It is immediately clear from these examples that any experimental method which provides information on the relationship between m_1 and $\bar{c}$ or on $(\overline{M}_w/M_1)$ and $\bar{c}$ may be used to test the possibility that a system is associating in the definite mode and to estimate the values of the appropriate equilibrium constants. It should be stressed at the outset that the latter endeavour is difficult within available experimental precision when several equilibrium constants of different magnitude govern the successive equilibria. A particular case of definite self-association frequently arises, however, in which the system closely approximates a two state system $nP_1 \rightleftharpoons P_n$ and when one equilibrium constant suffices to describe the system. When $n > 2$, the improbability of multiple-bodied collisions suggests that intermediates must coexist with monomer and the higher polymer; but there is no thermodynamic reason why the product of the equilibrium constants up to K_n may not be greater than any of the preceding products of constants. In that event, the system in experimental terms will closely approximate a two-state system for which expressions for $\bar{c}$ and for $(\overline{M}_w/M_1)$ may readily be written to aid the evaluation of K_n. This type of analysis is appropriate to several micellar systems as has been recently discussed (Nichol and Ogston, 1981; Nichol, Owen and Winzor, 1982).

4.1.1.2 Isodesmic indefinite self-associations

This type of system arises when n in equation (4.1) has no limit as may arise with a bivalent monomer undergoing an "head-to-tail" association in which essentially linear chain polymers are formed rather than a closed structure. Consideration of this type of

system was markedly simplified by Van Holde and Rossetti (1967) who considered a case where the standard free energy of addition of monomer to the polymer chain was identical at each step so that a single equilibrium constant, K_I, defined in terms of molar concentrations suffices to describe all successive equilibria. At first sight, this may seem an unrealistic assumption, but in fact it has been shown to be entirely reasonable in relation to several protein systems including lysozyme (Wills, Nichol and Siezen, 1980) and glutamate dehydrogenase (Nichol, Siezen and Winzor, 1978).

An indefinitely self-associating system governed by a single K_I is termed isodesmic for which equation (4.4) may be rewritten as:

$$\bar{c} = M_1 m_1 \sum_{i=1}^{i=\infty} i(K_I m_1)^{i-1}. \tag{4.8}$$

The summation in equation (4.8) is an open form, $1 + 2K_I m_1 + 3K_I^2 m_1^2 + \ldots + \infty$, but may be summed as a standard variation of a geometric progression, provided the common ratio $K_I m_1 < 1$. Thus:

$$\bar{c} = \frac{M_1 m_1}{(1 - K_I m_1)^2}, \tag{4.9}$$

similarly a closed solution for the reduced weight-average molecular weight is written as (Tang, Powell, Escott and Adams, 1977):

$$\frac{\overline{M}_w}{M_1} = \frac{1 + K_I m_1}{1 - K_I m_1}; \quad K_I m_1 < 1. \tag{4.10}$$

It is noteworthy that in this connection indefinitely self-associating systems have been considered in which the monomer is f-valent so that three-dimensional network formation arises in addition to linear chains (Nichol, Sculley, Jeffrey and Winzor, 1984). These workers showed that the relationship between the total base molar concentration $\bar{m}$, and the molar monomer concentration, m_1, was

$$m_1 = \bar{m} \{[(1 + 8k\bar{m})^{1/2} - 1]/4k\bar{m}\}^f \tag{4.11}$$

where k is the single site-binding constant governing all equilibria. Such an association cannot however be termed isodesmic except where $f = 2$, a situation where twice the site binding constant may be identified with the stoichiometric equilibrium constant K_I and equation (4.11) may be rearranged directly to give equation (4.9). When $f > 2$, an infinite series of stoichiometric equilibrium constants govern the equilibria each being related to k by a statistical factor formulated originally by Flory (1953).

4.1.1.3 Indefinite associations involving two equilibrium constants

A. Combination of definite and indefinite associations

It is perhaps not surprising that attempts have been made to combine the concepts of definite and indefinite associations in analysing experimental results which have been shown to conform to neither considered alone. A case in point is a particular interpretation of the association of zinc-free insulin which will be discussed in more detail later. It suffices here to note that it was proposed by one group of workers that a dimerization of the monomer occurred described by the definite association constant K_2 and that the dimer isodesmically self-associated, a second equilibrium constant K_I thereby being introduced into the formulation of the mathematical description of the system (Jeffrey, Milthorpe and Nichol, 1976).

The required formulation is not difficult in that it is again based on equation (4.4) and involves the summing of a geometric progression as in equation (4.8) the dimer being considered the basic associating protomer: necessarily a term for monomer is held apart from the summation of the infinite series and dimer concentration is written as $K_2 m_1^2$. The resulting expression arranged in simplest form is:

$$\bar{c} = \frac{M_1 m_1 [(1 - K_2 K_I m_1^2)^2 + 2K_2 m_1]}{(1 - K_2 K_I m_1^2)^2}. \qquad (4.12)$$

Jeffrey, Milthorpe and Nichol (1976) also utilized equation (4.6) to formulate the following expression for the weight-average molecular weight:

$$\frac{\overline{M}_w}{M_1} = \frac{M_1 m_1}{\bar{c}} + \frac{4M_1 K_2 m_1^2 (1 + K_2 K_I m_1^2)}{\bar{c}(1 - K_2 K_I m_1^2)^3}. \qquad (4.13)$$

Evidently other combinations of definite and indefinite associations may be envisaged (Tang *et al.*, 1977), but equations (4.12) and (4.13) suffice to illustrate the approach and to provide a basis for a later discussion on the association pattern of insulin. There remains one other variation on the theme which must be introduced before a full discussion of insulin is possible.

B. "Head-to-head" and "tail-to-tail" association

A bivalent molecule is considered which unlike lysozyme interacts by a combination of like domains rather than between unlike faces. In more formal terms, the monomer possesses two independent non-identical self-association sites, designated α and β, both capable of self-interaction. Two types of dimer are formed, one involving an α-α interaction, leaving two β-sites exposed and governed by an association constant k_α; the other involving β-β interaction, leaving two α-sites exposed and governed by an association constant k_β. Linear chain growth proceeds by successive addition of monomer so that all polymers, both odd- and even-numbered, coexist in equilibrium. Each of these polymers possesses alternating α-α and β-β bonds with even-numbered polymers having either two α-sites or two β-sites exposed and odd-numbered polymers having an α-site at one end and a β-site at the other. This distinction proved helpful in that Nichol *et al.* (1984) were able to show that:

$$c_i = iM_1(4k_\alpha k_\beta)^{(i-1)/2} m_1^i; \qquad i \text{ odd} \qquad (4.14a)$$

$$c_j = jM_1(k_\alpha + k_\beta)(4k_\alpha k_\beta)^{(j-2)/2} m_1^j; \qquad j \text{ even.} \qquad (4.14b)$$

Thus,

$$\bar{c} = M_1 m_1 \left[\sum_{i=1}^{i=\infty} i(4k_\alpha k_\beta)^{(i-1)/2} m_1^{i-1} + \sum_{j=2}^{j=\infty} j(k_\alpha + k_\beta)(4k_\alpha k_\beta)^{(j-2)/2} m_1^{j-1} \right] \tag{4.15}$$

which on summation yielded:

$$\bar{c} = M_1 m_1 \left[\frac{(1 + 2k_\alpha m_1)(1 + 2k_\beta m_1)}{(1 - 4k_\alpha k_\beta m_1^2)^2} \right]. \tag{4.16}$$

A useful correlation is noted by placing $k_\alpha = k_\beta$ whereupon equation (4.16) becomes equation (4.9), that describing an isodesmic self-association with $f = 2$ and twice the site binding constant being identified with K_I. It will become apparent, however, that the recent derivation of equation (4.16) finds greater use when $k_\alpha \neq k_\beta$. It is indeed a symmetrical and elegant mathematical description of the composition of a solution comprising an infinite array of species in solution of basically different types (odd- and even-numbered polymers). However, unlike all other patterns of associations thus far discussed, no expression is available from the literature for the weight-average molecular weight.

C. Derivation of $(\overline{M}_w/M_1)$ for a "head-to-head" and "tail-to-tail" self-association

Combination of equations (4.14a) and (4.14b) with equation (4.6) where $n = \infty$ yields:

$$\frac{\overline{M}_w}{M_1} = m_1 M_1 \left[\sum_{i=1}^{i=\infty} i^2 (4k_\alpha k_\beta)^{(i-1)/2} m_1^{(i-1)} + \sum_{j=2}^{j=\infty} j^2 (k_\alpha + k_\beta)(4k_\alpha k_\beta)^{(j-2)/2} m_1^{(j-1)} \right] \Big/ \bar{c}. \tag{4.17}$$

The first sum in the numerator may be expanded as, $1 + 9(4k_\alpha k_\beta)m_1^2 + 25(4k_\alpha k_\beta)^2 m_1^4 + 49(4k_\alpha k_\beta)^3 m_1^6 + \ldots + \infty$ which is in the general form of $1 + 3^2x + 5^2x^2 + 7^2x^3 + \ldots$

$+ \infty$ where $x = 4k_\alpha k_\beta m_1^2$. When $|x| < 1$ this series converges to (Dwight, 1961) $(1 + 6x + x^2)/(1 - x)^3$. Thus:

$$\sum_{i=1}^{i=\infty} i^2 (4k_\alpha k_\beta)^{(i-1)/2} m^{(i-1)} = \frac{1 + 24k_\alpha k_\beta m_1^2 + 16k_\alpha^2 k_\beta^2 m_1^4}{(1 - 4k_\alpha k_\beta m_1^2)^3}. \tag{4.18}$$

The second sum when expanded gives $4(k_\alpha + k_\beta)m_1[1 + 4x + 9x^2 + 16x^3 + \ ... + \infty]$; $x = 4k_\alpha k_\beta m_1^2$ which when $|x| < 1$ also may be written in closed form (Dwight, 1961), so that:

$$\sum_{j=2}^{j=\infty} j^2 (k_\alpha + k_\beta)(4k_\alpha k_\beta)^{(j-2)/2} m_1^{j-1} = \frac{4m_1(k_\alpha + k_\beta)[1 + 4k_\alpha k_\beta m_1^2]}{(1 - 4k_\alpha k_\beta m_1^2)^3}. \tag{4.19}$$

Substitution of equations (4.18) and (4.19) into equation (4.17) followed by substantial rearrangement leads to:

$$\frac{\overline{M}_w}{M_1} = \frac{P}{Q} \tag{4.20a}$$

where

$$P = 16k_\alpha^2 k_\beta^2 m_1^4 + 16k_\alpha k_\beta (k_\alpha + k_\beta) m_1^3 + 24k_\alpha k_\beta m_1^2 + 4(k_\alpha + k_\beta)m_1 + 1 \tag{4.20b}$$

$$Q = (1 - 4k_\alpha k_\beta m_1^2)(1 + 2k_\alpha m_1)(1 + 2k_\beta m_1). \tag{4.20c}$$

When $k_\alpha = k_\beta$, that is sites are equivalent, equation (4.20) reduces to the same form as equation (4.10) with $2k_\alpha = 2k_\beta = K_I$, as required. From the first derivative of equation (4.20) it can be shown that there are no critical points in the allowable range of $0 < 4k_\alpha k_\beta m_1^2 < 1$ and nor were any points of inflection evident from numerical examples. Thus it appears that the simultaneous set of equations (4.16) and (4.20) describe a smooth monotonically increasing dependence of $(\overline{M}_w/M_1)$ on $\bar{c}$, illustrations of which will be presented later.

4.1.2 A Review of Patterns Invoked to Describe the Self-Association of Zinc-Free Insulin in Solution

The pattern of self-association of zinc-free insulin (monomer molecular weight, ≈ 5750) has been extensively studied by a wide variety of techniques including nuclear magnetic resonance (Bradbury, Remesh and Dodson, 1981), circular dichroism (Goldman and Carpenter, 1974), sedimentation velocity (Fredericq, 1956), sedimentation equilibrium (Jeffrey, Milthorpe and Nichol, 1976) and light scattering (Steiner, 1952). Several basic models have been proposed to describe the self-association under various conditions. Jeffrey and Coates (1966) working at pH 2.0 proposed a definite association pattern consisting of monomer, dimer, tetramer and hexamer. The same pattern was later shown by Goldman and Carpenter (1974) to be consistent with results obtained at pH 8.0. Evidently there is difficulty in justifying this type of association in terms of equation (4.1) in that odd-numbered species have been excluded. On the other hand as we have noted in relation to two-state micellar systems it is not impossible for certain products of equilibrium constants to be small in relation to others so that just three equilibrium constants K_2, K_4 and K_6 would suffice to describe the system, and, indeed, the workers have reported values of these constants obtained by analysing weight-average molecular weight data in terms of the appropriate closed solution for this type of definite association. As the pH approaches 5.6, the isoelectric point of insulin (Tanford and Epstein, 1954), the extent of insulin association approaches a maximum. Solubility limitations, however, prohibit a comprehensive study at this pH. Accordingly, emphasis has been given recently to studies at pH 7.0, the "physiological pH", where the extent of association is quite pronounced and the protein is reasonably soluble to a limit of approximately 4 g/litre. Some workers have proposed that at pH 7.0, the association is definite like that proposed at pH 2.0 and 8.0 (Holladay, Ascoli and Puett, 1977; Wu 1974). This, however, does not account for the fact that at pH 7.0 species considerably larger than hexamer are present in solution at concentrations of insulin as low as 2 g/litre (Pekar and Frank, 1972). In an attempt to account for this observation, Pekar and Frank (1972) proposed a combined definite and indefinite association pattern in

which monomer and dimer were in equilibrium with hexamer which then isodesmically self-associated to give polymers of the hexamer species. This combination of definite and indefinite association patterns differs from that discussed earlier, in that the concentrations of all species intermediate between dimer and hexamer have been taken as negligible. The self-association pattern at pH 7.0 was also investigated by Jeffrey, Milthorpe and Nichol (1976). These workers tested a number of models including that of Pekar and Frank (1972) and an isodesmic indefinite self-association [equations (4.9) and (4.10)]. They showed that when non-ideality was taken into consideration the only model capable of fitting the data was one where monomer was in equilibrium with dimer which then acted as the basic protomer for a further isodesmic indefinite self-association. Equations (4.12) and (4.13) are explicitly relevant to the description of this system.

From this brief review of the self-association pattern of insulin several questions emerge. They are:

1. Does the fundamental nature of the association pattern change as the pH is varied or is a single pattern operative, despite the variation attributed to the system by different investigators?
2. Is it correct to confer special stability on the zinc-free hexamer species, as has been done in all work reported except that of Jeffrey, Milthorpe and Nichol (1976)?
3. Is the assumption, shared by all models thus far suggested, valid that the association proceeds in a manner in which certain polymers assume negligible equilibrium concentrations?

Some light may be shed on these questions by a brief outline of the known three-dimensional structure of insulin. As porcine insulin has been the most extensively studied in this regard, comment will be restricted to this insulin, though it should be noted that except for a few isolated examples the primary and secondary structure of mammalian insulins is highly conserved (Blundell *et al.*, 1972). The insulin monomer consists of two polypeptide clains, the A chain with 21 amino acid residues and the B chain with 30 residues (Ryle, Sanger, Smith and Kitai, 1955; Brown, Sanger and Kitai, 1955). Included in the primary structure of insulin are two interchain and one intrachain disulphide bridges which convey structural stability on the molecule (Ryle *et*

al., 1955). The tertiary structure has been elucidated to high resolution by several crystallographic studies, summarized by Blundell *et al.* (1972) and performed with crystals containing either two or four zinc ions per hexamer. Less detailed studies have been performed on insulins crystallized in the presence of other divalent transition metal cations. In the presence of zinc, insulin preferentially crystallizes as a cyclic hexamer as shown in Figure 4.1, this particular structure referring to the particular form in which two zinc ions are coordinated to histidine residues on the threefold axis of symmetry above and below the plane shown. In the present context, the noteworthy feature emerging from inspection of Figure 4.1 is that each monomer unit in the hexameric structure is linked to two others at different faces. In the nomenclature of Blundell *et al.* (1972) the two reactive domains, both capable of self-interaction, occur, one along the twofold axis OP and the other along the twofold axis OQ. These domains involve 20 and 24 residues respectively, those in the OP domain being predominantly hydrophobic with the notable exception of glutamic acid B13. In contrast the interactions between the OQ domains involve predominantly hydrogen bonding between the two tyrosines A14 and also between glutamic acid A17 and phenylalanine B1. There seems little doubt that the visualization of the cyclic hexameric structure in X-ray crystallography influenced the workers who chose conceptually to give it predominance as a stable species in solutions free of zinc. Jeffrey, Milthorpe and Nichol (1976) disagreed with this concept: they showed in a separate study (Milthorpe, Nichol and Jeffrey, 1977) that the addition of the stoichiometric quantity of zinc ions to zinc-free insulin resulted in a marked favouring of species with the molecular weight of hexamer, but insisted that in the absence of zinc ions the hexamer assumed no particular predominance as a species in the series of polymers formed by the isodesmic indefinite association of the dimer. It is entirely possible therefore that the hexameric structure in zinc-free solutions is not of the precise cyclic form observed in the crystal (Figure 4.1). Indeed in crystals grown in the absence of zinc, X-ray studies have indicated the formation of linear chains, main contacts still being made through the OP domain and involving residues of OQ domain along with residues A9 and A10 (Dodson, Dodson, Lewitova and Sabesan, 1978). It

Figure 4.1: The structure of the 2-zinc-insulin hexamer as determined by X-ray crystallography [reproduced from Figure 20 of Blundell *et al.* (1972)]. The uppermost diagram represents the complete hexamer viewed along the threefold symmetry axis and specifies the OP and OQ reaction domains referred to in the text. The second figure is the dimer unit, the basic asymmetric unit of the hexamer structure, where again the OP and OQ reaction domains are shown. These become more apparent in the lowest figure which shows two monomer units in juxtaposition to form one particular form of dimer.

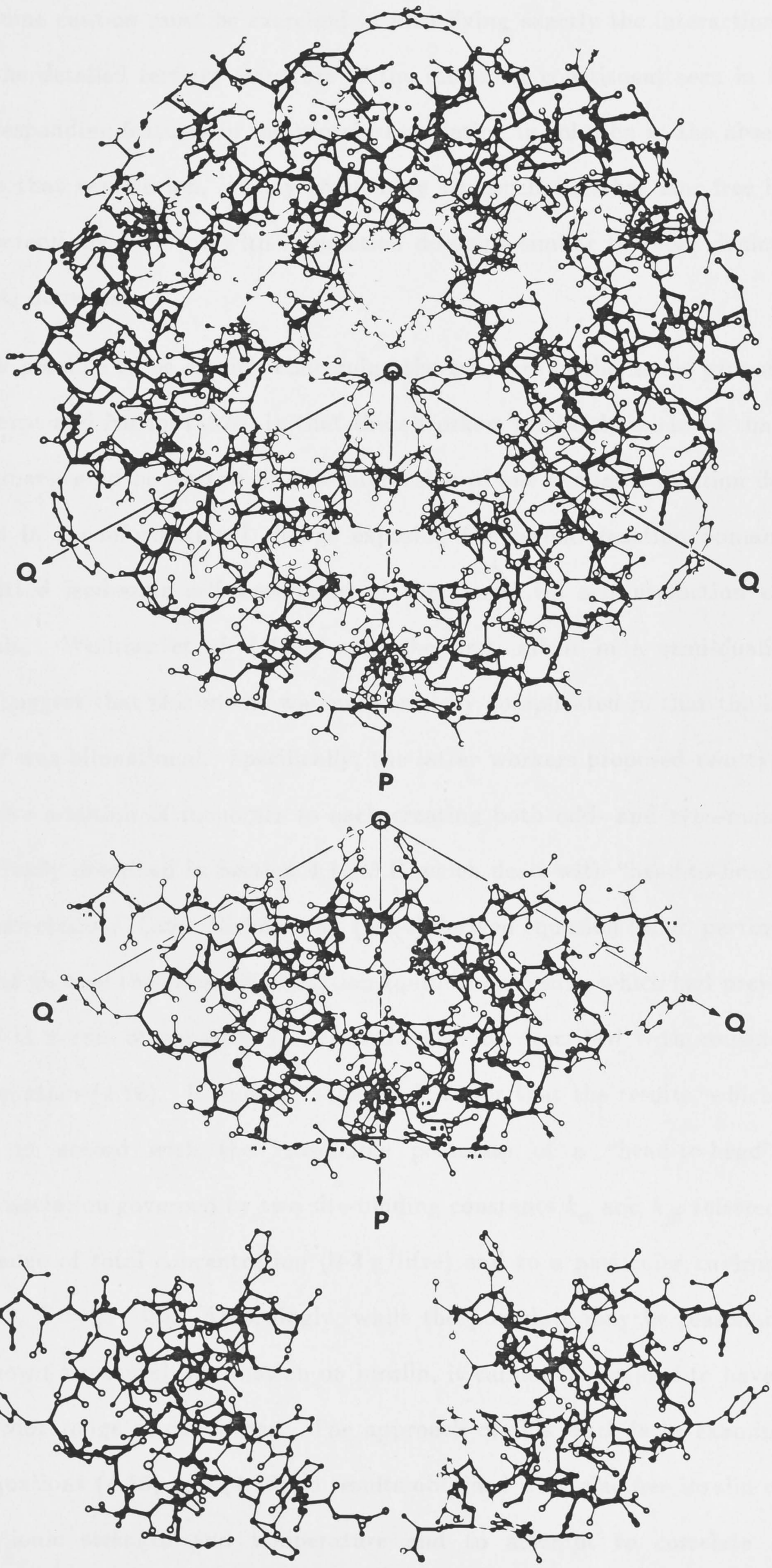
P
Q
Q
P
Q
Q
P

follows that some caution must be exercised in identifying exactly the interaction faces (and indeed the detailed tertiary structure of the monomer constituent seen in Figure 4.1) with corresponding features in the protein associating in solution in the absence of zinc. Despite that reservation, it may reasonably be concluded that zinc-free insulin monomer is potentially bivalent with interaction domains similar to those depicted as the OP and OQ domains.

It is now possible to be explicit concerning the criticism of the model proposed by Jeffrey, Milthorpe and Nichol (1976) in that these workers implicitly assumed that only one type of dimer would be formed by self-interaction of one available reaction domain which resulted in a conformational change exposing the second reaction domain and thereby permitted isodesmic self-association of the dimer via self-interaction of this exposed domain. Wollmer *et al.* (1980) were the first, albeit in a semi-qualitative treatment, to suggest that this model was unnecessarily complicated in that the insulin monomer itself was bifunctional. Specifically, the latter workers proposed two types of dimer, successive addition of monomer to each creating both odd- and even-numbered polymers as already described in Section 4.1.1.3.B which dealt with "head-to-head" and "tail-to-tail" association. Later Nichol *et al.* (1984) derived equation (4.16) pertinent to this concept and showed that the sedimentation equilibrium results which had previously been analysed in terms of equation (4.12) could also be described with considerable precision by equation (4.16). It must be stressed however that the results, which were shown to be in accord with the reasonable postulate of a "head-to-head" and "tail-to-tail" association governed by two site-binding constants k_α and k_β, referred only to a limited range of total concentration (0-3 g/litre) and to a particular environment (pH 7.0, I = 0.2, T = 25 °C). Accordingly, while the postulate may be reasonable on the basis of known structural information on insulin, it cannot be claimed to have been tested over a wide range of conditions. The approach of this work is to examine the relevance of equations (4.16) and (4.20) to results obtained with zinc-free insulin over a range of pH, ionic strength and temperature and to attempt to correlate albeit empirically observed variations in k_α and k_β with variation in the behaviour of the

constituent residues in the OP and OQ reaction domains. The method selected for this study was sedimentation equilibrium, because it is capable of yielding with considerable precision information on the dependence on total concentration of both $(\overline{M}_w/M_1)$ and on the concentration of the monomer m_1.

4.1.3 Sedimentation Equilibrium

4.1.3.1 Basic equations

In a sedimentation equilibrium experiment, a dialysed solution of protein in buffer is inserted into one sector of a double-sector cell and matched with equilibrium diffusate in the other sector. The cell is inserted into a rotor which is spun at constant angular velocity, ω (radians/second), and constant temperature, T (absolute), until the resulting distribution of total concentration, $\bar{c}$ (g/litre), *versus* radial distance from the axis of rotation, x, becomes invariant with time. The equilibrium distribution in this work was recorded photographically as a Rayleigh interferogram, which was measured according to the method of Richards, Teller and Schachman (1968), described in detail in Chapter 6. In the examination of solutions of a single solute containing a mixture of states of different molecular weight, it was assumed that the specific refractive increment of each state was identical with that of the monomer. This permits the distribution recorded in the equilibrium interferogram to be plotted as $\bar{c}$ *versus* x, the interpretation of which requires detailed comment.

Consider first a single solute species, i, which is not associating. At sedimentation equilibrium, the total potential is constant at each point in the cell: in other words, the variation with radial distance of the centrifugal potential, ψ_i, tending to cause sedimentation, is exactly balanced by the variation with radial distance of the chemical potential, μ_i, tending to cause back-diffusion. The mathematical statement of sedimentation equilbrium at constant temperature may therefore be written as (Fujita, 1962):

$$\frac{d\psi_i}{dx} - \frac{d\mu_i}{dx} = 0. \qquad (4.21)$$

The first term in equation (4.21) may be formulated as $M_i x\omega^2 dx$ where M_i is the molecular weight of the species i, and the second is obtained by partial differentiation of $\mu_i = \mu_i^0 + RT \ln a_i$ where μ_i^0 is the standard chemical potential per mole and a_i is the thermodynamic activity, of species i:

$$\frac{d\mu_i}{dx} = \left(\frac{\partial \mu_i}{\partial a_i}\right)_{T,P} \frac{\partial a_i}{\partial x} + \left(\frac{\partial \mu_i}{\partial P}\right)_{T,a_i} \frac{\partial P}{\partial x}. \tag{4.22}$$

The following standard transformations are now introduced together with the assumption that the solution is incompressible:

$$\left(\frac{\partial \mu_i}{\partial P}\right)_{T,a_i} = M_i \bar{v}_i; \qquad \frac{\partial P}{\partial x} = x\omega^2 \rho; \tag{4.23}$$

where $\bar{v}_i$ is the partial specific volume of species i and ρ is the density of the solution. Combination of equations (4.21), (4.22) and (4.23) yields, on noting $\partial a_i/\partial x = da_i/dx$:

$$\frac{d \ ln \ a_i(x)}{d(x^2)} = \frac{M_i \omega^2 (1 - \bar{v}_i \rho)}{2RT} \tag{4.24}$$

which may be integrated utilizing the reasonable assumption that the buoyancy term $(1 - \bar{v}_i \rho)$ is constant with respect to the radial distance, and hence to pressure variation, to give:

$$a_i(x) = a_i(x_F) \ exp\{\phi_i M_i (x^2 - x_F^2)\}; \tag{4.25a}$$

$$\phi_i = \frac{(1 - \bar{v}_i \rho)\omega^2}{2RT} \tag{4.25b}$$

where x and x_F are any two radial distances between the meniscus, x_m, and the base of the solution column x_b. The formulation of the basic sedimentation equilibrium equations (4.24) and (4.25) has assumed that species i is a non-electrolyte; but the same

formulation applies to a charged macromolecular species provided the solution has been dialysed and it is understood that the component i refers to the electroneutral component as defined by Casassa and Eisenberg (1964).

Consider now a single solute which self-associates to form an equilibrium mixture of states of different molecular weight. It has been shown (Nichol and Ogston, 1965) that equation (4.25) written for each state satisfies not only the conditions of sedimentation equilibrium, but also satisfies the condition that chemical equilibrium is maintained at each point in the cell. This may readily be illustrated by formulating the following ratio for a monomer-dimer system based on equation (4.25).

$$\frac{a_2(x)}{a_1^2(x)} = \frac{a_2(x_F)\ exp\{\phi_2 2M_1(x^2 - x_F^2)\}}{a_1^2(x_F)\ exp\{2\phi_1 M_1(x^2 - x_F^2)\}} \tag{4.26}$$

when $\phi_1 = \phi_2$, the situation which arises when the partial specific volumes of monomer and dimer are identical and there is no volume change on reaction. It is clear that the exponential terms in equation (4.26) cancel and that the dimerization constant K_2 is identical at each point in the cell, as required. Howlett, Jeffrey and Nichol (1970) have likewise shown that equation (4.26) is valid even when a volume change accompanies dimerization by predicting with it the correct dependence of the equilibrium constant on pressure, consequent on changing radial distance. It is noteworthy in this connection that pressure variation in sedimentation equilibrium experiments conducted with insulin is small and that there has been no suggestion that any marked volume change accompanies the self-association of insulin. The important point emerges that equation (4.25) and its differentiated form apply to the distribution of all insulin species subjected to sedimentation equilibrium.

4.1.3.2 **The omega analysis**

It has been shown (Milthorpe, Jeffrey and Nichol, 1975) that the experimentally obtained plot of $\bar{c}$ *versus* x may be analysed to yield the activity of monomer, a_1, as a function of the total weight concentration $\bar{c}$. This was achieved by defining a parameter Ω(x) operationally as:

$$\Omega(x) = \frac{\bar{c}(x)\ exp\{M_1\phi(x_F^2 - x^2)\}}{\bar{c}(x_F)} \tag{4.27}$$

where the point $[\bar{c}(x_F),\ x_F]$ is selected as a reference position within the experimental distribution. Evidently the use of equation (4.27) permits values of $\Omega(x)$ to be evaluated at corresponding values of $\bar{c}(x)$ across the entire distribution. A plot of $\Omega(x)$ *versus* $\bar{c}(x)$ is then constructed and extrapolated to infinite dilution to yield a value for Ω°. The significance of this extrapolated value may be seen by rewriting equation (4.27) utilizing equation (4.25), whereupon:

$$\Omega(x) = \frac{a_1(x_F)\bar{c}(x)}{\bar{c}(x_F)a_1(x)}. \tag{4.28}$$

As $\bar{c}(x) \rightarrow 0$, $a_1(x) \rightarrow c_1(x)$ since the activity coefficient tends to unity and in addition $\bar{c}(x) \rightarrow c_1(x)$ since dilution favours dissociation. Thus:

$$\lim_{\bar{c}\rightarrow 0} \Omega(x) = \Omega^\circ = \frac{a_1(x_F)}{\bar{c}(x_F)}. \tag{4.29}$$

The validity of this limit argument has been examined rigorously by Milthorpe, Jeffrey and Nichol (1975) in terms of L'Hopital's rule. Combination of equations (4.28) and (4.29) gives:

$$a_1(x) = \frac{\Omega^\circ \bar{c}(x)}{\Omega(x)}. \tag{4.30}$$

This procedure offers advantages in addition to avoiding differentiation of experimental results. First, it is possible to utilize different reference points within the distribution to obtain the same final result: conventionally the midpoint is used but other selections permit an averaging of results if required. Secondly, the method permits correlation of results obtained in different experiments which must necessarily be conducted if a reasonable range of total concentration is to be examined. Thus even in the plot of $\Omega(x)$ *versus* $\bar{c}(x)$ overlapping of results from different experiments may be ensured by

selecting a value of $\bar{c}(x)$ common to both experiments. In a similar vein a method has been devised for coordinating results from three or more experiments (Milthorpe, Jeffrey and Nichol, 1975). There is also considerable advantage in obtaining as the final result of an Ω-analysis the thermodynamic activity of the monomer as a function of total weight concentration rather than an apparent quantity which defines non-ideality effects in a less explicit way. Indeed for a single non-associating solute it is noteworthy that this analysis yields directly the concentration dependence of the activity coefficient, y_i, since $a_i = y_i c_i$ (Jeffrey, Nichol, Turner and Winzor, 1977).

4.1.3.3 **Associating systems examined at low total concentration**

It is reasonable to suggest that over a range of low $\bar{c}$ the system may be considered to a good approximation as being thermodynamically ideal (all $y_i \approx 1$). In this region therefore the Ω analysis yields directly corresponding values of m_1 and $\bar{c}$ appropriate for use in equations (4.5), (4.9), (4.11), (4.12) and (4.16). In short, results are obtained which are directly useful in relation to available theory to explore the nature of the association pattern and to obtain first estimates of relevant equilibrium constants.

It is now timely to comment on the use of equation (4.24) which may be rewritten assuming that all $y_i \approx 1$, and all $\phi_i = \phi$, as:

$$\frac{d\ ln\ c_i(x)}{d(x^2)} = \phi M_i. \tag{4.31}$$

It follows that :

$$\frac{dc_i}{d(x^2)} = \phi M_i c_i; \quad \frac{d\bar{c}}{d(x^2)} = \phi \sum_i M_i c_i \tag{4.32}$$

and from equation (4.6) that:

$$\frac{d\bar{c}}{\bar{c}d(x^2)} = \frac{d\ ln\ \bar{c}}{d(x^2)} = \phi \overline{M}_w. \tag{4.33}$$

Thus the slope of the tangent to a plot of *ln* $\bar{c}$ *versus* x^2 obtained from a sedimentation equilibrium experiment yields, with knowledge of ϕ, the weight-average molecular weight of the system at the corresponding value of $\bar{c}$. Such analysis is undeniably useful in both determining M_1 (if this is unknown) as the limit of $\overline{M}_w$ as $\bar{c} \rightarrow 0$ and also in obtaining the first insight into the limit of association, if this exists. It is also noted that ($\overline{M}_w$, $\bar{c}$) values may also be used to evaluate a function developed by Steiner (1952):

$$\eta_w = \frac{(M_1/\overline{M}_w) - 1}{\bar{c}}. \tag{4.34}$$

Steiner showed that integration of equation (4.34) from $\bar{c} = 0$ to any other $\bar{c}$ gives:

$$\int_0^{\bar{c}} \eta_w d\bar{c} = ln(c_1/\bar{c}). \tag{4.35}$$

Thus by differentiating experimental results to find $\overline{M}_w$ values and then by integrating η_w values as the area under the plot of η_w *versus* $\bar{c}$ extrapolated to infinite dilution, it is also possible to obtain the fundamentally useful relation between the concentration of monomer and the weight-average molecular weight and thus obtain the dependence of the concentration of monomer on the total concentration. It should be noted that Steiner developed his approach in relation to light scattering results, obtained with insulin solutions (Steiner, 1952), where only weight-average molecular weights were available. The advantages of sedimentation equilibrium now become clear in that it can yield the same quantity if desired; but it also gives results which may be analysed by the omega method to give the activity of monomer directly.

4.1.3.4 **Examination at high values of $\bar{c}$: non-ideality effects**

It is now established that examination of a particular system exclusively in the range of low total concentration may lead to misinterpretation in the association pattern which pertains (Kim, Deonier and Williams, 1977). This is not surprising as even an

indefinitely self-associating system at sufficiently low total concentration consists predominately of monomer and dimer. A case in point is the progressive interpretations which were given to the association of lysozyme. Originally it was viewed as a monomer-dimer system (Adams and Filmer, 1966), reinterpreted as a monomer-dimer-trimer system (Milthorpe, Jeffrey and Nichol, 1975) and finally, with extended concentration studies, recognized as an isodesmic indefinite self-associating system (Wills, Nichol and Siezen, 1980). The advisable course of action is thus to perform at least some experiments at reasonably high $\bar{c}$ and it is in this region with globular proteins that allowance must be made for thermodynamic non-ideality.

Weight-average molecular weights determined either by light scattering or by sedimentation equilibrium using equation (4.33) should be termed $(\overline{M}_w/M_1)_{\text{apparent}}$ and it is noted that Adams and coworkers in an extensive series of papers (e.g. Adams and Fujita, 1963; Adams *et al.*, 1969) have developed methods based on the Steiner approach to evaluate equilibrium constants and a non-ideality coefficient, B, defined by the empirical relation $ln\ y_i = iM_1B\bar{c}$. This is equivalent to invoking the "Adams-Fujita" approximation that ${y_1}^i/y_i = 1$ and renders equation (4.4) written for an ideal system consistent with its rigorous formulation:

$$\bar{c} = M_1 \sum_i i \left\{ \prod_{l=1}^{l=i} K_l \right\} \frac{a_1^i}{y_i}. \tag{4.36}$$

However the "Adams-Fujita" approximation has been questioned (Ogston and Winzor, 1975) and has been shown by numerical example to be increasingly difficult to justify as $\bar{c}$ increases (Nichol, 1981). In this work an approach is adopted which acknowledges that activity coefficients are dependent upon the composition of a solution rather than on total concentration of solute and assesses non-ideality coefficients by statistical mechanics in terms of excluded volumes (Wills, Nichol and Siezen, 1980). In studies conducted on insulin the value of $\bar{c}$, never going beyond 6 g/litre, only the first term of the expansion of the logarithm of the activity coefficient of each species need be considered:

$$ln\ y_i = \sum_j \alpha_{ij} m_j \tag{4.37}$$

where each of the subscripts i,j is allowed to span the set of monomeric and polymeric species independently. The set of constant coefficients α_{ij} may be calculated utilizing the expression (Wills, Nichol and Siezen, 1980):

$$\alpha_{ij} = \frac{4\pi N(r_i + r_j)^3}{3} + \frac{Z_i Z_j (1 + \kappa r_i + \kappa r_j)}{2I(1 + \kappa r_i)(1 + \kappa r_j)} - M_j \bar{v}_j \tag{4.38}$$

where the first term denotes the covolume contribution based on spherical geometry, r_i and r_j being radii of the impenetrable spheres; the second term gives the charge-charge interaction in terms of the net charges, Z_i and Z_j, borne by the spheres, the ionic strength, I, and the Debye inverse-screening length, κ; and the third term expresses the molar volume of species j. Once the values of α_{ij} have been tabulated results may be analysed in terms of equation (4.37) by an iterative procedure based on that originally proposed by Nichol and Winzor (1976b). In more detail, the known values of a_1 obtained by the Ω method are used to obtain estimates of other a_i from equilibrium constants deduced from analysis of results obtained at low $\bar{c}$. These values of a_i including a_1 are inserted into equation (4.37) as first estimates of m_i to obtain first estimates of all y_i. Division of the a_i by the first estimates of y_i gives improved values for m_i appropriate to equation (4.37). This procedure is repeated until the values of y_i converge. This procedure may be applied at each $\bar{c}$ for which a_1 values are available and does involve, for an indefinitely self-associating system, truncation of those polymers which are assessed to contribute negligibly to the $\bar{c}$ under consideration. In the final step it is possible to test the appropriateness of the equilibrium constants employed by summing the weight concentration of each species obtained as $c_i = iM_1 a_i / y_i$ to enquire whether the predicted total concentration in fact agrees with the experimental total concentration corresponding to the particular a_1 value under consideration. If it does not, it is possible to refine the values of the equilibrium constants, due allowance having been made for the composition-dependence of the activity coefficients.

4.2 SEDIMENTATION EQUILIBRIUM STUDIES ON INSULIN

4.2.1 Experimental

All experiments were conducted with bovine insulin obtained from Commonwealth Serum Laboratories and designated crystalline and "single peak". The following steps were employed in the purification of the sample. First, the protein was dissolved in and exhaustively dialysed against 0.01 M HCl to form the apo-protein free of bound zinc ions (Jeffrey, Milthorpe and Nichol, 1976). The last stages of the dialysis were performed against a solution of 0.01 M HCl and 0.1 M NaCl. The second step involved subjecting the dialysed solution to gel filtration on Sephadex G-50 to remove traces of proinsulin. The final step involved adjusting the pH of the solution to 8.1 in accordance with the method of Chance, Root and Galloway (1976) and subjecting the solution to ion exchange chromatography on a column of DEAE-Cellulose to remove any traces of mono-desamido insulin. The electrophoretic homogeneity of purified samples was routinely checked on polyacrylamide gels and samples were stored in the freeze-dried state at -20 °C. Full details of chromatographic steps are to be found in Chapter 6.

Table 4.1 summarizes the composition of buffers employed in the sedimentation equilibrium studies. Solutions of insulin were prepared by dissolving the freeze-dried zinc-free insulin powder either directly in the appropriate buffer or (for experiments conducted at pH 7.0) initially in 0.01 M HCl. Solutions, filtered through 0.22 μm Millipore filters, were adjusted to approximately the desired concentration, and dialysed (Selbys type 8 cellulose tubing) for 18-24 hours against buffer with several changes of dialysate. Concentrations of solutions were determined spectrophotometrically at 276 nm employing an extinction coefficient of $\epsilon^{1\%}_{1\,\mathrm{cm}} = 10.5$ (Frank and Veros, 1968). Dilutions where necessary were performed with dialysate. Initial loading concentrations, $\bar{c}_0$, for the sedimentation equilibrium experiments were checked refractometrically employing either a Brice-Phoenix Differential Refractometer or by performing a synthetic boundary experiment in the ultracentrifuge using Rayleigh interference optics.

Table 4.1: The composition of buffers employed in sedimentation equilibrium studies on zinc-free insulin

Buffer Composition	pH[a]	Ionic Strength, I	Density[b] (g/ml)
5.3 mM Glycine, 14.7 mM HCl, 85.3 mM NaCl	2.0	0.10	1.0015_7
20 mM Tris, 18 mM HCl,[c] 79 mM NaCl, 1 mM EDTA	7.0	0.10	1.0025_0
20 mM Tris, 18 mM HCl, 29 mM NaCl, 1 mM EDTA	7.0	0.05	0.9995_0
5.3 mM Glycine, 3.2 mM NaOH, 95 mM NaCl	10.0	0.10	1.0012_5

[a] All pH values were measured at the temperature of the sedimentation equilibrium experiments.

[b] Densities of buffers were measured with an Anton Paar DMA 02C precision density meter accurate to ± 0.00001 g/ml.

[c] In two sedimentation equilibrium experiments conducted at 37 °C rather than 25 °C the pH of the Tris-HCl buffer was adjusted to pH 7.0 at 37 °C by addition of NaOH. The resulting density of the buffer was 0.9977_0 g/ml.

The specific refractive index of insulin was taken to be 1.789×10^{-4}g/litre (Milthorpe, 1977) which in a 12 mm ultracentrifuge cell leads to the conversion that 3.93 Rayleigh interference fringes corresponds to 1.0 g/litre, one fringe being equivalent to a displacement of 287 μm. For simplicity and consistency all concentrations in this work are reported directly on the grams per litre scale.

Sedimentation equilibrium experiments were performed in a Spinco model-E Analytical Ultracentrifuge equipped with an electronic speed control and temperatures were measured to within 0.1 °C with the aid of the R.T.I.C. unit. Final sedimentation equilibrium distributions were recorded as interferograms which were measured using a Nikon model-6C microcomparator according to the method of Richards, Teller and Schachman (1968). Full details of the measuring procedure, which includes the

determination of the concentration at the meniscus, $\bar{c}(x_m)$, are given in Chapter 6. Table 4.2 summarizes the basic parameters pertinent to each of the twelve sedimentation equilibrium experiments performed, the detailed compositions of the buffers used being given in Table 4.1. In what follows, use will be made of the first column of Table 4.2 in designating the particular experiment under consideration.

Table 4.2: A summary of the experimental parameters applicable to sedimentation equilibrium experiments conducted with zinc-free insulin

Experiment Number	pH	I	T (°C)	$\bar{c}_o$ (g/litre)	ω (rad/s)	x_b-x_m (cm)	$\bar{c}(x_m)$[a] (g/litre)
1	2.0	0.10	25	0.710	4609	0.684	≈ 0
2	2.0	0.10	25	1.823	3143	0.275	0.500
3	7.0	0.10	25	0.759	5028	0.666	≈ 0
4	7.0	0.10	25	0.476	2724	0.284	0.102
5	7.0	0.10	25	0.905	2094	0.269	0.331
6	7.0	0.05	25	0.879	5029	0.655	≈ 0
7	7.0	0.05	25	1.080	2094	0.279	0.318
8	7.0	0.05	25	0.989	2094	0.274	0.310
9	7.0	0.10	37	1.071	4610	0.666	≈ 0
10	7.0	0.10	37	1.055	2095	0.275	0.410
11	10.0	0.10	25	0.662	5450	0.556	≈ 0
12	10.0	0.10	25	1.870	3145	0.270	0.670

[a] The statement $\bar{c}(x_m) \approx 0$ g/litre defines an experiment of the meniscus depletion design (Yphantis, 1964) in which ω is selected so that the concentration at the meniscus at sedimentation equilibrium corresponds to an undetectable fringe displacement ($< 10\ \mu$m).

4.2.2 Parameters Used in the Interpretation of the Sedimentation Equilibrium Experiments

The molecular weight of the monomer of bovine insulin was taken to be 5734 (Ryle *et al.*, 1955) with a partial specific volume of 0.73 ml/g (Frank and Veros, 1968). As in previous studies (Jeffrey, Milthorpe and Nichol, 1976) it was assumed that the same partial specific volume characterized all polymeric states of insulin, the implicit assumption being that no measurable volume change accompanies the self-association of the protein. In accounting for the thermodynamic non-ideality effects according to equation (4.38) it is necessary to have estimates of both the effective Stokes radius of each state of the protein and the net charge borne by it. With respect to the former quantities the following relations pertain (Jeffrey, Nichol, Turner and Winzor, 1977):

$$r_i^H = (3M_i^H \bar{v}_i^H / 4\pi N)^{1/3} \tag{4.39a}$$

$$M_i^H = M_i^U (1 + w) \tag{4.39b}$$

$$\bar{v}_i^H = (\bar{v}_i^U + w v_1)/(1 + w) \tag{4.39c}$$

where the superscript H denotes the hydrated particle, the superscript U the unhydrated particle, w is the degree of hydration (the number of grams of solvent per gram of dry solute) and v_1 is the partial specific volume of the solvent (approximately unity). Combination of equations (4.39b) and (4.39c) yields:

$$M_i^H \bar{v}_i^H = M_i^U (\bar{c}_i^U + w v_1) \approx M_i^U , \tag{4.40}$$

since w for globular proteins is in the range 0.2-0.3 g/g. It follows then, on the basis of spherical geometry, that a reasonable approximation of the effective Stokes radius of the hydrated polymeric states of insulin may be calculated simply from:

$$r_i^H = (3iM_1^U/4\pi N)^{1/3} \tag{4.41}$$

where $i = 1$ denotes the insulin monomer. The net charges borne by the monomer of insulin at the different pH values used in this work were taken from the titration results of Tanford and Epstein (1954). The values were as follows: +5 (pH 2.0); -2 (pH 7.0)

and -5.5 (pH 10.0). It was assumed that charge was conserved in each step of the self-association to form higher polymers. The values of κ, the Debye inverse screening length, appropriate to equation (4.38) were calculated from the relationship $\kappa \approx 3.3 \times 10^{-7} \sqrt{I}$ (Jeffrey, 1981). These parameters and relations permit the ready computation of the non-ideality coefficients α_{ij}, which are then used in the iterative procedure previously described to estimate the activity coefficients y_i of each polymeric state. As is apparent from equation (4.37), it is necessary in the calculation of y_i for an indefinitely self-associating system to truncate the system at a tractable and realistic value of i.

In the range of total concentration explored at pH 7.0 it was found by numerical calculation that truncation at $i = 30$ sufficed to account for over 98% of the total concentration. Since, as will be seen, the extent of association is greater at pH 7.0 than at either pH 2.0 or pH 10.0, the truncation value of $i = 30$ was consistently used in the analysis of all results.

4.3 RESULTS

4.3.1 Studies at pH 7.0

Discussion is first directed toward results obtained at neutral pH, a condition which has been utilized in several previous studies to explore the self-association pattern of zinc-free insulin [Section 4.1.2]. In this work the ionic strength was held fixed at 0.1 and the temperature at 25 °C to permit a correlation of results over a range of total concentration 0.01-3.3 g/litre, which was achieved in three experiments, 3, 4 and 5 of Table 4.2, by employing different loading concentrations and angular velocities. Figure 4.2 presents a plot of the apparent weight-average molecular weight *versus* the total concentration found using equation (4.33). Values of $[d\ ln\ \bar{c}/d(x^2)]$ were obtained by differentiation of a polynomial expression used to fit the $ln\ \bar{c}$ *versus* $(x)^2$ data. Two points emerge from an inspection of Figure 4.2. Firstly, in accordance with all previous findings, it is apparent that the apparent weight-average molecular weight increases with increasing concentration to the extent that species with molecular weights greater

Figure 4.2: The dependence of the apparent weight-average molecular weight, $(\overline{M}_w)_{\text{apparent}}$, on total weight concentration of zinc-free insulin at pH 7.0, I = 0.10, 25 °C. Experimental values were obtained by differentiating sedimentation equilibrium results according to equation (4.33) and refer to experimental numbers defined in Table 4.2 as follows: 3 (△): 4 (o): 5(◇). The solid curve was computed using equation (4.20) with $k_\alpha = 2.05 \times 10^4\ \text{M}^{-1}$ and $k_\beta = 1.63 \times 10^4\ \text{M}^{-1}$, values found after allowance had been made for thermodynamic non-ideality effects.

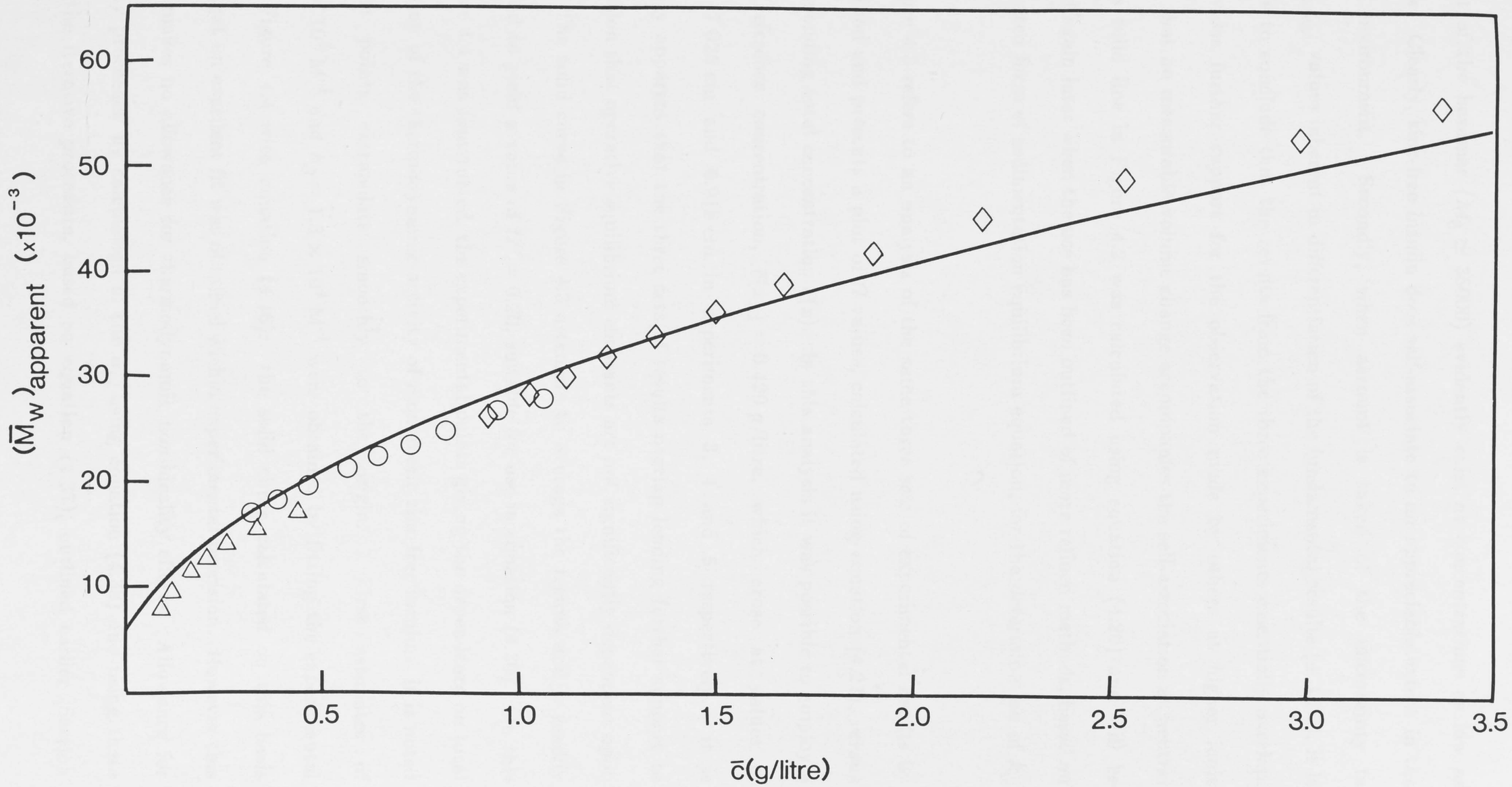
60
50
40
30
20
10
$(\bar{M}_w)_{apparent}$ $(x10^{-3})$
0.5
1.0
1.5
2.0
2.5
3.0
3.5
$\bar{c}$(g/litre)

than that of the hexamer ($M_6 \simeq 35000$) evidently exist at concentrations as low as 1.3 g/litre. Clearly, zinc-free insulin does self-associate to an appreciable extent in the specified environment. Secondly, when account is taken of the uncertainty in $(\overline{M}_w)_{\text{apparent}}$ values inherent in differentiation of the fundamental results ($\pm$ 10%), it is reasonable to conclude that the results from the three experiments essentially overlap. This provides further support for the observation made by others at higher ionic strengths that no measurable volume change accompanies the self-association at neutral pH. The solid line in Figure 4.2 was calculated using equation (4.20) and will be mentioned again later when the use has been outlined of more refined methods, based on the integrated form of sedimentation equilibrium equation, for the determination of k_α and k_β.

Figure 4.3 refers to an analysis of the same three sets of experimental results by the Ω-method and presents a plot of Ω values, calculated using equation (4.27), *versus* the corresponding total concentration $\bar{c}(x)$. In this analysis it was possible to employ a common reference concentration, $\bar{c}(x_F) = 0.420$ g/litre, which arose at values of 7.087 cm, 7.025 cm and 6.918 cm in experiments 3, 4 and 5 respectively. It is immediately apparent that the three sets of results overlap lending further support to the conclusion that operative equilibrium constants are not significantly dependent upon pressure. The solid curve in Figure 4.3 attempts to average the results and is readily extrapolated to yield a value of $\Omega^o = 0.20$, suitable for use in equation (4.30). On this basis Figure 4.4 was constructed, the experimental points giving the dependence on total concentration of the thermodynamic activity of monomeric zinc-free insulin. It is noted that these points extrapolate smoothly to the origin. First estimates of $k_\alpha = 2.5 \times 10^4$ M^{-1} and $k_\beta = 1.3 \times 10^4$ M^{-1} were obtained by fitting the experimental points in Figure 4.4 with equation (4.16): the solid curve calculated on this basis indicates that an excellent fit was obtained within experimental precision. However this procedure makes no allowance for thermodynamic non-ideality effects. Allowance for non-ideality proceeded by calculation of the α_{ij} using equation (4.38) and using these values in the iterative procedure, based on equation (4.37), outlined earlier [Section

Figure 4.3: An illustrative plot of the Ω-method used to analyse all sedimentation equilibrium results obtained with zinc-free insulin. This particular set of experimental points relates to experiments 3 (•), 4 (■), and 5 (▲) of Table 4.2. The ordinate values were obtained using equation (4.27) utilizing the common reference concentration reported in the text, while the abscissa values refer to the corresponding total concentrations for which Ω-values were determined. The solid curve attempts to average the data and the extrapolation to give $\Omega^\circ = 0.20$ is shown.

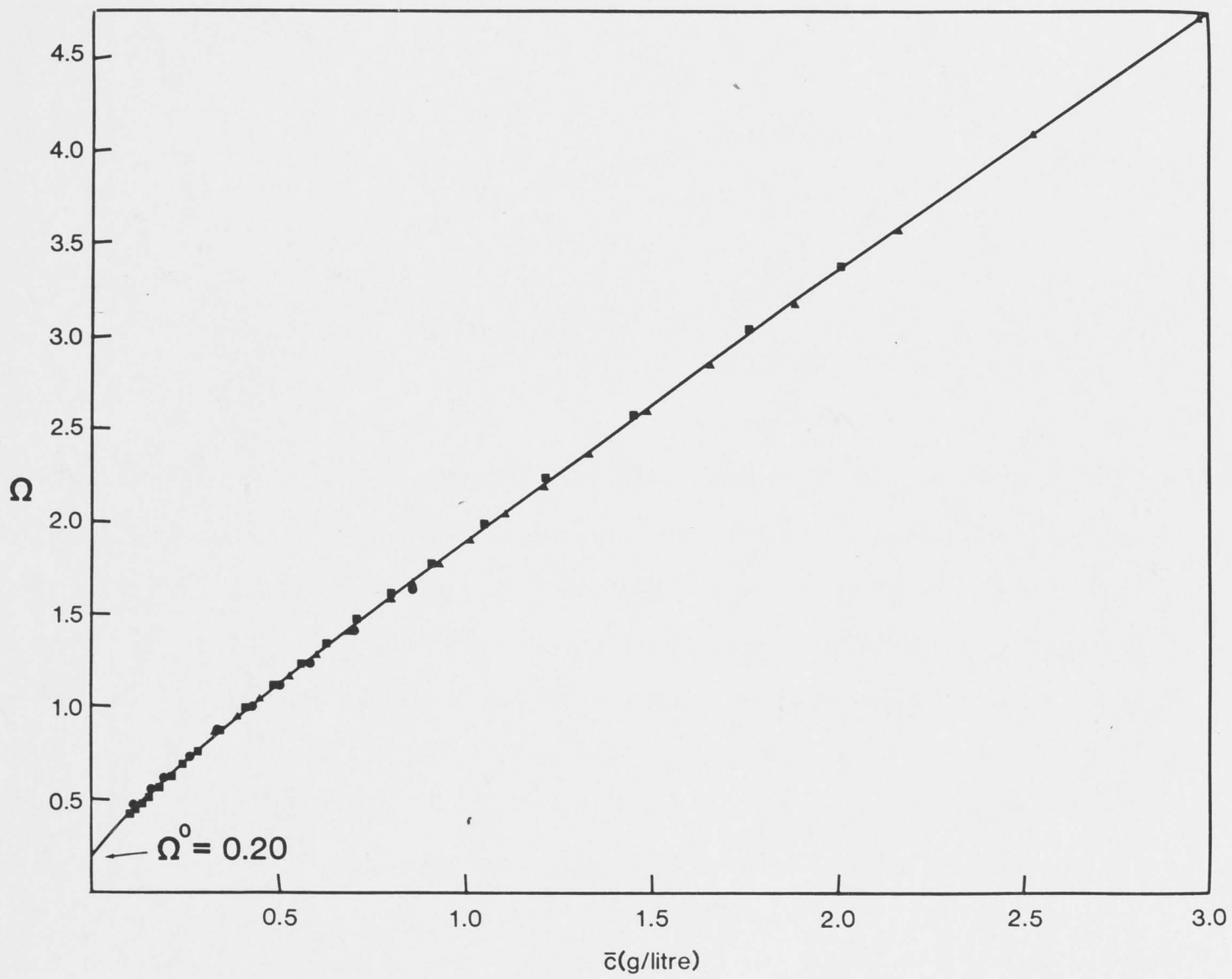
4.5
4.0
3.5
3.0
2.5
2.0
1.5
1.0
0.5
Ω
Ω° = 0.20
0.5
1.0
1.5
2.0
2.5
3.0
c̄(g/litre)

Figure 4.4: A plot of the thermodynamic activity of monomer, a_1 *versus* the total weight concentration found from sedimentation equilibrium experiments conducted with zinc-free insulin at pH = 7.0, I = 0.10, 25 °C. Equation (4.30) was used to calculate the experimental points from the smooth solid curve shown in Figure 4.3. The solid curve was calculated using equation (4.16) describing a "head-to-head" and "tail-to-tail" association pattern with first estimate values $k_\alpha = 2.5 \times 10^4\ \mathrm{M}^{-1}$ and $k_\beta = 1.3 \times 10^4\ \mathrm{M}^{-1}$ and shows the final result of the curve fitting procedure used to obtain these first estimates.

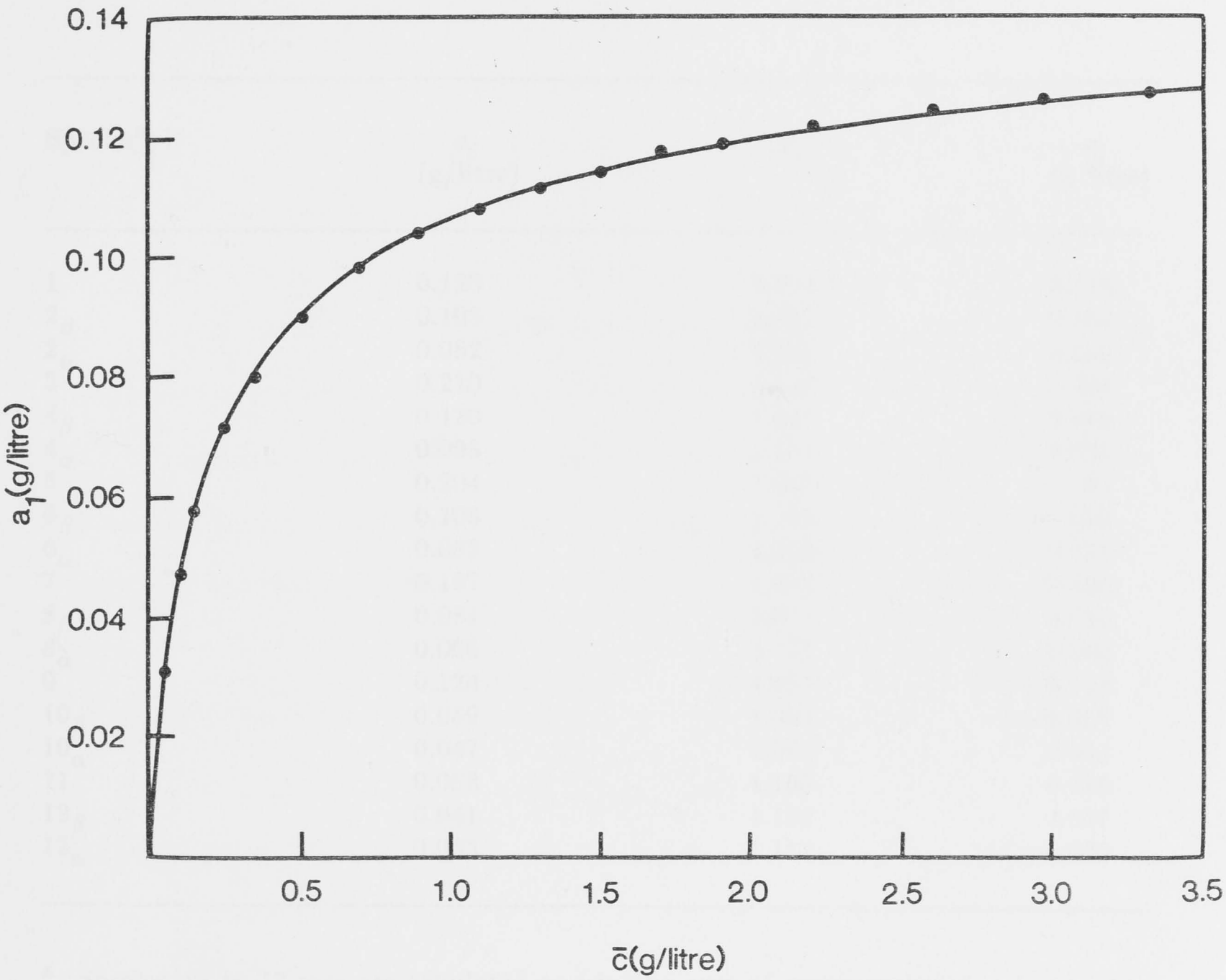
0.14
0.12
0.10
0.08
0.06
0.04
0.02
a_1(g/litre)
0.5
1.0
1.5
2.0
2.5
3.0
3.5
$\bar{c}$(g/litre)

Table 4.3: An illustration of the magnitude of the thermodynamic non-ideality effects in a solution (2.0 g/litre) of zinc-free insulin at pH 7.0, I = 0.1 and T = 25 °C.

Calculations were based on the experimentally determined value of the activity of monomer a_1, and $k_\alpha = 2.05 \times 10^4\ M^{-1}$ and $k_\beta = 1.63 \times 10^4\ M^{-1}$, appropriate to the postulated "head-to-head" and "tail-to-tail" association pattern.

Species[a], i	a_i (g/litre)	y_i	c_i (g/litre)
1	0.120	1.014	0.118
2_β	0.103	1.023	0.100
2_α	0.082	1.023	0.080
3	0.210	1.032	0.203
4_β	0.120	1.041	0.015
4_α	0.095	1.041	0.091
5	0.204	1.050	0.194
6_β	0.105	1.059	0.096
6_α	0.083	1.059	0.078
7	0.167	1.068	0.156
8_β	0.081	1.077	0.076
8_α	0.065	1.077	0.060
9	0.124	1.085	0.114
10_β	0.059	1.094	0.054
10_α	0.047	1.094	0.043
11	0.088	1.103	0.080
12_β	0.041	1.112	0.037
12_α	0.033	1.112	0.030

[a] Species up to 12-mer are tabulated and in the case of even-numbered polymers two entries are required to specify the detailed composition in terms of species with two free α sites denoted by the subscript α or with two free β sites denoted by the subscript β.

4.3.4]. This permitted refinement of the site-binding constants to $k_\alpha = 2.05 \times 10^4\ M^{-1}$ and $k_\beta = 1.63 \times 10^4\ M^{-1}$, which differ little from the values obtained neglecting non-ideality. It is stressed however that the allowance for non-ideality assumes greater importance in experimental environments where charge-charge interactions are increased in magnitude. In the environment presently under discussion, the magnitude of the non-ideality effects can be appreciated by inspection of Table 4.3, which presents in

column three the activity coefficients of monomer to 12-mer pertinent at a total concentration of 2.0 g/litre. The values of y_i increase systematically with the size of the polymer but attain a value little different from unity even for the 12-mer. It is also apparent from column four of Table 4.3 that the contribution to the total concentration of species larger than the 12-mer is not large, which indicates that the truncation at $i = 30$, used in practice, is certainly sufficient. In summary, Table 4.3 illustrates the potential of the present approach in defining the detailed composition of the solution at a given total concentration based on an association pattern involving "head-to-head" and "tail-to-tail" association. The appropriateness of this pattern to the results obtained at pH 7.0 is seen by the fit of the calculated solid curve to the experimental points in Figure 4.2 referring to the differentiated results. The relevance of the postulated self-association pattern will be inspected more critically in relation to the experimental results shown in Figure 4.4 after further discussion has been given of the treatment of non-ideality effects.

4.3.2 Studies at pH 2.0

A major point of interest is whether or not the "head-to-head" and "tail-to-tail" association pattern also suffices to describe the results obtained at pH 2.0, a value employed by other workers (Jeffrey and Coates, 1966) and one where zinc-free insulin is more soluble than at pH 7.0. An entirely similar procedure to that earlier described was used to obtain a plot of a_1 *versus* $\bar{c}$ using the Ω-method applied to results obtained in experiments 1 and 2 of Table 4.2. Again overlapping of the results from the different experiments was found. The iterative procedure to calculate activity coefficients of species at selected concentrations in the experimental range 0.1 to 5.8 g/litre led to the values shown in Figure 4.5 for the arbitrarily selected range of species $i = 1$ (monomer) to $i = 10$ (decamer). At pH 2.0 the charge on the monomer is +5 and thus the charge-charge interaction term in equation (4.38) is much larger at pH 2.0 than at pH 7.0. This may be illustrated by comparing, for example, the value $y_{10} = 1.094$ [Table 4.3] with that of $y_{10} = 1.50$ found at the same total concentration of 2.0 g/litre

Figure 4.5: Estimates of the activity coefficients of monomer and polymers of zinc-free insulin at pH = 2.0, I = 0.10, 25 °C plotted as a function of total weight concentration. Polymers up to decamer are shown although in numerical calculations designed to allow for the composition-dependence of the activity coefficients of constituent species, all polymers up to 30-mer were considered. These particular calculations, which were typical of others performed for different environmental conditions, were based on equations (4.37) and (4.38) using the values of $k_\alpha = 3.80 \times 10^4\ M^{-1}$ and $k_\beta = 0.03 \times 10^4\ M^{-1}$ obtained after the iterative procedure outlined in the text had been applied.

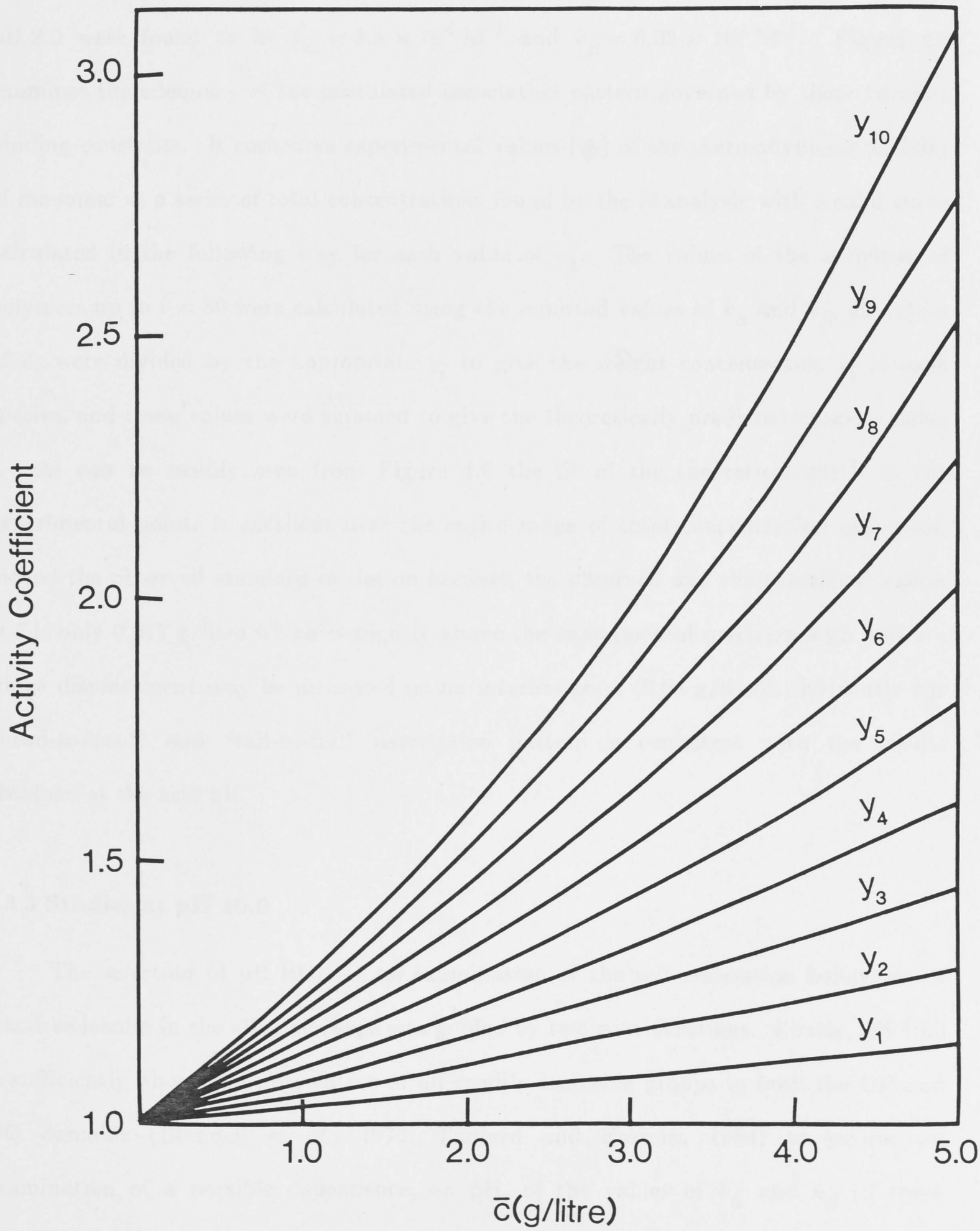
3.0
2.5
2.0
1.5
1.0
Activity Coefficient
y_{10}
y_9
y_8
y_7
y_6
y_5
y_4
y_3
y_2
y_1
1.0
2.0
3.0
4.0
5.0
$\bar{c}$(g/litre)

at the lower pH [Figure 4.5]. As Figure 4.5 shows, it is indeed possible to attain values of y_i exceeding 3.0 for the activity coefficients of species larger than the decamer at concentrations around 5 g/litre. When due allowance was made for composition-dependent non-ideality, the refined values of k_α and k_β which best fitted the results at pH 2.0 were found to be $k_\alpha = 3.8 \times 10^4$ M^{-1} and $k_\beta = 0.03 \times 10^4$ M^{-1}. Figure 4.6 examines the adequacy of the postulated association pattern governed by these two site binding constants. It compares experimental values (◆) of the thermodynamic activity of monomer at a series of total concentrations found by the Ω-analysis with a solid curve calculated in the following way for each value of a_1. The values of the activities of polymers up to $i = 30$ were calculated using the reported values of k_α and k_β, all values of a_i were divided by the appropriate y_i to give the weight concentration c_i of each species, and these values were summed to give the theoretically predicted abscissa value $\bar{c}$. As can be readily seen from Figure 4.6 the fit of the theoretical curve to the experimental points is excellent over the entire range of total concentration examined. Indeed the observed standard deviation between the observed and the calculated values of $\bar{c}$ is only 0.017 g/litre which is slightly above the experimental precision with which a fringe displacement may be measured on an interferogram (0.01 g/litre). Evidently the "head-to-head" and "tail-to-tail" association pattern is consistent with the results obtained at the acid pH.

4.3.3 Studies at pH 10.0

The selection of pH 10.0 for an examination of the self-association behaviour of zinc-free insulin in the alkaline range was guided by two considerations. Firstly, pH 10.0 is sufficiently above the pKa values of all readily ionizable groups in both the OP and OQ domains (Blundell *et al.*, 1972; Tanford and Epstein, 1954) to permit an examination of a possible dependence, on pH, of the values of k_α and k_β (if these continue to pertain). Secondly, it has been shown (Helmerhorst and Stokes, 1983) that the base catalysed cleavage of the inter- and intra-chain disulphide bridges, within the insulin structure, is negligible at pH 10.0 and only becomes a complicating factor at

Figure 4.6: The result of analysing sedimentation equilibrium results, by the Ω method, obtained at pH = 2.0, I = 0.10, 25 °C with zinc-free insulin [experiments 1 and 2 of Table 4.2]. The plot of the thermodynamic activity of monomer a_1 *versus* total weight concentration is analogous to that shown in Figure 4.4, but in this case the solid curve utilized refined values of k_α and k_β (3.80×10^4 M^{-1}, 0.03×10^4 M^{-1}, respectively) obtained after allowance had been made for composition-dependent non-ideality effects.

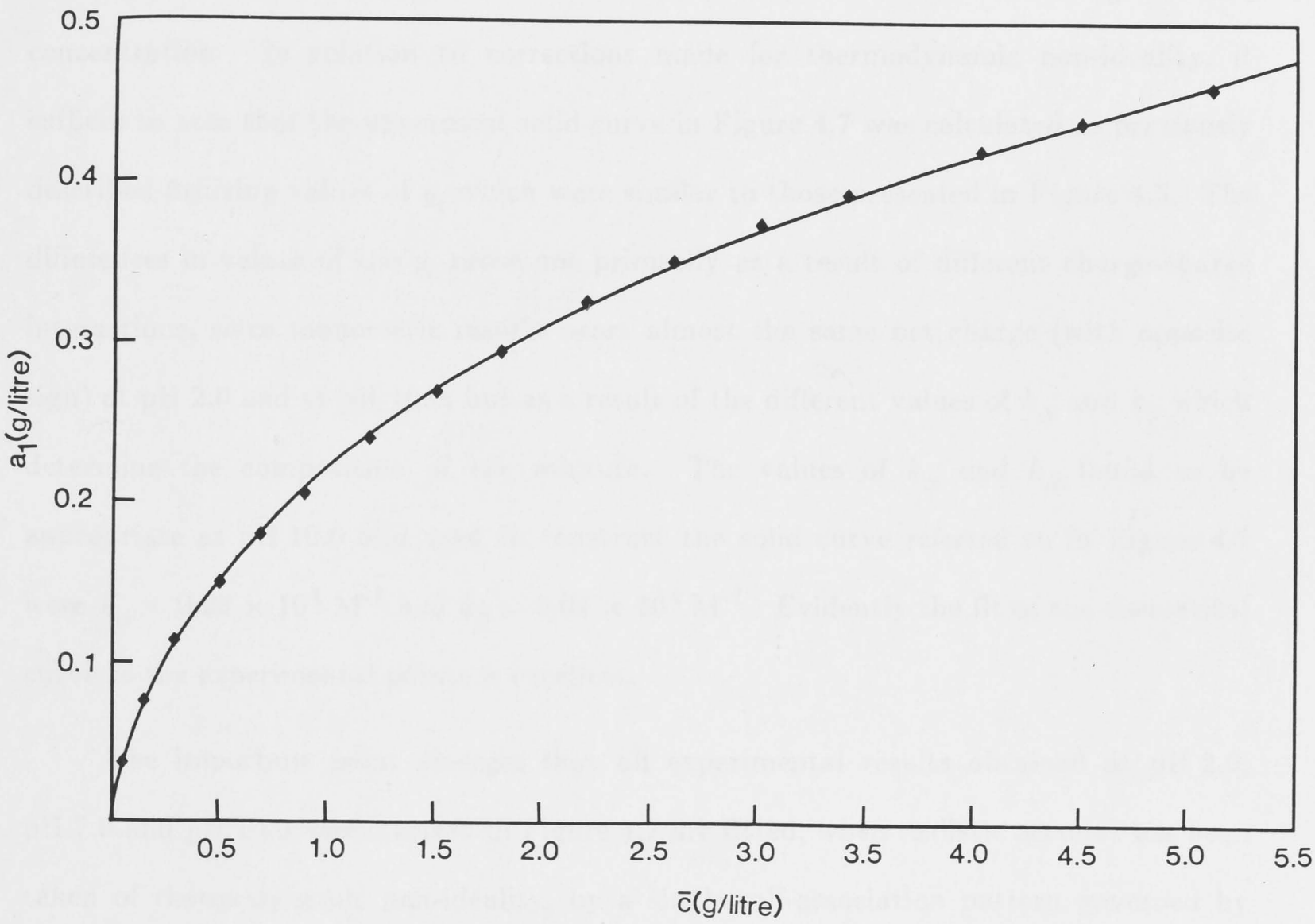
0.5
0.4
0.3
0.2
0.1
a_1(g/litre)
0.5
1.0
1.5
2.0
2.5
3.0
3.5
4.0
4.5
5.0
5.5
$\bar{c}$(g/litre)

higher pH values around 13. The discussion which follows refers to sedimentation equilibrium experiments 11 and 12 (Table 4.2).

The uppermost points (■) in Figure 4.7 are the results of the Ω-analysis, which, consistent with the results obtained at lower pH values, yielded overlap of curves relevant to the different experiments conducted to explore the indicated range of total concentration. In relation to corrections made for thermodynamic non-ideality, it suffices to note that the uppermost solid curve in Figure 4.7 was calculated as previously described utilizing values of y_i which were similar to those presented in Figure 4.5. The differences in values of the y_i arose not primarily as a result of different charge-charge interactions, since monomeric insulin bears almost the same net charge (with opposite sign) at pH 2.0 and at pH 10.0; but as a result of the different values of k_α and k_β which determine the composition of the mixture. The values of k_α and k_β found to be appropriate at pH 10.0 and used to construct the solid curve referred to in Figure 4.7 were $k_\alpha = 0.23 \times 10^4$ M^{-1} and $k_\beta = 0.04 \times 10^4$ M^{-1}. Evidently the fit of the theoretical curve to the experimental points is excellent.

The important point emerges that all experimental results obtained at pH 2.0, pH 7.0 and pH 10.0, summarized in Figure 4.7 are fitted, when realistic account has been taken of thermodynamic non-ideality, by a single self-association pattern governed by two association constants k_α and k_β. It is not suggested that the magnitudes of k_α and k_β are invariant with pH and to stress the point values already reported are summarized in Table 4.4. Even before a detailed examination of these values of k_α and k_β is made, it is evident from Figure 4.7 that at all total concentrations examined the weight-fraction of monomer increases in the order pH 10.0 > pH 2.0 > pH 7.0. In other words, the overall extent of association is maximal at neutral pH and increases in the order pH 7.0 > pH 2.0 > pH 10.0, a point made graphically in Figure 4.8 in terms of reduced weight-average molecular weights calculated using equation (4.20) with appropriate values of k_α and k_β.

Figure 4.7: A composite diagram which shows the dependence on total zinc-free insulin concentration of the thermodynamic activity of insulin monomer relevant to solutions I = 0.10, 25 °C and at the pH values shown against each curve. In each case the solid curves are those calculated on the basis of the refined estimates of k_α and k_β reported in Table 4.4, due allowance having been made for composition-dependent thermodynamic non-ideality effects. The figure is designed to show the appropriateness of the "head-to-head" and "tail-to-tail" association pattern for zinc-free insulin over a wide range of pH.

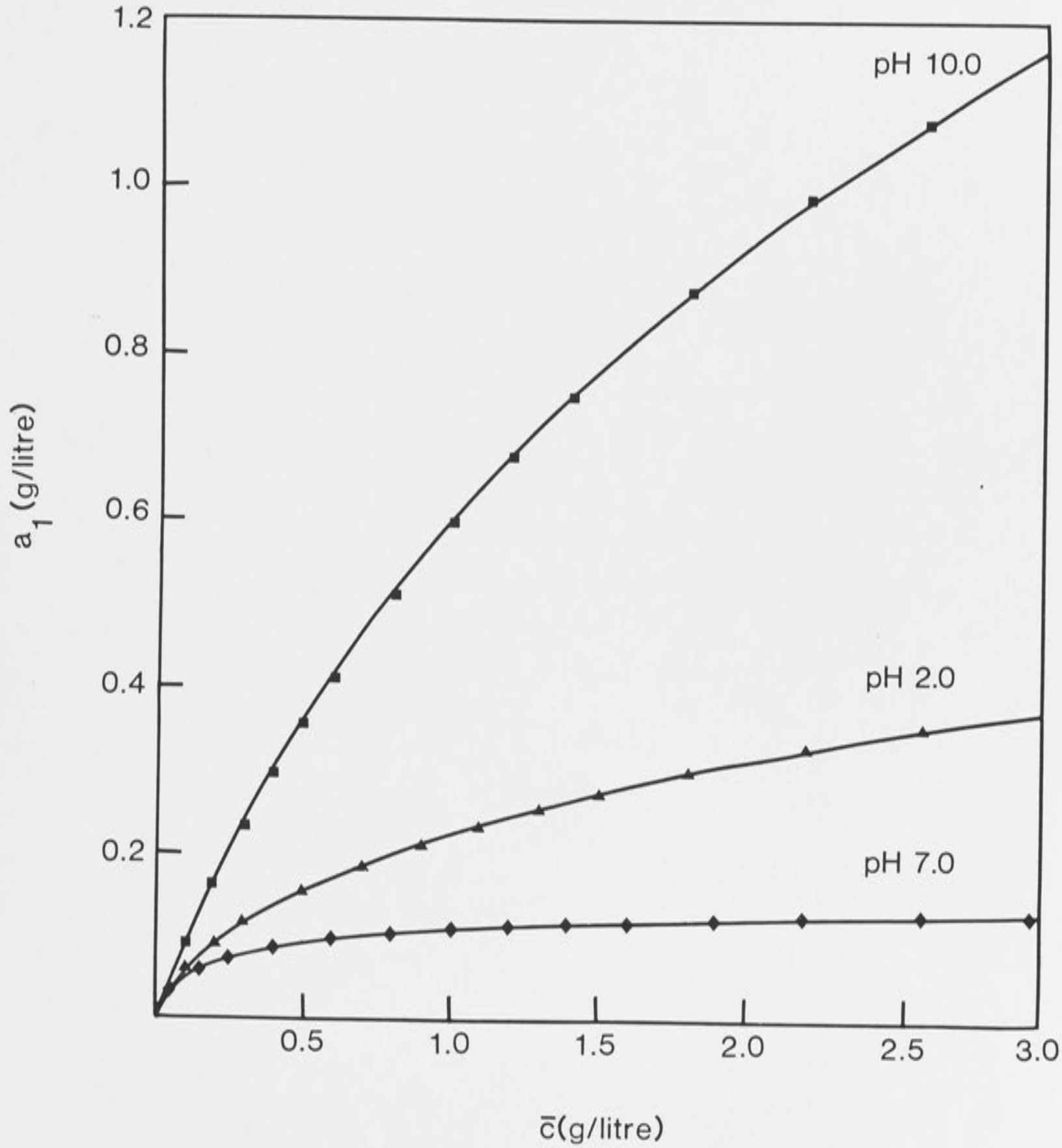
1.2
1.0
0.8
0.6
0.4
0.2
a_1 (g/litre)
pH 10.0
pH 2.0
pH 7.0
0.5
1.0
1.5
2.0
2.5
3.0
$\bar{c}$(g/litre)

Figure 4.8: The overall extent of association of zinc-free insulin at different pH values (as indicated) reflected in plots of the concentration-dependence of the reduced weight-average molecular weight. The curves were computed using equation (4.20) with the values of k_α and k_β reported in Table 4.4.

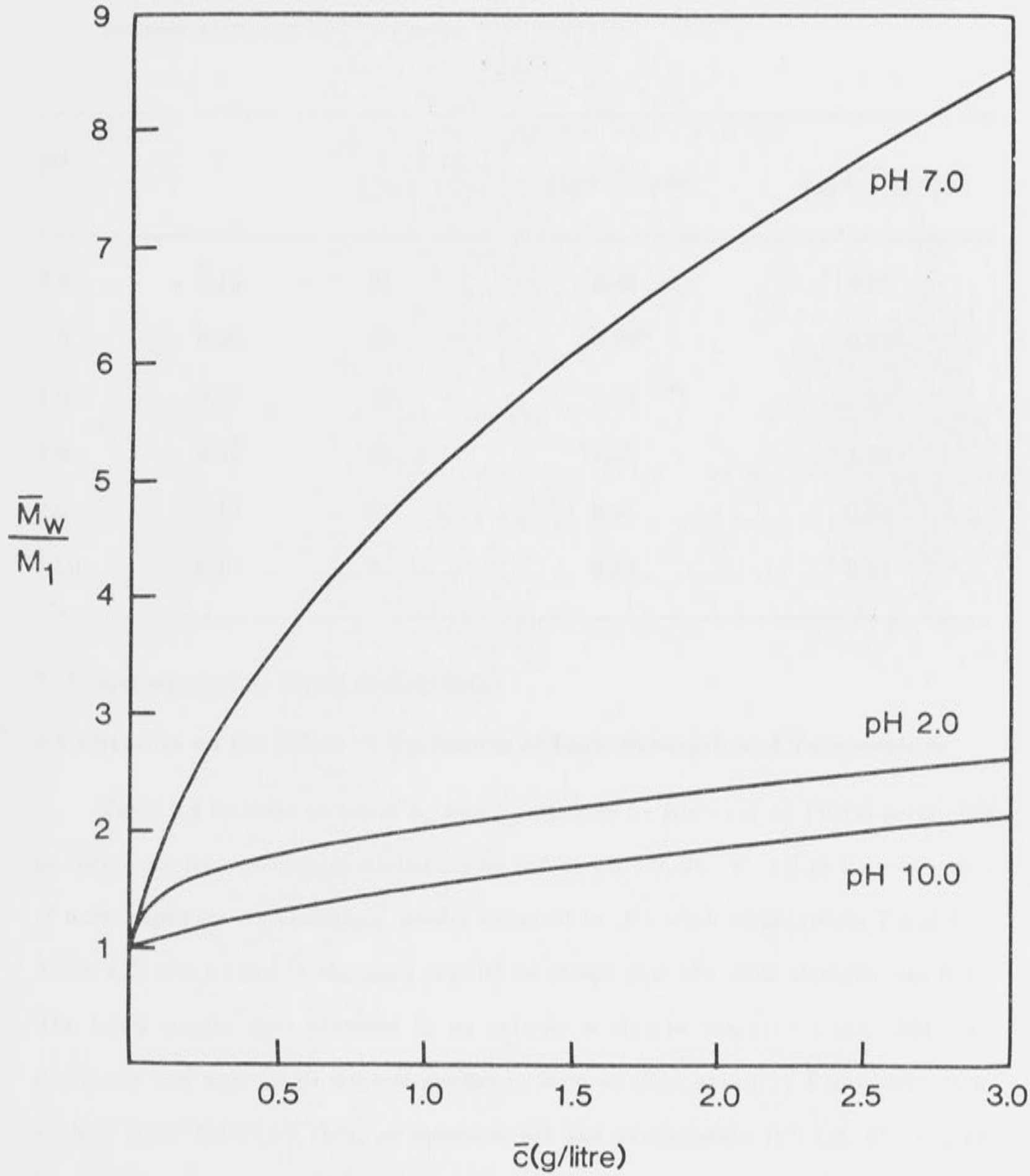
9
8
7
6
5
4
3
2
1
$\frac{\overline{M}_w}{M_1}$
pH 7.0
pH 2.0
pH 10.0
0.5
1.0
1.5
2.0
2.5
3.0
$\overline{c}$(g/litre)

Table 4.4: Summary of the values of k_α and k_β pertinent to the "head-to-head" and "tail-to-tail" association pattern of zinc-free insulin found from the analysis of sedimentation equilibrium results.

pH	I	T (°C)	k_α ($M^{-1} \times 10^{-4}$)	k_β ($M^{-1} \times 10^{-4}$)
2.0	0.10	25	3.80	0.03
7.0	0.20	25	5.75[a]	0.85[a]
7.0	0.10	25	2.05	1.63
7.0	0.05	25	1.52	1.40
7.0	0.10	37	3.85	0.39
10.0	0.10	25	0.23	0.04

[a] Values reported by Nichol *et al.* (1984).

4.3.4 Studies on the Effect of Variations of Ionic Strength and Temperature

Table 4.4 includes values of k_α and k_β reported by Nichol *et al.* (1984) pertaining to sedimentation equilibrium studies performed at pH 7.0, 25 °C and at ionic strength of 0.20, together wth additional results obtained in this work [experiments 7 and 8 of Table 4.2] which refer to the same conditions except that the ionic strength was 0.05. The latter results were obtained in an entirely analogous manner to that described previously and were in all respects similar in form to those shown in Figure 4.4. It is evident from Table 4.4 that, at constant pH and temperature (pH 7.0, 25 °C), an increase of ionic strength results in a small systematic increase in k_α, while the value of k_β remains essentially constant within experimental error, $1.3 \pm 0.4 \times 10^4$ M^{-1}.

The "physiological" pH of 7.0 was also employed in experiments 9 and 10 of Table 4.2 to investigate the association pattern at the elevated temperature of 37 °C. Results

in rows 3 and 5 of Table 4.4 may be compared in this regard since both were obtained at the same ionic strength of 0.10. While little significance can be attached to the numerical values of the standard enthalpy changes calculable from these two sets of results, it may be concluded within experimental precision that an increase of temperature results in an increase in k_α ($\Delta H^\circ > 0$) and to a decrease in k_β ($\Delta H^\circ < 0$). It is relevant to note that for the additional experiments reported in this section the "head-to-head" and "tail-to-tail" association continued to provide an excellent description of all results.

4.4 DISCUSSION

Several points merit comment in relation to the sedimentation equilibrium studies on zinc-free insulin. It is now clear that both the differentiated and integrated forms of basic sedimentation equilibrium equation may be used in complementary fashion. The former, employed in the construction of Figures 4.2 and 4.8, permits a ready visualization of the overall extent of the self-association of the protein. The latter permits, via the Ω-analysis, a simple and direct estimation of the thermodynamic activity of the insulin monomer at different total weight concentrations, as in Figures 4.4, 4.6 and 4.7, without recourse to the integration step inherent in the Steiner (1952) method of analysing apparent weight-average molecular weights in these terms. It is noted that the determination of the thermodynamic activity of monomer is independent of any assumption concerning the nature of the self-association pattern and provides the basis for the iterative method used to calculate the composition-dependence of the activity coefficients in relation to an assumed model of association, as in Figure 4.5.

It is possible to be somewhat critical concerning the nature of the assumptions on which the thermodynamic non-ideality effects are assessed, basically in terms of covolume and charge-charge interaction effects. Both spherical geometry and charge-conservation on polymerization have been assumed, the species being viewed as hard impenetrable spheres with Stokes radii taken as the effective radii appropriate to excluded volume calculations. Nevertheless, it must be stressed that the effects of

non-ideality in the present system are not large due to the relatively small size of, and net charges borne by, the protein and because of the restricted range of total concentration (never exceeding 6 g/litre) which was examined. The consideration of non-ideality effects is both realistic and important with certain systems, but it is evidently a second-order effect in the present system. The matter is put into perspective by observing that the activity coefficient of haemoglobin at the erythrocyte concentration of 320 g/litre (Ross and Minton, 1977) has been assessed as 62.8, whereas the largest value apparent in Figure 4.5 is 3, this value referring to a decamer of insulin in relatively low amount present at acid pH where charge-charge interactions were maximal in this study. Accordingly, there is less concern with the approximations used in the statistical mechanical calculation of non-ideality effects than with the requirement that some realistic account be taken of them in refining values of the equilibrium constants governing the association of zinc-free insulin.

The major point which emerges from the sedimentation equilibrium studies is that a single association pattern, termed "head-to-head" and "tail-to-tail", suffices to describe all results found over a wide pH range and (at pH 7.0) at different ionic strengths and temperatures. It is not suggested that each of these results viewed separately might not be fitted by an alternative model of association because, as we have seen, this has been done by various groups of workers and has led to a wide spectrum of patterns each claimed to be operative in a particular environment. It is, however, suggested that the weight of present evidence, including that available from X-ray crystallographic studies, strongly supports the view that the insulin monomer is bivalent and that it associates in the absence of zinc ions proceeding in an indefinite fashion by homogeneous bivalent interaction at two independent sites. The postulate does not invoke exclusion of particular polymeric species, such as odd-numbered polymers (Jeffrey, Milthorpe and Nichol, 1976) and nor does it require that emphasis be given to a particular species such as the zinc-free hexamer (Pekar and Frank, 1972). Indeed, it suggests an undeniably complicated detailed composition of each solution in which two types of even-numbered polymers are present (with identical but different interaction

domains at each end) and all odd-numbered polymers (with different interaction domains at each end) coexist in equilibrium with the monomer. The pertinent point is, despite this complexity, the detailed composition may be described in quite simple terms by equation (4.16), which involves only two thermodynamic constants, k_α and k_β. The fitting procedure used to obtain these quantities reported in Table 4.4 is quite sensitive and in this respect the precision given is warranted; but, at the same time, it is readily acknowledged that the experimental points derived from the Ω-analysis, which have been fitted, are themselves subjected to experimental error and thus it may be assessed that each reported value has an uncertainty of approximately 15%. The ability to fit all experimental results within experimental error to the two parameters k_α and k_β highlights the likely appropriateness of the "head-to-head" and "tail-to-tail" association pattern in describing the solution behaviour of zinc-free insulin. This finding may have general implication in relation to other self-associating protein systems, such as lysozyme and chymotrypsinogen A, where different association patterns have been invoked to explain results obtained in experimental environments (Wills, Nichol and Siezen, 1980; Tung and Steiner, 1974).

There are two interrelated reasons for further examining the values of k_α and k_β reported in Table 4.4. The first arises because of the symmetry evident in equation (4.16), which does not permit identification of α-α interaction, governed by k_α, or β-β interactions, governed by k_β, in relation to the OP- and OQ-type reaction domains shown in Figure 4.1. The second reason is that examination of the variation of k_α and k_β with pH, ionic strength and temperature might provide further support for the postulated association pattern in that trends should be at least consistent with the chemistry of constituent residues in the reaction domains, once defined. At the outset it is observed that the standard free energy changes associated with k_α and k_β are the sum of several interaction components, not least the free energy of repulsion between species of like charge. In this connection it is noted that the overall extent of association is greatest at pH 7.0 where the net charge repulsion is at a minimum, Figure 4.8. It follows that a detailed interpretation of standard free energy changes is somewhat

hazardous; but, with this reservation in mind, the following points are made. The value of k_α increases with increased temperature ($\Delta H^\circ > 0$) and increases with increasing ionic strength, both characteristics of interactions which are predominantly hydrophobic in nature (Kauzmann, 1959). This would suggest that the α-α interaction may be identified with reaction between groups in the OP domain. These groups are predominantly hydrophobic and form a region of secondary structure which is highly conserved between the various crystal structures obtained with porcine insulin in the presence and absence of zinc ions (Blundell *et al.*, 1972; Smith *et al.*, 1984; Dodson *et al.*, 1978). In these terms k_α (which in all experimental environments is greater than k_β) governs the equilibria forming the α-α (OP-OP) dimer and the addition of monomers also at the OP interface, to a free OP interface in the formation of higher polymers. The relatively small dependence of k_α on pH (compared with k_β), at fixed ionic strength and temperature, is consistent with this assignment and, moreover, the variation itself finds rational explanation when it is appreciated that the only ionizable groups in the OP domain of 2-zinc insulin are glutamic acid B13 (pK_a 4.7) and tyrosines B24 and B26 (pK_a 9.6) (Blundell *et al.*, 1972; Tanford and Epstein, 1954). From Table 4.4 it is clear that as the pH is increased from pH 2.0 to pH 10.0 the value of k_α decreases in accord with an increasing state of ionization of the three groups and the inherent increase in like charge repulsion opposing the hydrophobic attractions. The apparent corollary is that the formation of the β-β dimers and higher polymers involving like interfaces, governed by k_β, is associated with interactions of groups in the OQ domain which notably feature the ionizable groups tyrosine A14, phenylalanine B1 and glutamic acid A17. It is tempting to suggest that the negative enthalpy change associated with k_β, the maximal value of k_β at pH 7.0, and the slight decrease in k_β with increasing ionic strength at pH 7.0 are all consistent with interaction between hydrophilic groups especially glutamic acid A17 and the amino-terminal phenylalanine B1 which bear opposite net charges at pH 7.0. However a cautionary note is sounded in that such detailed interpretation in terms of the overall "free-energy balance sheet" is not strictly warranted, especially as it is by no means certain that the groups shown in the OQ

domain in Figure 4.1 are necessarily those involved in crystal formation or associated states of zinc-free insulin in free solution. In this connection it is noted that zinc-free porcine insulin crystallizes in the form of linear chains along a screw axis (Dodson *et al.*, 1978). Despite a warranted reluctance to provide a detailed interpretation of all variation shown in Table 4.4, it is fair to say that all observations at least find a rational explanation in terms of the "head-to-head" and "tail-to-tail" association pattern, that almost certainly the α-α interactions may be identified with OP-OP interactions and that while the details of the β-β interactions in solution remain to be elucidated, they most certainly exist.

CHAPTER 5

CONSIDERATION OF THE POSSIBLE RELEVANCE OF THE SELF-INTERACTION OF INSULIN IN THE BIOLOGICAL CONTEXT: INSULIN RECEPTOR BINDING

5.1 INTRODUCTION

The thermodynamic characterization of the self-association of insulin presented in the last chapter permits comment on the likely distribution of species in the serum, where the total concentration of unbound insulin is estimated to be in the range 0.7-3.0 ng/ml. This point is developed in the first section of this chapter, together with discussion of two constraints, the presence of space-filling macromolecules in the serum and the possibility of preferential binding of a specific secondary ligand, both of which might influence the distribution of insulin species *in vivo*. It must be said at the outset that, while not all possible constraints to the operative equilibria could be considered, the existing evidence strongly suggests that the monomeric form of insulin is the dominant unbound form of insulin in the serum. It follows that while the concepts developed in Chapter 2 might to some small extent apply to the overall binding of insulin to its receptor-matrix, it is unlikely that the self-association of this particular hormone-ligand in free solution in the serum will cause marked deviations from an hyperbolic binding response. Indeed, only if a polymeric form (present in exceedingly small relative concentration) were capable of binding preferentially to the receptors, could marked deviations originating on this basis be obtained. There is no evidence at present to support the latter hypothesis. The second part of this chapter examines the possible role receptor crosslinking may play in relation both to the form of the insulin binding response and the aggregation phenomenon observed in the system. It is recognized that while insulin monomer is effectively the only form of free ligand, multiple binding of it to more than one receptor may induce crosslinking effects both in solution and on a membrane surface. The postulate formulated by Jeffrey (1982), that the self-association acts as the source of the receptor aggregation is also examined critically utilizing experimentally obtained binding curves and theory developed in Chapter 3. The conclusion drawn in this section is that with an appropriate

cross-linking model a binding response resembling "negative cooperativity" in Scatchard format may be obtained. Such a response has been observed by different workers (Williams, Caterson and Turtle, 1984; Fujita-Yamaguchi *et al.*, 1983; Grigorescu, White and Kahn, 1983; Pollet, Standaert and Haase, 1977); but not by all (Kohanski and Lane, 1983; Donner, 1980). In theory such a crosslinking hypothesis may be tested experimentally based on the theoretical developments of this thesis pertaining to acceptor concentration-dependence effects. Attempts in this direction using partially purified receptor form the concluding section of the second part of the chapter.

The final part of the chapter discusses in critical vein the experimental approaches used to obtain insulin-receptor binding curves and the complications which ensue from utilizing intact cells where the binding of insulin forms the first step in a sequence of reactions. The potential for further studies utilizing purified receptors is emphasized. Such an approach together with the theory developed in this work may well provide basic information on crosslinking effects. Until such effects are further examined, it seems that interpretation of results obtained with intact cells, albeit the ultimate aim in this field, will remain ambiguous.

5.2 CONSIDERATION OF THE DISTRIBUTION OF INSULIN SPECIES IN THE SERUM

5.2.1 Weight-Fraction of Species: Theory and Calculation

As noted in Chapter 2, the distribution of species in an indefinitely associating system is usefully formulated in terms of the weight-fraction of species as a function of total concentration. No such expression has yet been formulated for the "head-to-head" and "tail-to-tail" indefinite self-association pattern pertinent, as we have seen in Chapter 4, to insulin.

The required expression may be formulated from the combination of equation (4.16), the expression for the total weight concentration, and equations (4.14a) and (4.14b) the weight concentrations of each of the odd- and even-numbered species respectively. The weight-fraction, ϕ_i, of each species, i, being given by:

$$\phi_i = \frac{c_i}{\bar{c}} = \frac{i\chi_i m_1^{(i-1)}(1 - 4k_\alpha k_\beta m_1^2)^2}{(1 + 2k_\alpha m_1)(1 + 2k_\beta m_1)} \qquad (5.1a)$$

where

$$\chi_i = (4k_\alpha k_\beta)^{(i-1)/2}; \qquad i \text{ odd} \qquad (5.1b)$$

$$\chi_i = (k_\alpha + k_\beta)(4k_\alpha k_\beta)^{(i-2)/2}; \qquad i \text{ even}. \qquad (5.1c)$$

By differentiating this expression with respect to $\bar{c}$ it is possible to determine whether the weight-fraction of a given species will pass through a maximum. It is noted in regard to this differentiation that χ_i is a constant independent of $\bar{c}$. The weight-fraction of a given species will pass through a maximum when $d\phi_i/d\bar{c} = 0$. It may be readily shown that this is only true when; $16(i+1)k_\alpha^2 k_\beta^2 m_1^4 + 8(i+2)k_\alpha k_\beta(k_\alpha + k_\beta)m_1^3 + 24k_\alpha k_\beta m_1^2 + 2(2-i)(k_\alpha + k_\beta)m_1 - (i-1) = 0$.

When $i = 1$ the last term disappears and, as there are no changes in sign within the polynomial, by Descartes' rule of sign, there can be no real roots for $d\phi_1/d\bar{c} = 0$. Thus the monomer weight-fraction must decrease monotonically with increasing $\bar{c}$ ($d\phi_1/d\bar{c} < 0$). For all $i > 1$ there is one change of sign and therefore one positive real root for $d\phi_i/d\bar{c}$. This means that the weight-fraction of all species other than monomer will pass through a single maximum as the total concentration of insulin is increased.

This point is demonstrated in Figure 5.1 which shows the weight-fractions of all species up to and including pentamer ($i = 5$) as a function of total concentration. The values for the weight-fraction of each species were calculated using equation (5.1) assuming the values for k_α and k_β given in Table 4.4 relating to the self-association of zinc-free insulin at pH 7.0, I = 0.1 and T = 25 °C. It should be noted that in order to account for the two types of dimer and the two types of tetramer separately it is necessary to expand the expression given in equation (5.1c). Figure 5.1 allows appreciation of the complex distribution of species within the insulin system in solution. It also stresses the importance of the odd-numbered species, the dominant species by weight, under these particular conditions. This underlines the contrast between this and

Figure 5.1: The weight-fractions (ϕ_i) of all species up to and including pentamer ($i = 5$) present in a solution of zinc-free insulin (pH 7.0, I = 0.1, T = 25 °C) as a function of total concentration ($\bar{c}$) is shown. The values for the weight-fractions were calculated using equation (5.1) assuming values for k_α and k_β of 2.05×10^4 M^{-1} and 1.63×10^4 M^{-1} respectively. The lines labelled α-Dimer and α-Tetramer refer to the species of dimer and tetramer with two exposed α-faces whereas the lines labelled β-Dimer and β-Tetramer refer to the species of dimer and tetramer with two exposed β-faces.

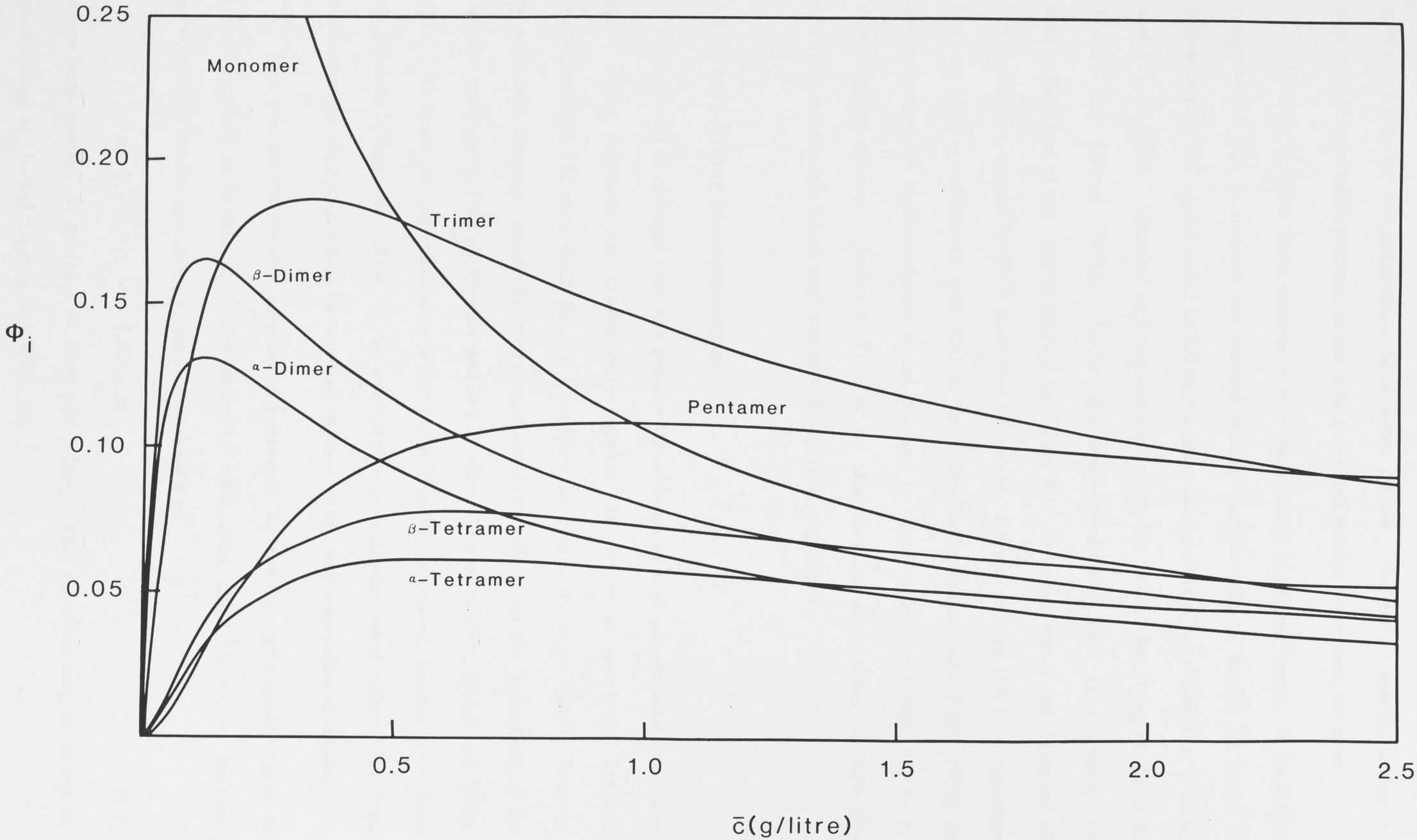
0.25
0.20
0.15
0.10
0.05
Φi
Monomer
Trimer
β–Dimer
α–Dimer
Pentamer
β–Tetramer
α–Tetramer
0.5
1.0
1.5
2.0
2.5
c̄(g/litre)

earlier models for the association of zinc-free insulin: the earlier models taking no account of the possible presence of any odd-numbered species other than monomer.

In order to place these comments into their proper biological context it should be remembered that in humans the normal resting concentration of insulin in serum is approximately 0.7 ng/ml rising to 3.0 ng/ml after the infusion of a glucose load (Fajans and Floyd, 1972). Maximal cell stimulation by insulin occurs by 10 ng/ml (Marsh, Westly and Steiner, 1984). Under the same conditions used to calculate the weight-fractions of the species plotted in Figure 5.1 a solution containing 10 ng/ml of insulin would comprise 99.987% monomer by weight. Results such as this have led some workers (Jeffrey, Milthorpe and Nichol, 1976; De Meyts, Bianco and Roth, 1976) to conclude that the self-association is not relevant to insulin's action *in vivo*, nor to *in vitro* binding studies. However, little or no attention has been given to naturally occurring constraints which may perturb the operative equilibria.

5.2.2 Space-Filling Macromolecules

It is well established that the presence in solution of high concentrations of inert space filling polymers can dramatically enhance the degree of association between macromolecules (Minton, 1981; Bosma, Voordouw, De Kok and Veeger, 1980). This can be explained thermodynamically in terms of covolume effects on the magnitude of the activity coefficients (Nichol, Ogston and Wills, 1981; Tellam, Sculley, Nichol and Wills, 1983). As blood plasma contains approximately 70 g/litre of protein, mostly in the form of albumin (Eastham, 1978), it is worthwhile to consider what effect this high concentration of protein would be expected to have on the self-association of insulin.

The two thermodynamic association constants, k_α and k_β are in essence ratios of thermodynamic activities (a_i). For example, considering only interactions between α-faces of the insulin monomer, k_α may be expressed as:

$$k_\alpha = a_{(n+1)}/a_n a_1; \quad n = 1,2,3,...\infty \tag{5.2}$$

where each species, n, contains at least one α-face. This equation may of course be re-expressed as (Nichol, Ogston and Wills, 1981):

$$k_\alpha = [m_{(n+1)}/m_n m_1][y_{(n+1)}/y_n y_1] \tag{5.3}$$

where m_i is the molar concentration and y_i the activity coefficient of species i. As discussed in detail in Chapter 4 the logarithm of each of these activity coefficients may be written as a multinomial expansion in terms of the concentrations of all solute species (Wills, Nichol and Seizen, 1980):

$$ln\ y_i = \sum_j \alpha_{ij} m_j + \text{higher terms.} \tag{5.4}$$

Normally, when experiments are conducted at low concentrations, it is assumed that the ratio of the activity coefficients $y_{(n+1)}/y_n y_1 \simeq 1$ (Adams and Fujita, 1963). An expression for the apparent value of k_α is thus given by:

$$k_\alpha^{app} = m_{(n+1)}/m_n m_1. \tag{5.5}$$

Although the assumption strictly holds only at infinite dilution it was demonstrated in Section 3 of Chapter 4 that for insulin it was still valid at concentrations in the range of 1 g/litre when insulin was the only macromolecular solute. The assumption cannot however, automatically be taken as valid where there are large concentrations of other macromolecular solutes such as in blood plasma. In these cases the observed association constant, k_α^{app} is related to the thermodynamic association constant, k_α, by the expression:

$$k_\alpha^{app} = k_\alpha[y_n y_1/y_{(n+1)}]. \tag{5.6}$$

In order to make the problem of obtaining an expression for the activity coefficients tractable it is necessary to assume that the space filling protein in serum is inert, uniform in size, and bears no net electrostatic charge (Tellam *et al.*, 1983). In situations where the concentration of the associating species is very low in comparison to the inert polymer, as in the case being considered, it can be readily shown that the higher terms in equation (5.4) can be ignored and reasonable estimates for the activity coefficients obtained by considering only the dominant terms $\alpha_{ip} m_p$; m_p referring to the concentration of the inert polymer (Nichol, Ogston and Wills: 1981): thus,

$$y_i = exp(\alpha_{ip} m_p). \tag{5.7}$$

A full expression for the virial coefficient was given in equation (4.38) and has already been discussed in relation to the allowance for non-ideality in the analysis of sedimentation equilibrium results. In essence, α_{ip} represents the volume of the solution excluded to a molecule of i by a molecule of p over and above the volume which the polymer molecule occupies (Nichol, Ogston and Wills, 1981). This may be written as (Nichol, Ogston and Wills, 1981):

$$\alpha_{ip} = U_{ip} - \bar{v}_p M_p \tag{5.8}$$

where U_{ip} is the molar covolume of i and p, $\bar{v}$ the partial specific volume and M_p the molar mass of the polymer. Combining equations (5.6), (5.7) and 5.8) it can be readily shown that:

$$k_\alpha^{app} = k_\alpha \, exp[(U_{np}+U_{1p}-U_{(n+1)p}-\bar{v}_p M_p)m_p]. \tag{5.9}$$

The quantity $U_{np} + U_{1p} - U_{(n+1)p}$ gives the decrease in covolume associated with the addition of monomer to the polymeric chain. The determination of this covolume decrement for a system undergoing an orientationally specific linear self-association has been considered by Tellam *et al.* (1983). They showed that if both the monomer and the inert macromolecule were considered as hard impenetrable spheres with radii of a and r, respectively, the covolume decrement was a constant given by $2N\pi r^2(3a+2r)/3$ where N is Avogadro's number. Thus far in this discussion only k_α (i.e. only interactions between α-faces) has been considered. It should, however, be obvious that because of the intrinsic symmetry of the "head-to-head"and "tail-to-tail" model, an identical equation could be written in terms of k_β. This may be expressed mathematically as:

$$k_\alpha^{app}/k_\alpha = k_\beta^{app}/k_\beta = exp[(2N\pi r^2(3a+2r)/3 - \bar{v}_p M_p)m_p]. \tag{5.10}$$

In order to quantify the effect of serum proteins on the self-association of insulin in the terms outlined above, estimates are needed for the radii of insulin, a, and the space-filling protein, r, as well as the concentration of the space-filling protein, m_p. In both cases it will suffice to calculate the radii from the molecular weights and the partial specific volumes assuming spherical geometries. Serum albumin ($M_w \simeq 68500$) will be used as the model for the inert polymer as it is by far the protein of highest

concentration in serum. Using $\bar{v} = 0.733$ g/litre (Edsall, 1953) the radius of serum albumin was calculated to be $r = 2.71$ nm. For insulin ($M_w = 5734$) the partial specific volume has been given previously as $\bar{v} = 0.73$ g/litre (Frank and Veros, 1968) which results in a radius of $a = 1.13$ nm. The values yield a covolume decrement of 83.1 M^{-1}. The protein concentration of 70 g/litre in serum translates to a concentration for the model protein ($M_w \simeq 68500$) of $m_p \simeq 1$ mM. After substitution into equation (5.10) these values yield a figure for the apparent enhancement of the two association constants for the self-association of zinc-free insulin in blood due to the covolume effects of serum proteins of $k_\alpha^{app}/k_\alpha = k_\beta^{app}/k_\beta \simeq 1.03$. Although this figure is based on a large number of assumptions and therefore should be considered only semi-quantitative it does give the order of magnitude of the likely effect. It is evident that a pronounced enhancement of the extent of self-association cannot reasonably be postulated on the basis of covolume effects.

5.2.3 The Effect of Secondary Ligands

When considering the homogeneous self-association of insulin in Chapter 4, great care was taken to exclude from the experiments species, such as zinc(II) ions, known to interact specifically with either the monomeric or polymeric forms of insulin. Such species, which will be termed secondary ligands for the purpose of this discussion, can have a marked effect on an interacting system by preferentially stabilizing a given polymeric state (Tellam, Winzor and Nichol, 1978; Howlett and Nichol, 1972). An example of this is the formation by insulin of a cyclic hexamer in the presence of zinc(II) ions (Milthorpe, Nichol and Jeffrey, 1977; Blundell *et al.*, 1972). Therefore, when considering the nature of insulin in solution in a biological context, or in regard to *in vitro* binding studies, the question that must be asked is: are any components of the system capable of interacting with insulin and, if so, what will be the overall effects of such interactions on the self-association of insulin?

Besides zinc, insulin has been shown to bind a wide range of divalent cations (Goldman and Carpenter, 1974). Insulin also binds D-glucose and the binding of a

number of other hexose sugars has been postulated (Anzenbacker and Kalous, 1975; Milthorpe, 1977). The most relevant of these secondary ligands to consider in the present context are calcium, magnesium and D-glucose. Each of these molecules is found not only in significant quantities in blood plasma (Eastham, 1978) and is commonly included in binding-study buffers, but has also been implicated in the modification of the insulin binding response (De Meyts *et al.*, 1973; Williams, Caterson and Turtle, 1984; Lonnroth, Di Girolamo and Smith, 1983). Although the binding of magnesium and calcium ions to insulin has in the past received little attention, recent studies have shown that calcium binds to the B13 carboxylates of insulin and acts, along with zinc(II) ions, to stabilize the hexameric structure found in two-zinc insulin crystals (Alameda *et al.*, 1985; Storm and Dunn, 1985). To date no studies have been conducted to determine the effect of either of these ions on the self-association of zinc-free insulin.

Several attempts to determine the effect of glucose on the self-association of zinc-free insulin have been made. These studies stem from the work of Anzenbacker and Kalous (1975) who found that at pH 7.9 insulin bound eight glucose units per monomer. At high concentration (77.6 g/litre), Jeffrey (1974) showed that glucose tended to cause higher insulin polymers to disassociate though this may have been due to solvent effects (Milthorpe, 1977). Further studies by Milthorpe (1977) at lower concentrations proved inconclusive. In order to determine the overall effect of these secondary ligands on the self-association of insulin two sedimentation equilibrium experiments were conducted under conditions approximating those commonly used in studies on the binding of insulin to whole cells. The buffer used was based on that of Gambhir, Archer and Carter (1977) and consisted of Tris, 50 mM; Hepes, 50 mM; $MgCl_2$, 10 mM; $CaCl_2$, 10 mM; NaCl, 50 mM: KCl, 5 mM; D-glucose, 10 mM; pH 8.0 at 15 °C. Each of the inorganic ions and D-glucose was included at a concentration approaching that found in serum (Eastham, 1978). In addition ethylenediaminetetra-acetic acid (EDTA), 2 mM, was added to eliminate possible contamination by zinc(II) ions. The original binding buffer also contained 0.1% serum albumin. As this would cause severe interference in the sedimentation equilibrium experiments it was omitted. The two sedimentation

equilibrium experiments, the parameters for which are given in Table 5.1, were designed and conducted using the method previously outlined in Chapter 4. Both experiments were analysed by the Ω-method, again applied as described in Chapter 4. Figure 5.2 presents a plot of Ω *versus* $\bar{c}$, the Ω values being calculated using equation (4.27), utilizing a common reference concentration of 0.625 g/litre. Figure 5.2 was included to show the excellent overlap achieved between the two experiments, thus demonstrating the efficacy of the Ω-method even when applied to a heterogeneously associating system. The solid line in Figure 5.2 attempts to average the data and, as shown, is readily extrapolated to $\Omega^o = 0.18$. Using equation (4.30) and the above value for Ω^o, the dependence on total concentration of the thermodynamic activity of the insulin monomer was calculated from the experimental results; as shown in Figure 5.3. The solid line in Figure 5.3 was calculated from equation (4.16) using as values for k_α and k_β, 5.0×10^4 M^{-1} and 0.3×10^4 M^{-1} respectively. Again it is clear that the composition of the solution in terms of the distribution of insulin species shown in Figure 5.1 would be little altered on this basis. While not all possible constraints have been examined, it may be concluded that there is no evidence at present which questions the postulate that the monomeric form of insulin is the dominant species in physiological environments paralleling that of the serum.

5.3 BINDING STUDIES TO SOLUBLIZED INSULIN RECEPTOR

5.3.1 A Review of the Structure of the Insulin Receptor and its Interaction with Insulin

Several comprehensive reviews (Jacobs and Cuatrecasas, 1983; Houslay and Heyworth, 1983; Czech, 1984) have recently appeared on the nature of the insulin receptor. It will suffice, therefore, to give only a summary of the more relevant details.

The insulin receptor is an intrinsic membrane protein though it may be readily separated from the membranes by solubilizing in a variety of non-ionic detergents and still retain its insulin binding capacity (Jacobs and Cuatrecasas, 1983). The solubilized receptor consists of two glycoprotein subunits; the α-subunit ($M_w \simeq 125{,}000$) and the

Figure 5.2: The Ω plot used in the analysis of results from sedimentation equilibrium experiments conducted using zinc-free insulin in the presence of the buffer whose composition is given in Table 5.1. The values of Ω were calculated from equation (4.27), utilizing the common reference concentration of 0.625 g/litre, for each of the two experiments, 1 (▼) and 2 (■) outlined in Table 5.1. This plot is included in order to demonstrate the excellent overlap between the two experiments carried out under these conditions.

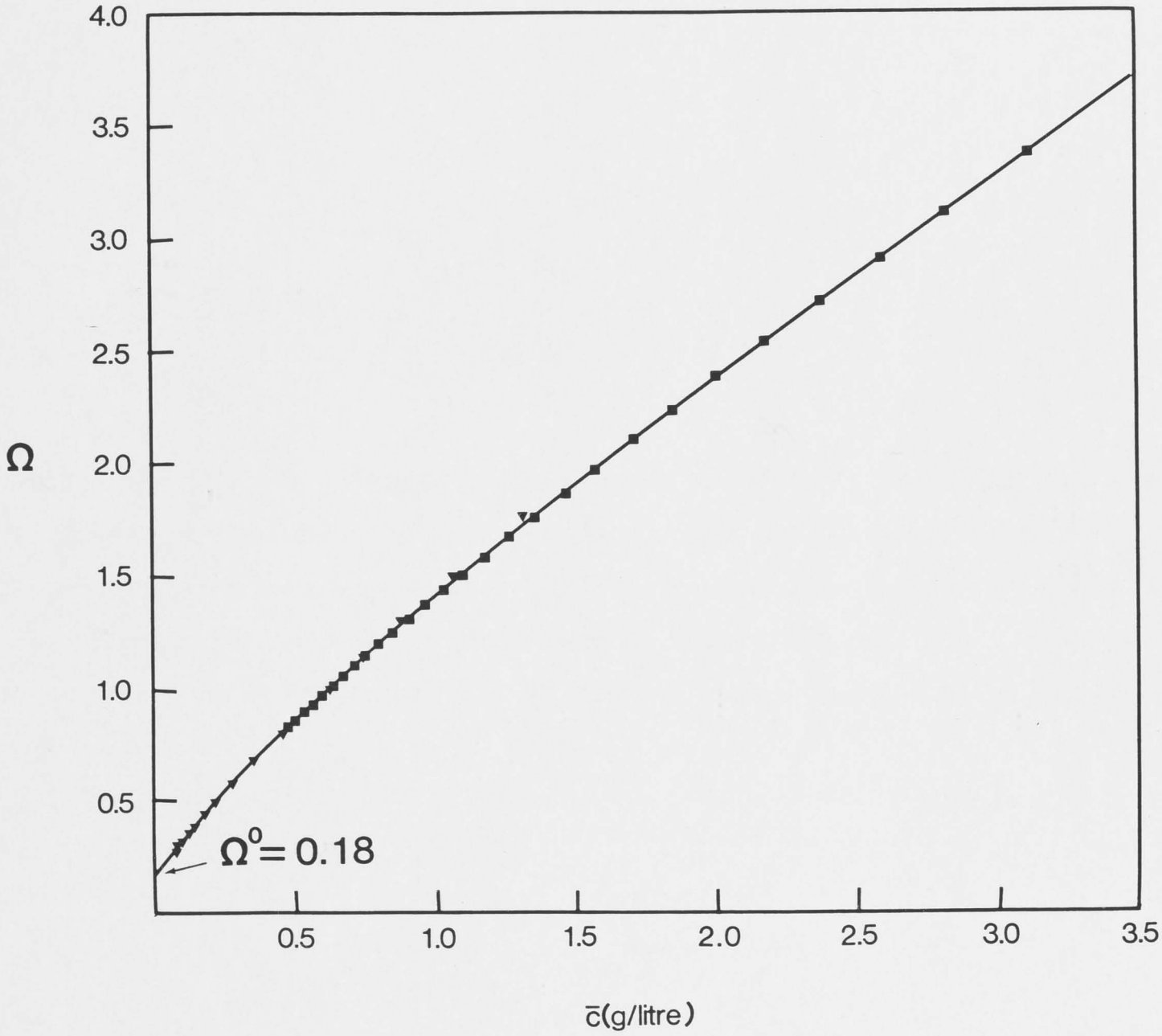
4.0
3.5
3.0
2.5
2.0
1.5
1.0
0.5
Ω
$\Omega^0 = 0.18$
0.5
1.0
1.5
2.0
2.5
3.0
3.5
$\bar{c}$(g/litre)

Figure 5.3: The result of analysing sedimentation equilibrium data, by the Ω method, obtained under conditions approximating those commonly used to investigate the binding of insulin to its receptor. The results relate to experiments 1 and 2 of Table 5.1 with the solid line being a line of best fit calculated using equation (4.16) assuming values for k_α and k_β of 5.0×10^4 M^{-1} and 0.3×10^4 M^{-1}, respectively.

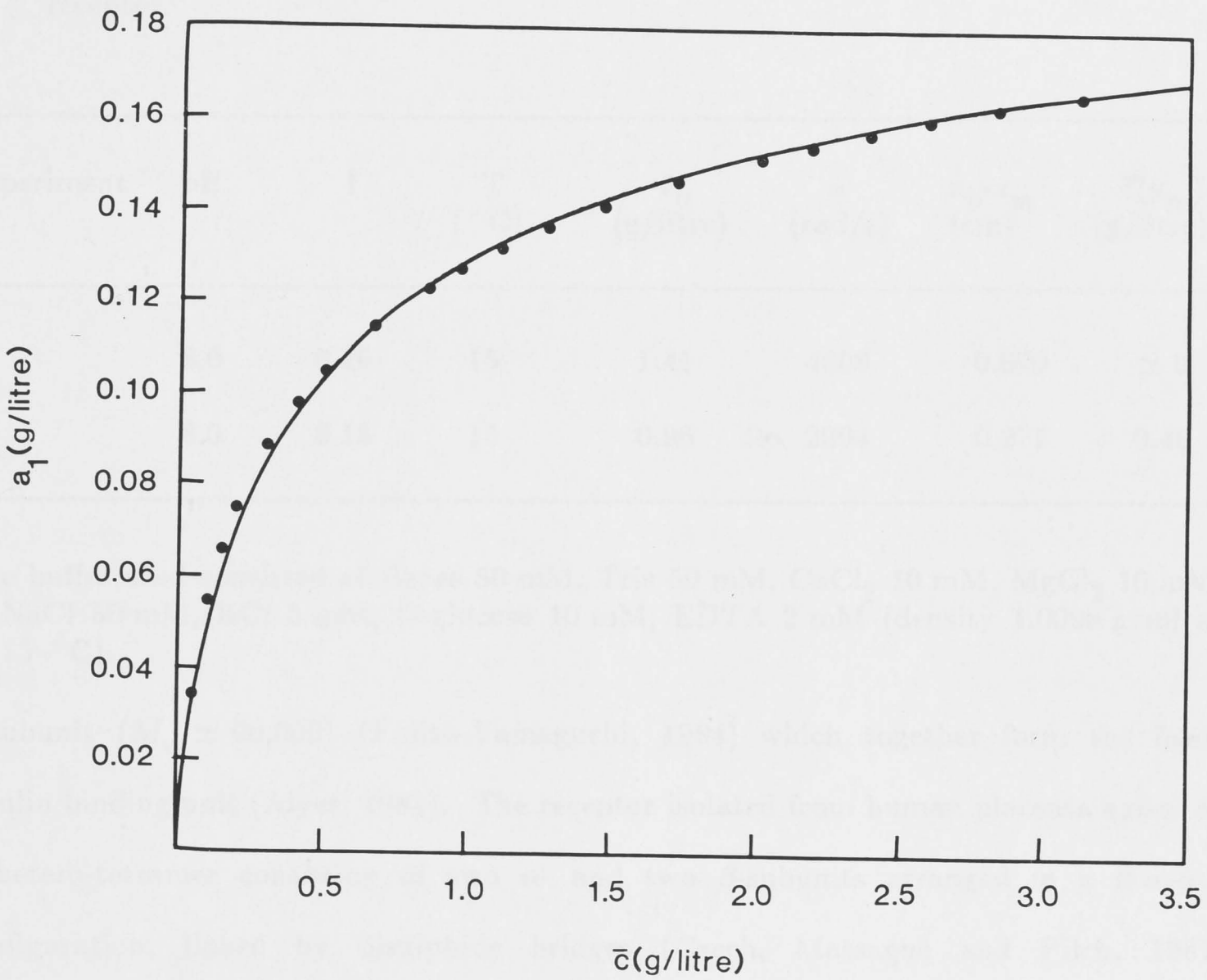
0.18
0.16
0.14
0.12
0.10
0.08
0.06
0.04
0.02
a_1(g/litre)
0.5
1.0
1.5
2.0
2.5
3.0
3.5
$\bar{c}$(g/litre)

Table 5.1: A summary of the experimental parameters applicable to sedimentation equilibrium experiments performed using zinc-free insulin under conditions approaching those commonly used to investigate the binding of insulin to its membrane receptor.

Experiment	pH	I	T (°C)	$\bar{c}_0$ (g/litre)	ω (rad/s)	x_b-x_m (cm)	$\bar{c}(x_m)$ (g/litre)
1	8.0	0.16	15	1.41	4608	0.670	$\simeq 0$
2	8.0	0.16	15	0.96	2094	0.271	0.46

The buffer used consisted of Hepes 50 mM, Tris 50 mM, $CaCl_2$ 10 mM, $MgCl_2$ 10 mM, NaCl 50 mM, KCl 5 mM, D-glucose 10 mM, EDTA 2 mM (density 1.0098 g/ml at 15 °C).

β-subunit ($M_w \simeq 90{,}000$) (Fujita-Yamaguchi, 1984) which together form the basic insulin binding unit (Aiyer, 1983). The receptor isolated from human placenta exists as a hetero-tetramer consisting of two α- and two β-subunits arranged in a β-α-α-β configuration, linked by disulphide bridges (Czech, Massague and Pilch, 1981; Fujita-Yamaguchi, 1984). Each of the subunits is glycosylated in such a way that the carbohydrate chains project into the extracellular medium and are believed to play a role in the orientation of the receptor within the membrane (Salzman, Wan and Rubin, 1984). The carbohydrate moieties may also play some role in the actual formation of the insulin binding site (Ronnett and Lane, 1981). This lies predominantly on the α-subunit, though there is some evidence from chemical crosslinking studies that the β-subunit may also be involved (Jacobs and Cautrecasas, 1983). Unlike the α-subunit, the β-subunit is a transmembrane protein extending into both the inter- and intra-cellular media. The β-subunit possesses a tyrosine specific phosphokinase activity which appears to play a role in transmembrane signalling associated with the hormone's action (Houslay and Heyworth, 1983). Few details in regard to the actual process of

insulin binding to its receptor are known. Due to its symmetry the receptor is believed to be bivalent, but this has been contested by some workers (Pang and Shafer, 1983; 1984). Insulin is believed to interact with the receptor through a region of the monomer involving mainly the same residues as those discussed in Chapter 4 as lying in the α self-interaction face (Pullen *et al.*, 1976). This implies that all insulin species with exposed α-sites may potentially bind to the receptor, a possibility supported by the work of Jeffrey (1985) who, in reanalysing the kinetic results of De Meyts (1980) in the light of the new model for the self-association of insulin, showed that species other than the insulin monomer must, in fact, be able to bind to the receptor.

The group of insulin species which have at least one exposed α-site include all odd-numbered species, dimers formed by the interaction of β-faces and all similarly formed higher even-numbered polymers. Thus, insulin has the potential not only to bind the receptor in long chains in a manner analogous to that considered in Chapter 2 but may also be able to crosslink the insulin receptors by virtue of the bifunctional even-numbered polymers. The question that must be asked is: are such considerations relevant in *in vitro* binding studies? It has already been shown that only monomeric insulin is present at the physiological insulin concentration in blood serum. *In vitro* binding studies, however, are conducted over a much wider concentration range.

Figure 5.4 shows the weight-fractions of both the α- and β-dimers and that of the trimer over the range of total insulin concentration normally examined in binding studies calculated using equation (5.1) assuming $k_\alpha = 2.05 \times 10^4\ \mathrm{M}^{-1}$ and $k_\beta = 1.63 \times 10^4\ \mathrm{M}^{-1}$. The broken line in Figure 5.4 gives the sum of the weight-fractions of all species, other than monomer, in the solution over the same concentration range. The first point to note in relation to Figure 5.4 is that, in contrast to the situation found in serum, significant quantities of polymeric insulin are present during insulin binding studies. This, as will be seen later, has important implications in the analysis of binding data. The other obvious feature of Figure 5.4 is that, to a reasonable first approximation, insulin acts as a monomer-dimer system over this concentration range. Therefore equations developed in Chapter 3 to describe the binding

Figure 5.4: The dependence of the weight-fractions (ϕ_i) of the α-dimer, the dimer with two exposed α-faces; the β-dimer, the dimer with two exposed β-faces and the trimer of insulin, on the total concentration of insulin over the concentration range normally used in insulin insulin-receptor binding studies. The curves were calculated using equation (5.1) assuming $k_\alpha = 2.05 \times 10^4\ M^{-1}$ and $k_\beta = 1.63 \times 10^4\ M^{-1}$ figures appropriate to pH 7.0, I = 0.1 and T = 25 °C. The broken line represents the sum of the weight-fractions of all species, other than monomer, in solution under the same conditions.

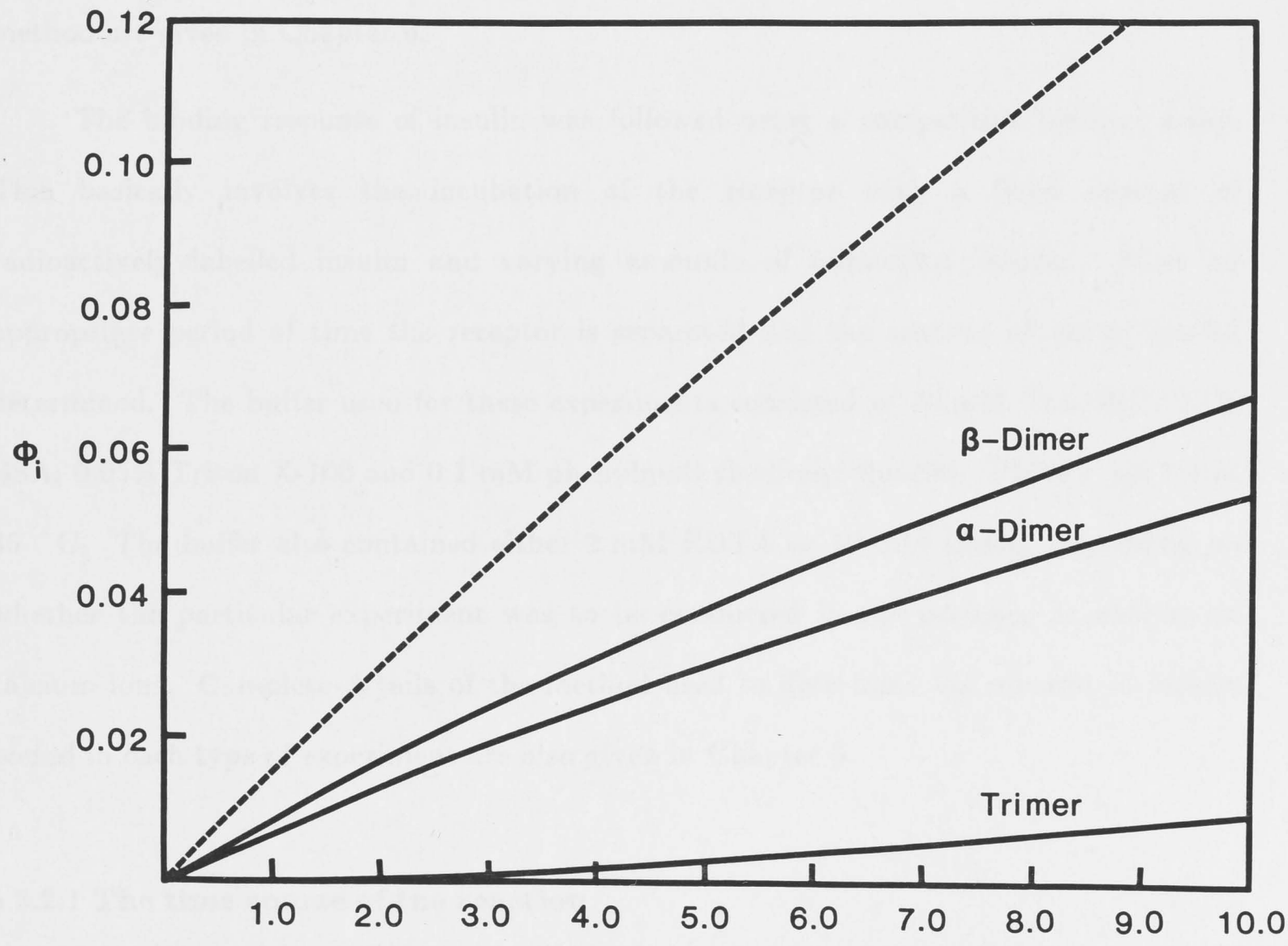
0.12
0.10
0.08
0.06
0.04
0.02
Φ_i
β–Dimer
α–Dimer
Trimer
1.0
2.0
3.0
4.0
5.0
6.0
7.0
8.0
9.0
10.0
$\bar{c}$(μg/ml)

of a dimerizing ligand to a bivalent acceptor may be directly applicable to the insulin system.

5.3.2 The Basic Form of the Binding Response

All work presented in this section relates to binding experiments conducted using human placental insulin receptors which had been solubilized in Triton X-100 and partially purified by affinity chromatography on wheat-germ-agglutinin Sepharose in accordance with the method of Fujita-Yamaguchi *et al.* (1983). Full details of this method are given in Chapter 6.

The binding response of insulin was followed using a competitive binding assay. This basically involves the incubation of the receptor with a fixed amount of radioactively labelled insulin and varying amounts of unlabelled insulin. After an appropriate period of time the receptor is separated and the amount of bound insulin determined. The buffer used for these experiments consisted of 50 mM Tris/HCl, 0.1% BSA, 0.05% Triton X-100 and 0.1 mM phenylmethylsulfonyl fluoride (PMSF); pH 7.4 at 35 °C. The buffer also contained either 2 mM EDTA or 10 mM $CaCl_2$, depending on whether the particular experiment was to be conducted in the presence or absence of calcium ions. Complete details of the method used to determine the amount of insulin bound in each type of experiment are also given in Chapter 6.

5.3.2.1 The time course of the reaction

In order to ascertain the time taken for the binding of insulin to its solubilized receptor to reach equilibrium, a series of time course experiments were conducted under conditions to be used in later binding experiments. The results are summarized in Figure 5.5 which shows, as a function of time, the amount of insulin bound as a percentage of the equilibrium value in the presence and absence of 10 mM calcium ions. Although Figure 5.5 shows results only for the first 120 minutes the reaction in both cases was followed until no increase in binding was observed for 60 minutes. The equilibrium value was taken to be the average obtained over this 60 minute period.

Figure 5.5: The time-course of insulin receptor binding at 35 °C. The experiments were conducted with solubilized receptors of human placenta in a buffer containing 50 mM Tris/HCl, 0.1% BSA, 0.05% Triton X-100 and 0.1 mM PMSF, pH 7.4 at 35 °C. The effect of calcium was determined by conducting the experiments in the presence of either 10 mM $CaCl_2$ (■) or 5 mM EDTA (▲). The results are expressed as the amount of insulin bound as a percentage of the equilibrium value and the solid lines represent attempts to average the data.

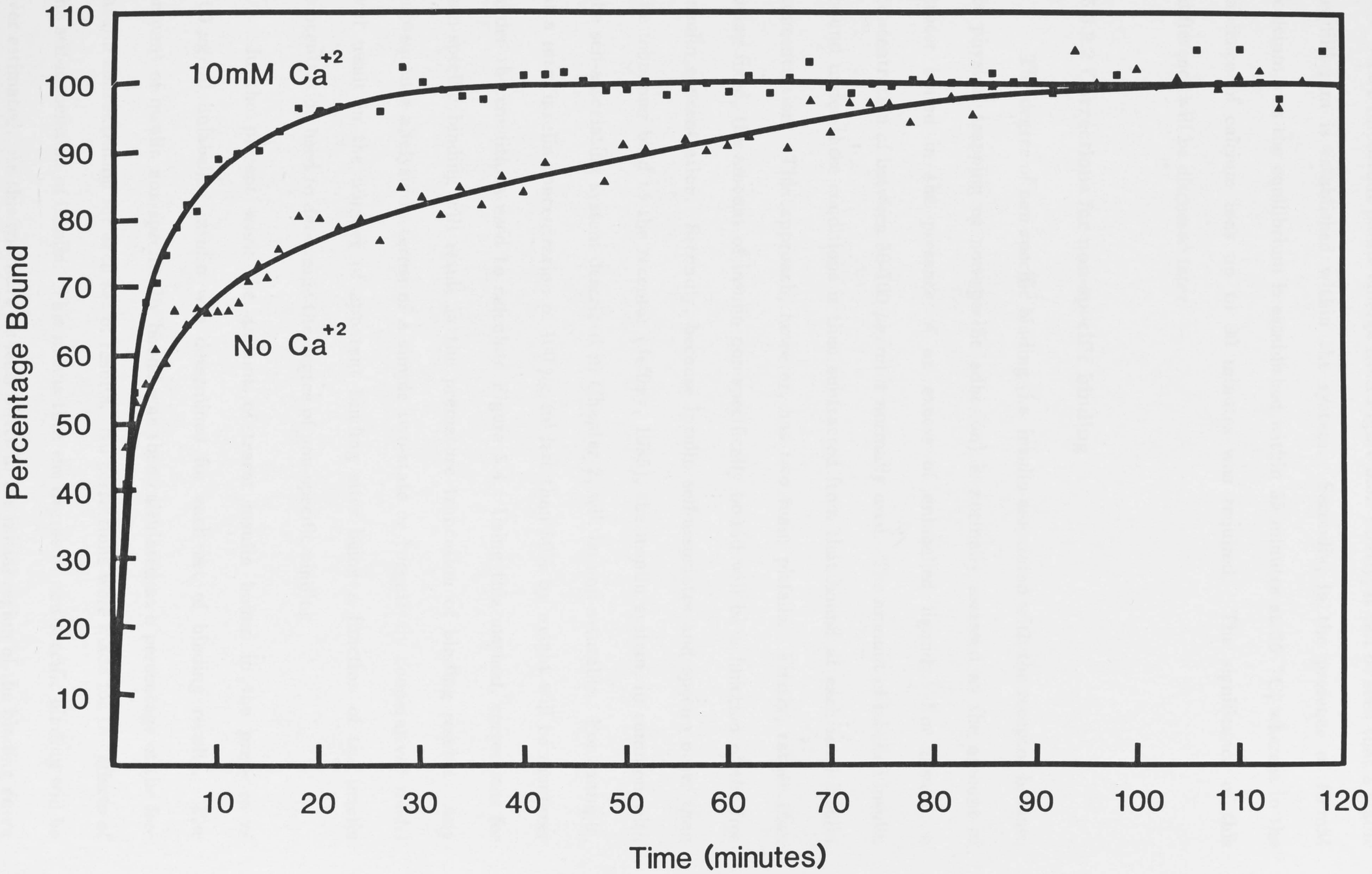
110
100
90
80
70
60
50
40
30
20
10
Percentage Bound
10mM Ca+2
No Ca+2
10
20
30
40
50
60
70
80
90
100
110
120
Time (minutes)

Two important points emerge from Figure 5.5. Firstly, it can be seen that a stable equilibrium is established within the system. Secondly, in the presence of 10 mM calcium ions the equilibrium is established within 35 minutes at 35 °C, whereas in the absence of calcium ions up to 90 minutes was required. The significance of this difference will be discussed later.

5.3.2.2 Corrections for non-specific binding

The degree of non-specific binding (i.e. insulin associated with the receptor because of physical trapping or non-specific adhesion) is normally assessed as the amount of tracer bound in the presence of an excess of unlabelled ligand. For insulin, a concentration of between 50-100 μg/ml is normally used. The amount of labelled insulin bound under these conditions is then subtracted from that bound at each total insulin concentration. This approach, however, has two main pitfalls. Firstly, rather than being fixed, the amount of insulin non-specifically bound will be a function of the free insulin concentration. Secondly, because insulin self-associates and species other than the monomer bind to the receptor (Jeffrey, 1985), the insulin system, in common with the self-associating system described in Chapter 2, will be non-saturable. For example, at a total insulin concentration of 100 μg/ml less than 50% by weight will be monomer under the conditions used to calculate Figure 5.4. Using this method, corrections for non-specific binding will result in the premature truncation of binding results. Any subsequence analysis in terms of a simple two-state or "negatively cooperative" model will result in the number of apparent binding sites being a function of the insulin concentration used to determine the degree of non-specific binding.

In the present work the amount of tracer insulin bound in the presence of 100 μg/ml unlabelled insulin was determined for each set of binding results. The amount of insulin non-specifically bound was then calculated as a percentage of the free insulin concentration for each set of results. No corrections were made for the effects of the self-association of insulin. This means that the degree of non-specific binding will be over estimated. As this will have its least effect in the initial region of the binding curve

(i.e. low free insulin concentration), discussion of the form of the curve will be concentrated on this region. Control experiments were conducted to ensure no component of the non-specific binding was due to the precipitation of free insulin.

5.3.2.3 Binding results: the form of the Scatchard plot

Figure 5.6 shows, in Scatchard format, the binding response obtained when insulin interacts with its partially purified solubilized receptor in a simple buffering system devoid of divalent cations. As can be seen, the binding response under these conditions is characterized by a curve convex to the abscissa. The solid line in Figure 5.6 is a theoretical curve which has been fitted to the data and will be discussed later. The results in Figure 5.6 have been presented in terms of the total amount of insulin bound rather than in terms of binding function, r, as defined in Chapter 2. This was necessary because it is not possible to determine the concentration of the receptor within the system without first assuming a model for the binding of insulin to its receptor.

The form of the curve presented in Figure 5.6 is consistent with the curvilinear Scatchard plots obtained by Williams, Caterson and Turtle (1984) and thus refutes the claim of Eckel and Reinauer (1984) that the removal of calcium linearizes the Scatchard plot. This point is significant as the majority of studies on the binding of insulin to solubilized receptors have been conducted in the presence of calcium ions. It has been well established (Williams, Caterson and Turtle, 1984; Desai, Zinman, Steiner and Hollenberg, 1978) that the addition of calcium not only increases the insulin binding affinity but also decreases the time taken to reach equilibrium, as shown in Figure 5.5. It is thus reasonable to assert that Figure 5.6 represents the true form of the insulin binding response. Similar results having been obtained in the vast majority of studies conducted to date irrespective of the source or purity of the receptor (Finn *et al.*, 1984; Fujita-Yamaguchi *et al.*, 1983; Grigorescu, White and Kahn, 1983).

Figure 5.6: A Scatchard plot pertaining to the binding of insulin to partially purified solubilized receptors from human placenta in the absence of divalent cations. Experiments were conducted as described in the text in a 50 mM Tris/HCl buffer containing 0.1% BSA, 0.05% Triton X-100, 0.1 mM PMSF, 5 mM EDTA, pH 7.4 at 35 °C. The line was computed using equations (3.28) and (3.30) which relate to the binding of a dimerizing ligand system to a bivalent acceptor. The monomeric form of the ligand being monovalent and the dimeric form being divalent. This theoretical curve which attempts to fit the data was calculated using $k_1 = 1 \times 10^{10}\ \mathrm{M}^{-1}$, $k_2 = 1 \times 10^{9}\ \mathrm{M}^{-1}$, $K_2 = 1 \times 10^{11}\ \mathrm{M}$, and $\bar{m}_A = 1 \times 10^{-11}\ \mathrm{M}$.

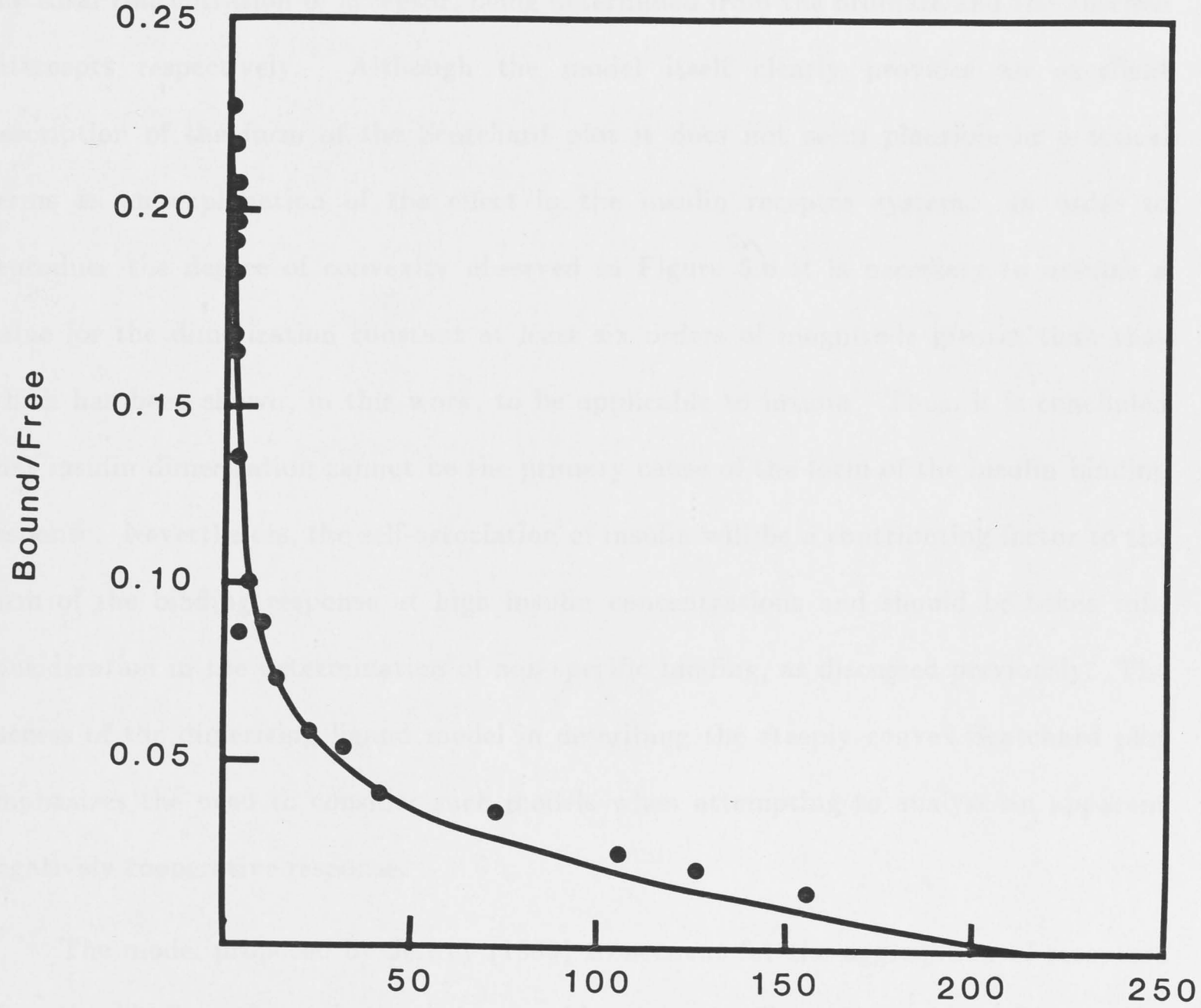
0.25
0.20
0.15
0.10
0.05
Bound/Free
50
100
150
200
250
Insulin Bound (ng/ml)

5.3.2.4 Interpretation of the basic convexivity of the Scatchard plot

The solid line in Figure 5.6 was generated using equations (3.28) and (3.30) which relate to a dimerizing ligand system in which the monomer and dimer are capable of interacting with a divalent acceptor as described in Chapter 3. The curve was calculated with $k_1 = 1 \times 10^{10}\ \mathrm{M}^{-1}$, $k_2 = 1 \times 10^{9}\ \mathrm{M}^{-1}$, $K_2 = 2 \times 10^{11}\ \mathrm{M}^{-1}$, and $\bar{m}_A = 1 \times 10^{-11}$ M, with the values of k_1, the monomer association constant, and $\bar{m}_A$, the total concentration of acceptor, being determined from the ordinate and the abscissa intercepts respectively. Although the model itself clearly provides an excellent description of the form of the Scatchard plot it does not seem plausible in practical terms as an explanation of the effect in the insulin receptor system. In order to reproduce the degree of convexity observed in Figure 5.6 it is necessary to assume a value for the dimerization constant at least six orders of magnitude greater than that which has been shown, in this work, to be applicable to insulin. Thus, it is concluded that insulin dimerization cannot be the primary cause of the form of the insulin binding response. Nevertheless, the self-association of insulin will be a contributing factor to the form of the binding response at high insulin concentrations and should be taken into consideration in the determination of non-specific binding, as discussed previously. The success of the dimerizing ligand model in describing the steeply convex Scatchard plot emphasizes the need to consider such models when attempting to analyse an apparent negatively cooperative response.

The model proposed by Jeffrey (1985) to account for the aggregation of receptors after the binding of insulin was also considered in detail in Chapter 3. This model envisaged the association of acceptor-ligand complexes initiated by the binding of ligand to the receptor. In regard to the insulin system, Jeffrey (1985) viewed the association as occurring through insulin dimer bridges. Although this model should be recognized as one of the first attempts to account for the observed aggregation phenomenon, it cannot explain the form of the binding response as it was clearly shown in Chapter 3 that only binding curves concave to the abscissa in Scatchard format are predicted by this model.

A third model developed in Chapter 3 viewed the insulin monomer as a

crosslinking agent which could undergo a conformational change on binding to permit the association of receptors via a single ligand bridge. This model is also capable of producing a binding curve convex to the abscissa in Scatchard format and when fitted to the experimental data, as shown in Figure 5.7, yields more realistic values for the two association constants, k_1 describing the binding of insulin to the receptor and k_2 the subsequent crosslinking to a second receptor molecule. It is evident from the theoretical line in Figure 5.7 that the model in its basic form is capable of generating only an approximate fit to the experimental data. For this reason it cannot be regarded as an entirely satisfactory description of the mechanism operating in the insulin system. Nevertheless, the basic postulate that the binding of insulin could initiate the aggregation of the receptors, possibly with an A_2B stoichiometry, though not necessarily involving insulin as a bridging ligand, is worthy of further exploration. In this connection it is especially noteworthy that just such a two state equilibrium is consistent with the kinetic and equilibrium insulin binding studies of Lipkin, Teller and de Haen (1986b).

5.3.3 Fine Details of the Binding Response

5.3.3.1 Binding curve sigmoidicity

In a recent article Marsh, Westly and Steiner (1984) asserted that at free insulin concentrations below 10 ng/ml insulin binding curves exhibit sigmoidicity and hence a maximum in the Scatchard plot. This would be consistent with the competitive but preferential binding of polymeric insulin over that of the monomer [Chapter 3 Section 3]. Figure 5.8 shows the initial portion of the Scatchard plot presented in Figure 5.6 corresponding to free insulin concentrations between 0.05 and 20.0 ng/ml. The solid line is a linear least squares line of best fit calculated giving all points equal weight. The magnitude of the errors associated with the determinations are also shown on this plot and were included in order to stress the experimental difficulty faced when attempting to detect minor features in the form of the Scatchard plot. The amplification of errors is a major problem with derived plots such as the Scatchard plot. Nevertheless, Figure 5.8

Figure 5.7: An attempt to fit the binding data presented in Figure 5.6 to a model in which the binding of an initially monovalent ligand to a bivalent acceptor induces a conformational change in the ligand which permits the crosslinking of receptors through a single ligand bridge. The theoretical line was calculated on the basis of equations (3.14) and (3.15) using $k_1 = 2.5 \times 10^9$ M^{-1}, $k_2 = 2.0 \times 10^{11}$ M^{-1}, and $\bar{m}_A = 1.3 \times 10^{-11}$ M.

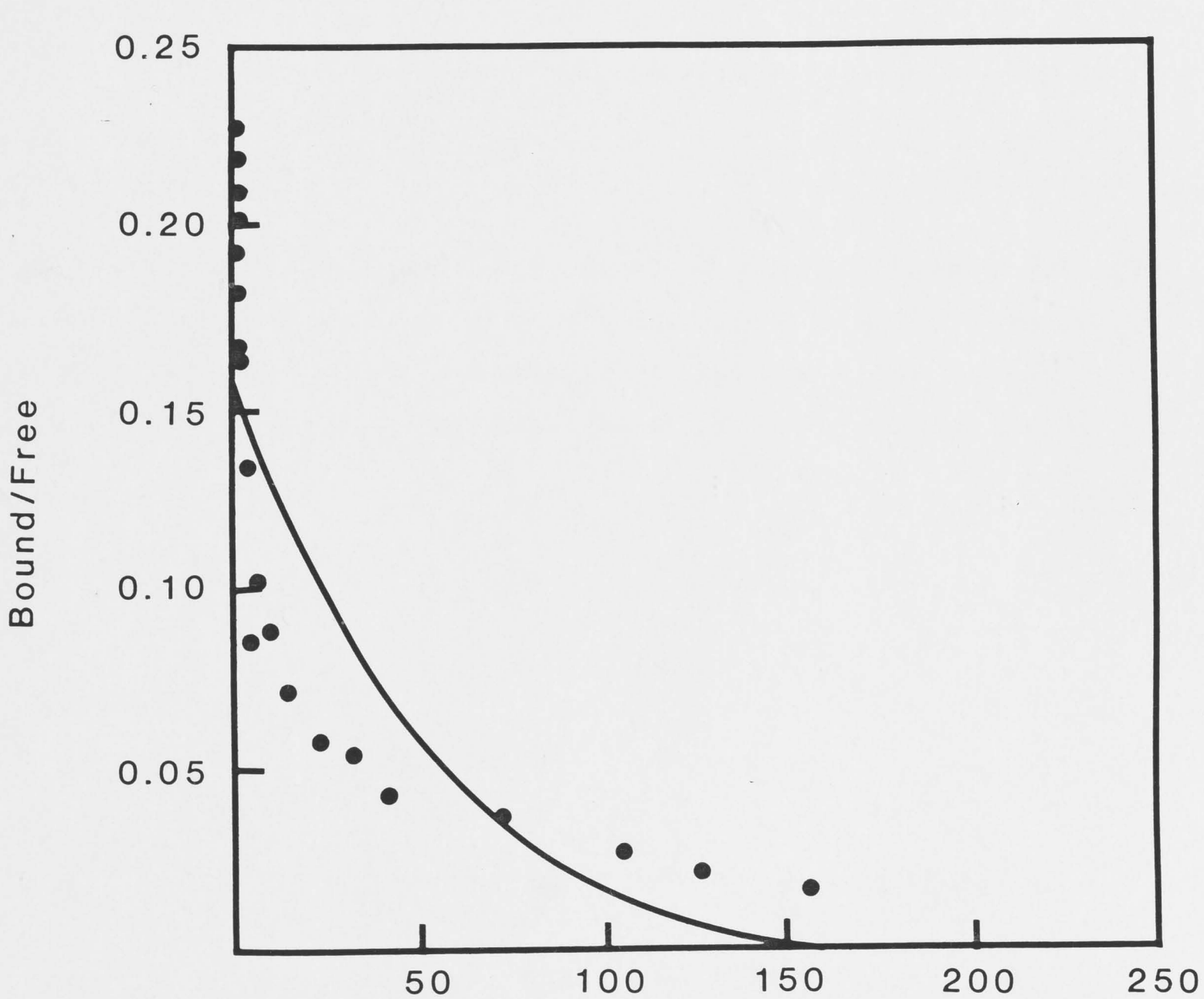
0.25
0.20
0.15
0.10
0.05
Bound/Free
50
100
150
200
250
Insulin Bound (ng/ml)

Figure 5.8: The initial region of the Scatchard plot presented in Figure 5.6 is shown in expanded format. The figure demonstrates that to within experimental error this region can best be described by a straight line. The solid line is a linear least squares regression of best fit giving all points equal weighting.

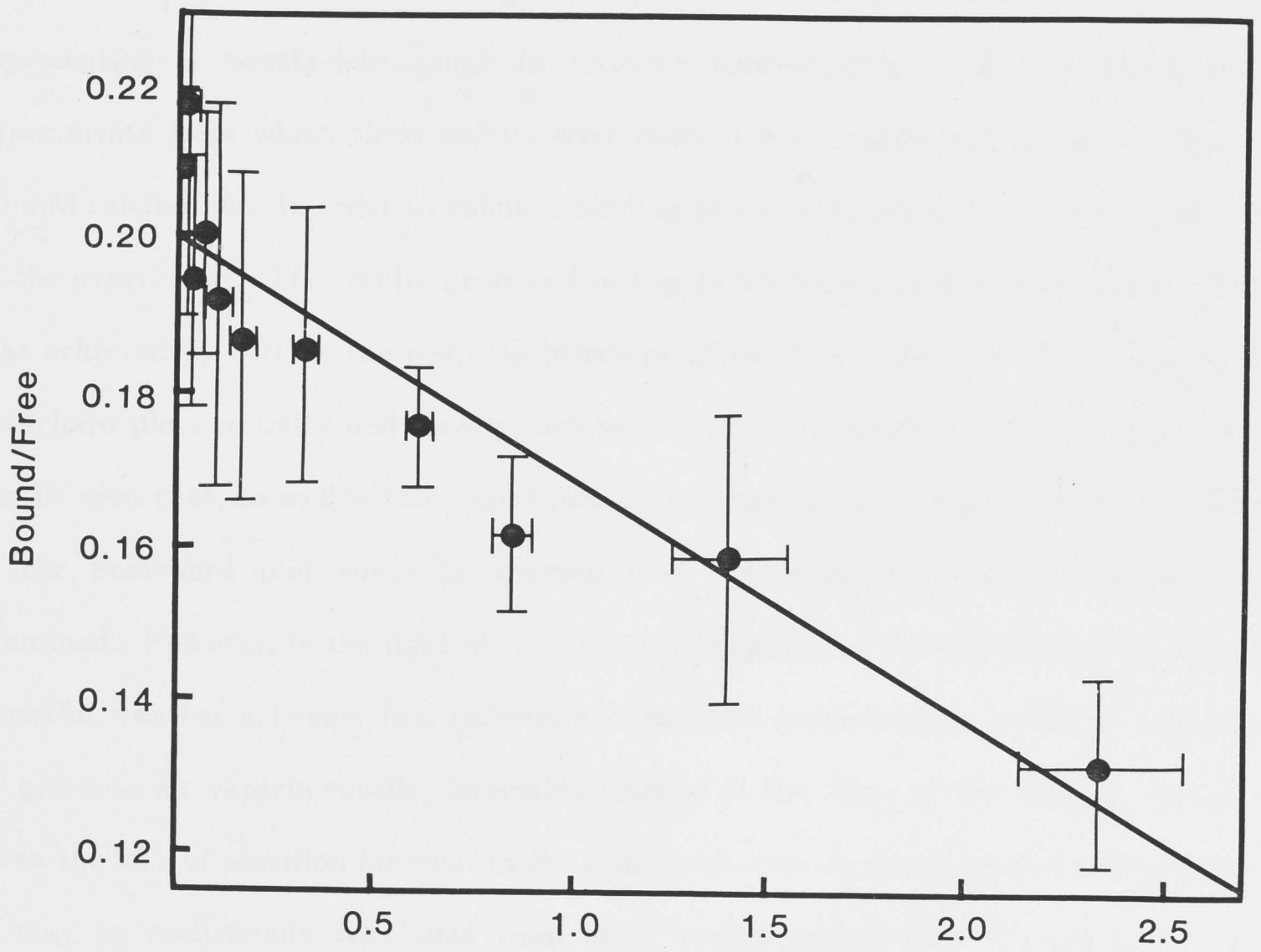
0.22
0.20
0.18
0.16
0.14
0.12
Bound/Free
0.5
1.0
1.5
2.0
2.5
Insulin Bound (ng/ml)

clearly demonstrates that under these conditions the Scatchard plot contains no observable maximum.

5.3.3.2 Receptor concentration dependence

Theoretical developments in Chapter 3 showed that one consequence of a binding mechanism involving crosslinking would be the dependence of the form of the binding response on the concentration of the receptor. Figure 5.9 shows the superposition of the low free insulin concentration region (0.02 to 20 ng/ml) of two Scatchard plots representing a twenty-fold range in receptor concentration. The initial binding experiments from which these results were derived were conducted in the presence of 10 mM calcium ions in order to enhance binding and thus increase the overall sensitivity of the experiment. The results presented in Figure 5.9 have also been normalized. This was achieved by setting the ordinate intercept of the line of best fit of the respective Scatchard plots to unity and scaling each set of data appropriately. From Figure 5.9 it can be seen that, to well within experimental uncertainty, no change in the initial form of the Scatchard plot could be claimed over the range of receptor concentration examined. However, in the light of the numerical examples discussed in Chapter 3, it is doubtful whether a twenty-fold difference in receptor concentration would be sufficient to generate an experimentally detectable change in the form of the binding response given the lack of precision inherent in the assay procedure as demonstrated in Figure 5.8. It may be realistically concluded from these considerations that binding curves for receptor concentrations ranging between 10^{-8} and 10^{-11} M would be needed for rigorous testing of a cross-linking hypothesis. Unfortunately, such a concentration range was not attainable with the partially purified receptor preparation. Thus, the results presented in Figure 5.9 cannot be taken as definitive.

5.4 THE BINDING OF INSULIN TO INTACT CELLS

5.4.1 The Present Picture

In whole cells the binding of insulin to its receptor is but the first step in a series of

Figure 5.9: Receptor concentration dependence in the binding of insulin to receptors from human placenta. Scatchard plots of the initial region of binding curves obtained with solubilized receptor are shown for concentrated receptor (•) and a 1:20 dilution (▲) of the concentrated receptor preparation. The binding was carried out in a 50 mM Tris/HCl buffer containing 0.1% BSA, 0.05%, Triton X-100, 0.1 mM PMSF and 10 mM $CaCl_2$, pH 7.5 at 35 °C. In order to superimpose the result each data set was normalized by setting the ordinate intercept of a line of best fit to unity.

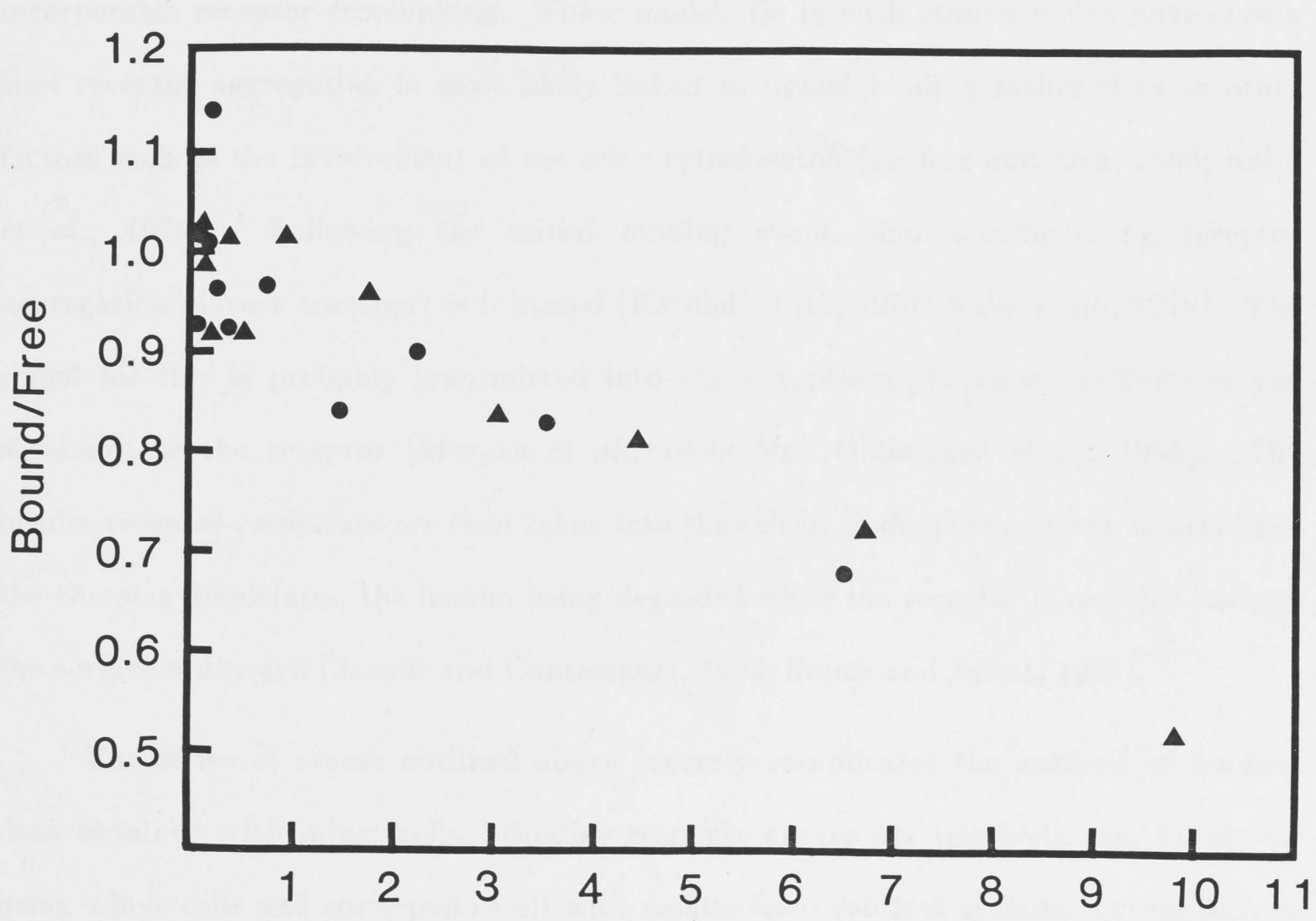
Bound/Free
1.2
1.1
1.0
0.9
0.8
0.7
0.6
0.5
1
2
3
4
5
6
7
8
9
10
11
Insulin Bound (ng/ml)

events leading to a cascade of metabolic and growth effects (Kahn *et al.*, 1981; Denton, Brownsey and Belsham, 1981). Among the first of these events is the initiation of receptor aggregation, possibly associated with conformational changes in either the receptor or insulin itself (Houslay and Heyworth, 1983; Dodson *et al.*, 1983). Although receptor aggregation apears to be required for the generation of transmembrane signals, little is known about the mechanism by which it occurs (Jeffrey, 1982; Kahn *et al.* 1981). In the main body of this chapter an attempt has been made to address this question. Models have been proposed for the interaction between insulin and its receptor which incorporates receptor crosslinking. These models tie in with studies which have shown that receptor aggregation is most likely linked to ligand binding rather than to other factors such as the involvement of the cell's cytoskeleton (Heffetz and Zick, 1986; Kahn *et al.*, 1978). Following the initial binding event, and accompanying receptor aggregation glucose transport is initiated (Karnieli *et al.*, 1981; Kahn *et al.*, 1978). The signal for this is probably transmitted into the cytoplasm via kinase activity of the β-subunit of the receptor (Morgan *et al.*, 1986; Van Obberghen *et al.*, 1985). The insulin-receptor complexes are then taken into the cell by endocytosis. Once internalized the complex dissociates, the insulin being degraded while the receptor is recycled back to the surface of the cell (Jacobs and Cuatrecasas, 1983; Smith and Jarett, 1983).

The series of events outlined above severely complicates the analysis of binding data obtained with intact cells. Binding response curves are relatively easy to obtain using whole cells and correspond well with results from cell-free systems, curves convex to the abscissa being found by most (de Vries and Van der Veen, 1985; Peterson *et al.*, 1983; Pollet, Standaert and Haase, 1977), but again not all (Lipkin, Teller and de Haen, 1986a), workers. However, it is doubtful whether these results represent the true equilibrium situation between receptors on the cell's surface and insulin free in solution. The first complication arises as a result of a process known as "down regulation", where the number of receptors expressed on the surface of a cell will not be constant throughout the course of the experiment (Capeau *et al.*, 1985; Chun *et al.*, 1984). "Down regulation" results from the exposure of a cell to insulin, studies on erythrocytes

having shown that the number of cell-surface receptors decrease by up to 70% within three hours during incubation with 1 μg/ml of insulin at 15 °C (Peterson *et al.*, 1983). Secondly, correcting for non-specific binding is difficult as much of the insulin trapped internally within a cell will not be associated with receptor (Jacobs and Cuatrecasas, 1983). The problem of insulin degradation is also contentious (Davidson and Vankatesan, 1982), one worker claiming that if corrections are made for the binding of hormone fragments the Scatchard plot is linearized (Donner, 1980). This is not meant to imply that binding studies with the whole cells are unimportant, but rather to assert that to make detailed mechanistic conclusions on the basis of such studies is premature. This point is exemplified by the debate between proponents of "negative cooperativity" and a two-state receptor hypothesis for the binding of insulin to its receptor (Bonen *et al.*, 1984; Corin and Donner, 1982; De Meyts, Bianco and Roth, 1976; De Meyts *et al.*, 1973). Both models are capable of reproducing the form of the binding response and while neither can account for insulin-induced receptor aggregation, either might be at least in part correct. To distinguish between them is, however, not possible on the basis of binding data obtained with intact cells alone.

5.4.2 Conclusions and Future Approaches

The results presented in this chapter have led both to the sounding of cautionary notes and to the development of a concept which may be further tested in the future. On the negative side, the possibility that the self-association of insulin plays a primary role in the determination of the convex binding response has been eliminated (Fig. 5.6). Moreover, problems with experimental systems involving intact cells and the need for further study using highly purified receptors have both been highlighted. Clearly, there is at present a danger [pointed out by Klotz and Hunston (1984) on theoretical grounds] of drawing inappropriate mechanistic conclusions on the basis of results from binding studies presented in this work and elsewhere.

On the positive side, it does seem reasonable to suggest that there may well be a direct link between association of receptors initiated by the binding of insulin and, at

least in part, the convexity in the form of the binding response plotted in Scatchard format. In this connexion, the exclusion of the model proposed by Jeffrey (1985) on the theoretical grounds developed in Chapter 3, and the illustrative fit, albeit relatively poor, of the theoretical convex plot in Figure 5.7 to experimental results are advances in this complicated area. It may well be that association of receptors via a single ligand (insulin) bridge is simplistic or only one of the factors contributing to the convexity observed. Nevertheless, the possibility of crosslinking of receptors can no longer be ignored and, as highly purified receptor becomes available, studies, such as those exemplified in Fig. 5.9, should be possible to explore the concept further. It is fair to claim that the theoretical developments in this thesis may assist in this endeavour.

CHAPTER 6
MATERIALS AND METHODS

6.1 MATERIALS

6.1.1 Chemicals

Standard laboratory chemicals used in this work were of analytical reagent grade supplied by either Ajax Chemicals Ltd., British Drug Houses Ltd. or Merck. Tris(hydroxymethyl)amino-methane (Tris), N-2-hydroxylethylpiperazine-N'-2-ethane-sulfonic acid (HEPES), phenylmethylsulfonyl fluoride (PMSF) and and N-acetylglucosamine were obtained from the Sigma Chemical Co., polyethylene glycol (6000) was supplied by Fluka A.G. while Triton X-100 was obtained from Bio Rad. British Drug Houses Ltd. electran grade acrylamide and bisacrylamide were used for analytical polyacrylamide gel electrophoresis. Except where stated in the text all chemicals were used without further purification.

6.1.2 Buffers

The composition of all buffers employed in this work has been specified in the text. Buffers were prepared using glass-distilled water and analytical grade reagents. A Radiometer pH meter (model 26) equipped with a combination electrode (GK2321C) was used to determine pH values, measurements being made either at the cited temperature or at 20 °C with corrections effected employing α(pH)/dT coefficients (McKenzie, 1969). Before storage at 4 °C all buffers were partially sterilized by passage through a 0.22 μm Millipore filter.

6.1.3 Proteins

6.1.3.1 Ultracentrifugation studies

Crystalline "single peak" bovine zinc-insulin was purchased from the Commonwealth Serum Laboratories, Australia (Batch 601-153-459, 24.2 units/mg). The insulin was freed of zinc by dialysis at 4 °C, of a solution of zinc-insulin (10 mg/ml in 0.01 M

HCl) against 100 times its volume of 0.01 M HCl for 48 hours with three changes of dialysate. This procedure has been demonstrated to result in a zinc concentration of less than 0.1 ppm (Milthorpe, 1977). A combination of gel filtration and ion-exchange chromatography was then used to obtain the highly purified product required for the ultracentrifugation studies.

6.1.3.2 **Gel filtration**

The first chromatographic purification step involved gel filtration to remove traces of proinsulin and other high molecular weight impurities such as covalently linked insulin polymers. A column (1.7 cm by 60 cm) of G-50 superfine Sephadex gel (Pharmacia Fine Chemicals) was poured and equilibrated with a solution consisting of 0.01 M HCl containing 0.1 M NaCl following the procedure recommended by the manufacturer. A sample of crude zinc-free insulin (100 mg in 2 ml of equilibrating solution) was applied to the column and the column eluted at a flow rate of 10 ml/hour with the aid of a peristaltic pump. Figure 6.1 shows a typical elution profile from this column, the elution of protein being monitored by way of the optical density of the elutant at 276 nm. In the example shown in Figure 6.1 2.5 ml fractions were collected, fractions 28 to 33 being pooled and concentrated using an Amicon YM2 ultrafiltration membrane.

6.1.3.3 **Ion-exchange chromatography**

The final purification step involved ion-exchange chromatography on diethylaminoethyl-cellulose (DEAE-celluose) and was specifically directed toward the removal of monodesamido-insulin, a degradation product of insulin and a common impurity in commercial preparations (Chance, Root and Galloway, 1976). A chromatographic column (2.6 cm by 20 cm) of DEAE-cellulose (Watman DE-52) was prepared in accordance with manufacturer's directions, the gel being pre-equilibrated with the appropriate buffer (0.01 M Tris/HCl, 7.0 M Urea, 0.001 M EDTA, pH 8.1 at 25 °C) before the column was poured. The urea used in this buffer was deionized by

Figure 6.1: A plot of the optical density at 276 nm as a function of the fraction number obtained from column chromatography of zinc-free "single-peak" bovine insulin at pH 2.0 on Sephadex G-50 gel.

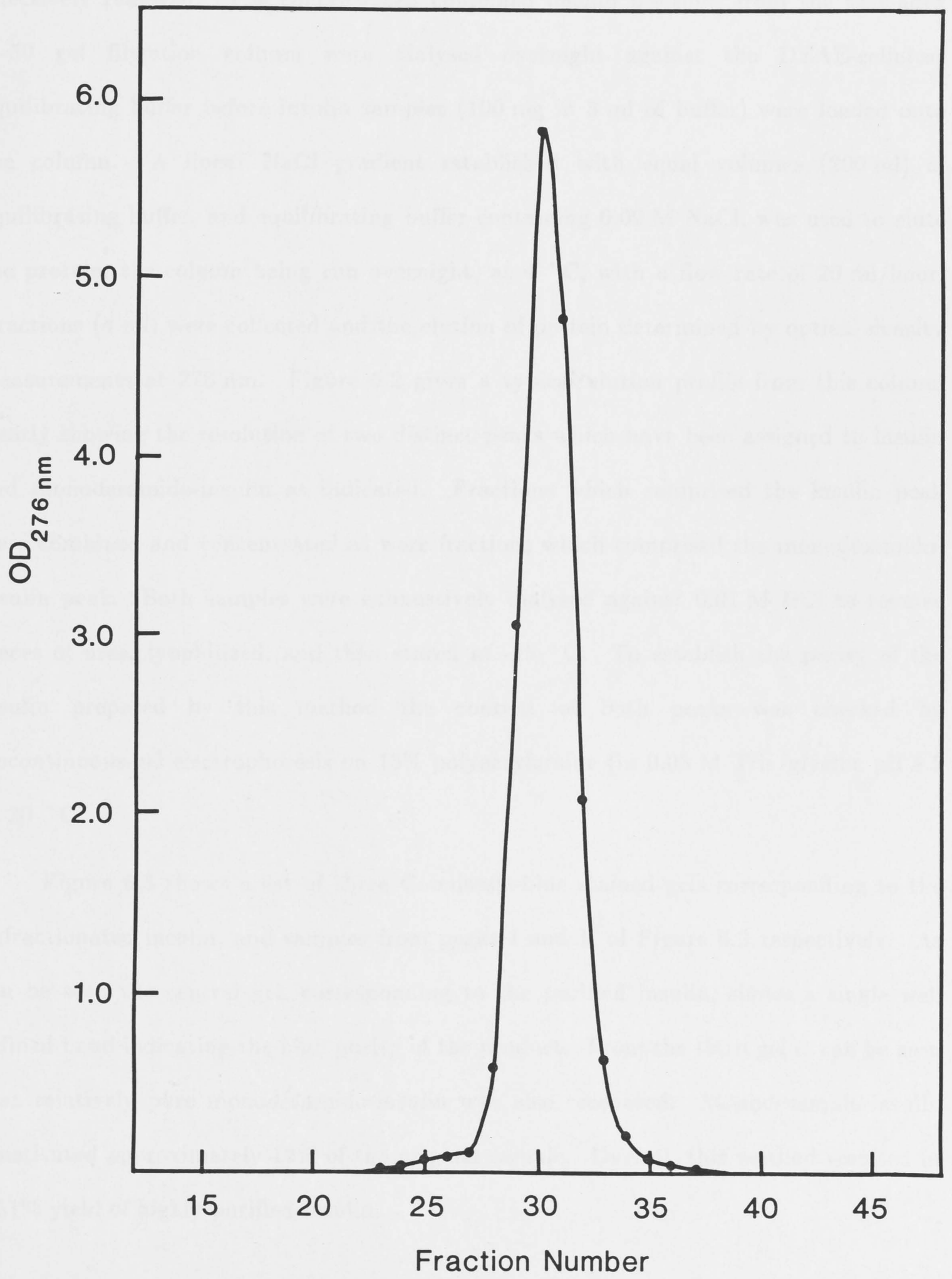
6.0
5.0
4.0
3.0
2.0
1.0
OD276 nm
15
20
25
30
35
40
45
Fraction Number

passage down a mixed-bed ion-exchange column (Bio Rad AG 501-AX) immediately prior to the buffer being constituted (Busse and Carpenter, 1976), with conductivity measurements being used to establish that contaminating isocyanate ions had been effectively removed. The concentrated combined insulin fractions from the Sephadex G-50 gel filtration column were dialysed overnight against the DEAE-cellulose equilibrating buffer before insulin samples (100 mg in 5 ml of buffer) were loaded onto the column. A linear NaCl gradient established with equal volumes (200 ml) of equilibrating buffer, and equilibrating buffer containing 0.09 M NaCl, was used to elute the protein; the column being run overnight, at 4 °C, with a flow rate of 20 ml/hour. Fractions (4 ml) were collected and the elution of protein determined by optical density measurements at 276 nm. Figure 6.2 gives a typical elution profile from this column clearly showing the resolution of two distinct peaks which have been assigned to insulin and monodesamido-insulin as indicated. Fractions which comprised the insulin peak were combined and concentrated as were fractions which comprised the monodesamido-insulin peak. Both samples were exhaustively dialysed against 0.01 M HCl to remove traces of urea, lyophilized, and then stored at -15 °C. To establish the purity of the insulin prepared by this method the content of both peaks was checked by discontinuous-gel electrophoresis on 15% polyacrylamide (in 0.05 M Tris/glycine pH 8.3 at 20 °C.

Figure 6.3 shows a set of three Coomassie-blue stained gels corresponding to the unfractionated insulin, and samples from peaks I and II of Figure 6.2 respectively. As can be seen the central gel, corresponding to the purified insulin, shows a single well defined band indicating the high purity of the product. From the third gel it can be seen that relatively pure monodesamido-insulin was also recovered. Monodesamido-insulin constituted approximately 12% of the original sample. Overall, this method resulted in a 51% yield of highly purified insulin.

6.1.4 **Receptor Binding Studies**

Receptor grade [^{125}I-Tyr^{A14}]-monoiodinated porcine insulin (Lot No. N366260,

Figure 6.2: A plot of the optical density of 276 nm as a function of the fraction number, obtained as a result of rechromatographing the insulin eluted from the Sephadex G-50 gel filtration column on DEAE-cellulose. The column was eluted using a linear NaCl gradient 0.0 to 0.09 M. Peak I corresponds to insulin while peak II corresponds to monodesamido-insulin.

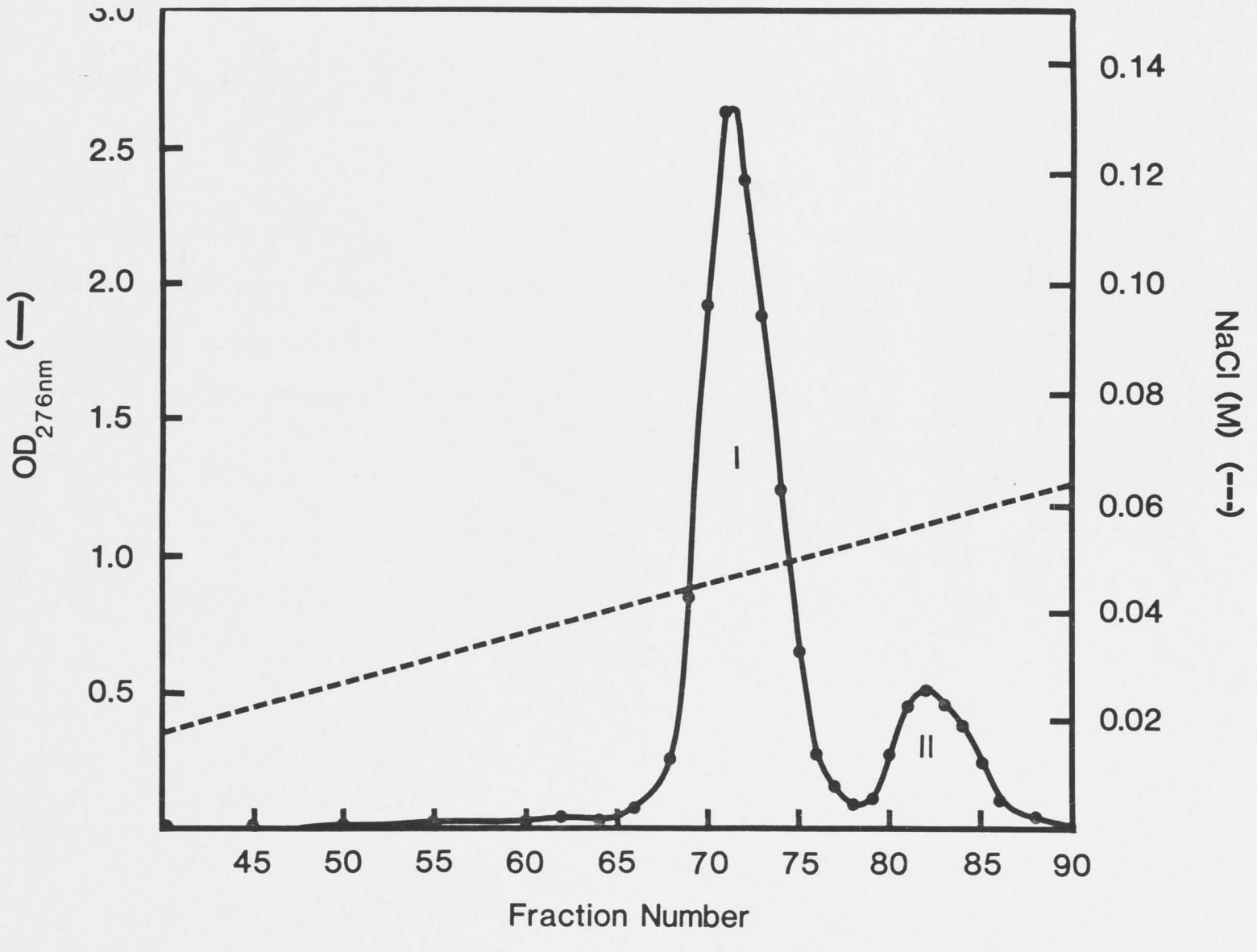
3.0
2.5
2.0
1.5
1.0
0.5
OD_{276nm} (—)
0.14
0.12
0.10
0.08
0.06
0.04
0.02
NaCl (M) (---)
I
II
45
50
55
60
65
70
75
80
85
90
Fraction Number

Figure 6.3: A series of Comassie blue stained polyacrylamide gels comparing unfractionated insulin with insulin from peaks I and II eluted from the DEAE-cellulose column [Figure 6.2]. The electrophoresis was performed at pH 8.3 on 15% acrylamide gels as described in the text. The bands corresponding to insulin and monodesamido-insulin are indicated.

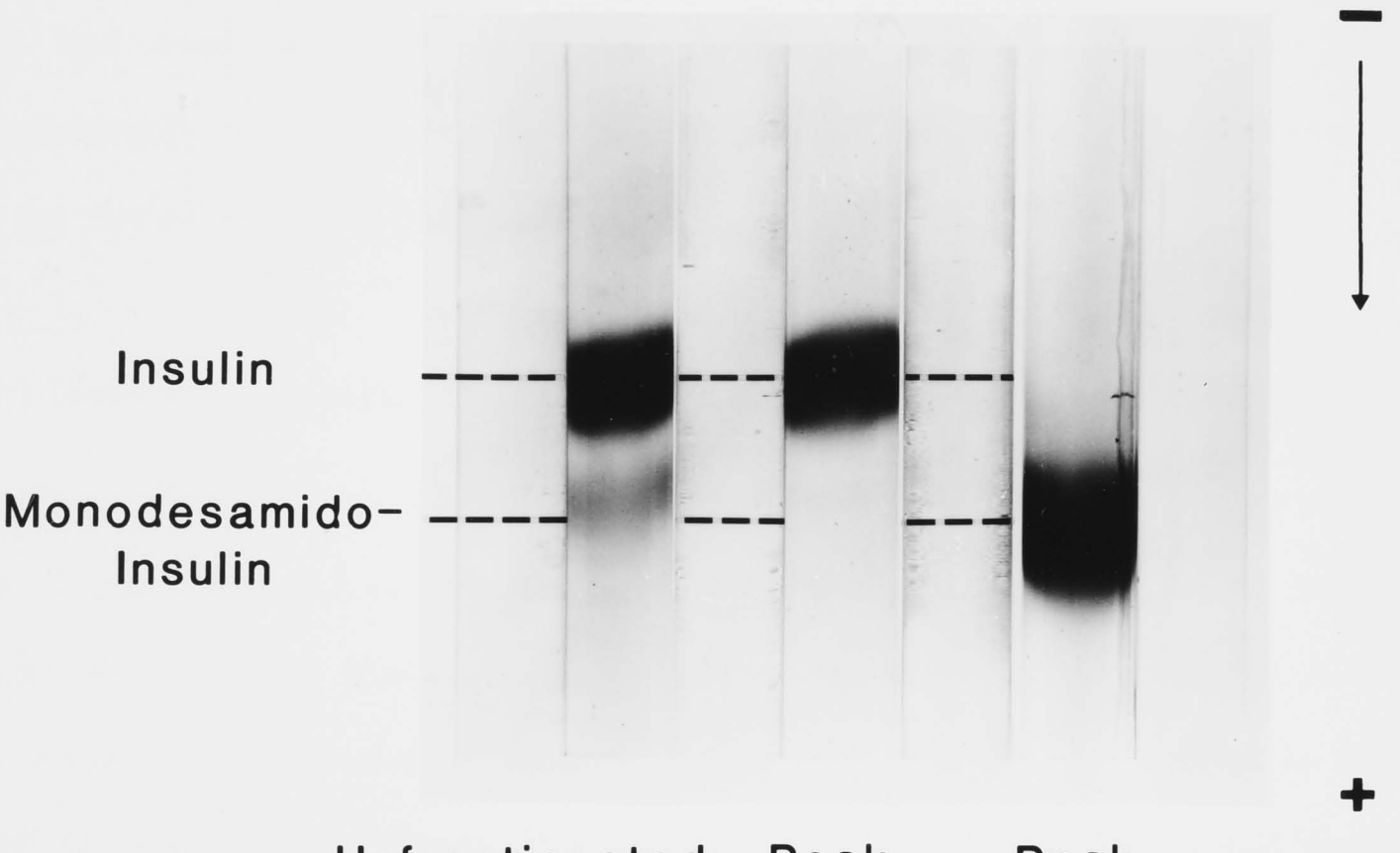

Unfractionated Insulin | Peak I | Peak II

2200 Ci/mmole), New England Nuclear Research Products, was used, without further purification, as a tracer in all binding experiments. This derivative has been reported to have binding characteristics indistinguishable from those of native porcine insulin (Peavy *et al.*, 1984). Crystalline porcine insulin (Batch 646.172.520, 25.7 units/mg) was obtained from the Commonwealth Serum Laboratories, Australia and apart from being freed of zinc in accordance with the method outlined previously, was used without further purification. Bovine serum albumin (BSA) (Fraction V, Lot No. 53F0255) and bovine γ-globulin (Cohn Fraction II, Lot. No. 14F0554) were purchased from Sigma Chemical Co. and were also used without further purification.

All binding experiments were conducted using human placental insulin receptors which had been solubilized in Triton X-100 and partially purified by affinity chromatography on wheat germ agglutinin Sepharose (WGA-Sepharose) in accordance with the method of Fujita-Yamaguchi *et al.* (1983) as described below.

6.1.4.1 **Isolation of placental plasma membranes**

Fresh normal human placentas were obtained within 1 hour of delivery from the labour wards of Royal Canberra and Calvary hospitals. The placentas were stored on ice until collected and, where possible, subsequent operations were conducted at 4 °C. Each placenta was trimmed of amnion and chorion before being washed in 0.25 M sucrose to remove excess blood. The soft placental tissue was then scraped from the vascular matrix using a scalpel. This tissue was again washed in 0.25 M sucrose before being transferred to a Waring blender containing an equivalent volume of homogenizing buffer (50 mM Tris/HCl, 0.25 M Sucrose, 0.1 mM PMSF, 1.0 mM EDTA, pH 7.5 at 4 °C). The tissue was homogenized for four periods of 15 second duration at top speed. The resulting homogenate was centrifuged at 15,000 xg for 20 minutes, the pellet discarded and the supernatant recentrifuged at 100,000 xg for 90 minutes.

The pelleted membranes were washed twice by suspending in 10 volumes of Tris/HCl buffer (50 mM Tris/HCl, 0.1 mM PMSF, 1.0 mM EDTA, pH 7.4 at 4 °C)

using a Potter-Elvehjem homogenizer and recentrifuging at 100,000 xg for 90 minutes. Membranes which could not be used immediately were stored until required at -60 °C.

6.1.4.2 Solubilization and chromatography on WGA-Sepharose

Placental membrane proteins were solubilized in 5 volumes of a 50 mM Tris/HCl buffer, pH 7.4 at 4 °C, containing 2% Triton X-100 and 0.1 mM PMSF for two hours at 4 °C with stirring. Centrifugation of this solution at 100,000 xg for 90 minutes yielded a clear supernatant which was diluted with three volumes of WGA-washing buffer (50 mM Tris/HCl, 0.1% Triton X-100, 10 mM $MgCl_2$, 0.1 mM PMSF, pH 7.4 at 4 °C) and mixed with 20 ml of WGA-Sepharose (Wheat Germ Lectin Sepharose 6MB, Lot Nos. 1A28518 and GC19083, Pharmacia Fine Chemicals) which had been previously equilibrated with the washing buffer.

The resulting suspension was gently stirred overnight after which time the gel was transferred to a column (1.5 cm by 11 cm) and washed with 200 ml of the WGA-washing buffer. The column was then eluted with a 50 mM Tris/HCl buffer, pH 7.4 at 4 °C, containing 0.1% Triton X-100, 0.3 M N-acetylglucosamine and 0.1 mM PMSF. As the column was being eluted the optical density of the elutate at 280 nm was recorded and fractions were assayed for insulin binding activity using a modification of the PEG-precipitation method of Cuatrecasas (1972). Figure 6.4 shows the superposition of a typical set of insulin binding activity and optical density elution profiles from this column.

In this example the column was eluted at a flow rate of 20 ml/hour with 2.5 ml fractions being collected. Fractions containing insulin binding activity were pooled and the protein concentrated by precipitation in 15% PEG(6000) at 4 °C, the preciptate being isolated by high speed centrifugation (100,000 xg for 90 minutes). This procedure not only rapidly concentrated the receptor from a large volume of eluent but also allowed for the simultaneous exchange of buffers. The protein pellet was reconstituted in a minimum volume of the buffer appropriate to the study to be undertaken and

Figure 6.4: The elution of insulin binding activity from a column of Wheat Germ Lectin Sepharose 6MB in the presence of 0.3 m N-acetylglucosamine. The insulin binding activity of each fraction was determined using a modification of the PEG-precipitation method of Cuatrecasas (1972), details of which are given in the text. A plot of the optical density of 280 nm of each fraction has been superimposed on the figure showing that the bound protein elutes in conjunction with the insulin binding activity.

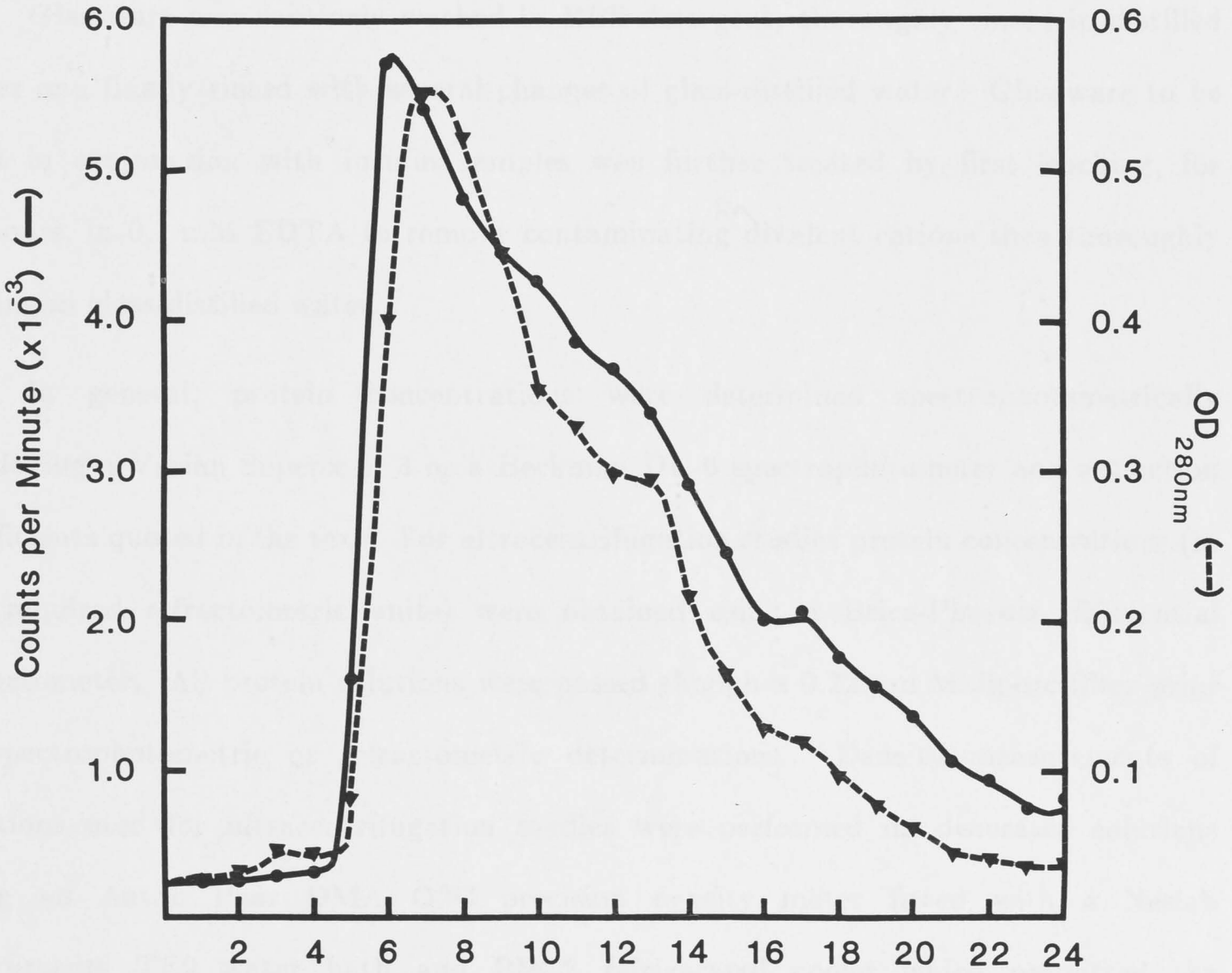
6.0
5.0
4.0
3.0
2.0
1.0
Counts per Minute (x10^{-3}) (—)
0.6
0.5
0.4
0.3
0.2
0.1
OD$_{280nm}$ (---)
2 4 6 8 10 12 14 16 18 20 22 24
Fraction Number

dialysed (Spectrapor 2, M_w cutoff 12,000-14,000) overnight to ensure complete removal and residual amounts of PEG, N-acetylglucosamine and magnesium ions. Receptor prepared by this method was used within 48 hours being stored until required at 4 °C in the presence of the protease inhibitor PMSF.

6.2 METHODS

6.2.1 General Laboratory Methods

Glassware was routinely washed in RBS detergent, thoroughly rinsed in distilled water and finally rinsed with several changes of glass-distilled water. Glassware to be used in conjunction with insulin samples was further treated by first leaching, for 24 hours, in 0.1 mM EDTA to remove contaminating divalent cations then thoroughly rinsing in glass-distilled water.

In general, protein concentrations were determined spectrophotemetrically employing a Varian Superscan 3 or a Beckman DU-6 spectrophotometer and extinction coefficients quoted in the text. For ultracentrifugation studies protein concentrations (in the required refractometric units) were obtained using a Brice-Phoenix differential refractometer. All protein solutions were passed though a 0.22 μm Millipore filter prior to spectrophotometric or refractometric determinations. Density measurements of solutions used for ultracentrifugation studies were performed on deaerated solutions using an Anton Paar DMA O2C precision density meter fitted with a Neslab Instruments TE9 water bath and PBC2 refrigerated cooler which permitted the temperature to be controlled to within ± 0.02 °C with a subsequent precision in density measurements of 4×10^{-6} g/ml (Milthorpe, 1977).

All dialyses were performed at 4 °C using Selby's type 8 dialysis tubing or Spectrapor No. 2 membrane tubing (M_w cutoff 12,000-14,000) for work involving insulin and the insulin-receptor respectively. In both cases the tubing was pre-treated by immersion in boiling 20 mM $NaHCO_3$ containing 1 mM EDTA for 30 minutes and thoroughly rinsed in glass-distilled water before use. Solutions were normally dialysed against 100 volumes of buffer for at least 24 hours with the buffer being changed at least

twice. Before use in ultracentrifugation experiments solutions were allowed to equilibrate for at least 10 hours after the final buffer change.

6.2.2 Electrophoresis

Polyacrylamide gel electrophoresis was performed in accordance with the method of Davis (1964). Acrylamide gels (15% acrylamide, 0.4% bis-acrylamide; in 0.375 M Tris/HCl buffer, pH 8.9 at 20 °C) were produced in glass tubes (0.5 by 7.5 cm) to a depth of 7 cm, spacer gels were not employed. Polymerization, which was conducted at 4 °C to reduce cracking and shrinkage, was initiated by the presence of ammonium-persulphate (0.001%) and N,N,N',N'-tetramethylethylenediamine (0.025%). Insulin samples, which had been weighted by the addition of glycol (50%) and contained bromophenol blue (0.01%) as a marker dye, were loaded onto the gels (20 μg of insulin per tube) under the electrophoresis buffer (0.025 M Tris, 0.192 M Glycine, pH 8.4 at 20 °C) with the aid of a Gilson automatic pipette.

The gels were initially electrophoresed at 2.5 mA per tube until the samples had moved into the gels at which time the current was increased to 5 mA per tube for a further 4 hours or until the dye front had left the end of the gel. The gels were stained in a 0.5% solution of Coomassie Blue in aqueous 2-propanol (25% v/v) and acetic acid (10% v/v) for 2 hours before being electrophoretically destained in aqueous 2-propanol (10% v/v) and acetic acid (10% v/v).

6.2.3 Sedimentation Equilibrium Studies

6.2.3.1 Conduct of experiments

A Spinco Model E analytical ultracentrifuge fitted with an electronic speed control was used to conduct all sedimentation equilibrium experiments which were of either short column (Richards, Teller and Schachman, 1968) or Chervenka (1970) meniscus depletion design. A Rayleigh interference optical system in conjunction with a symmetrical limiting aperture was used to follow the progress of all experiments, with interferograms being recorded photographically on Kodak IIG plates. Throughout the

course of an experiment the temperature of the rotor was controlled to within ± 0.1 °C of the value quoted in the text by the RTIC and refrigeration units of the ultracentrifuge. All experiments were conducted using an aluminium AN-D rotor in conjunction with a 12 mm double-sector cell with a filled-epon centrepiece, sapphire windows and teflon gaskets. Where possible each sedimentation equilibrium experiment was preceded by a synthetic boundary experiment to determine the initial concentration of protein in refractometric units (Richards, Teller and Schachman, 1968). When a synthetic boundary experiment was not conducted the initial protein concentration, in the required refractometric units was determined using a Brice-Phoenix differential refractometer and checked spectrophotometrically employing the calibration curve of Milthorpe (1977).

The protocol used for the short column sedimentation equilibrium experiments was as follows, 0.02 ml of the inert fluorocarbon FC-43 was introduced into both sectors of a double sector cell fitted with a standard centrepiece. This was followed by the addition of 0.10 ml of dialyzed protein solution and 0.101 ml dialysate (Casassa and Eisenberg, 1964) into the right- and left-hand sectors, respectively, to give a column height of 3 mm. Immediately after the rotor reached its final speed and before significant diffusion of the solute had occurred a reference baseline photograph was taken. Experiments were designed so that the total concentration of insulin at the base of the cell was well below the solubility limits of insulin. Selection of the required conditions was based on previously published parameters of the system (Jeffrey and Coates, 1966; Milthorpe, 1977; Pekar and Frank, 1972). It had been previously shown (Milthorpe, 1977) that 24 hours was sufficient to ensure equilibrium had been established. Nevertheless the attainment of equilibrium was always checked by comparing the interferograms after 20 and 24 hours.

For the Chervenka (1970) meniscus depletion design experiments a double sector cell with a capillary-type synthetic boundary centrepiece was used. Again fluorocarbon was added to both sectors followed by the introduction of 0.05 ml of dialyzed protein solution into the right-hand sector and 0.45 ml of dialysate into the left-hand sector. As

the rotor is accelerated the solution levels equilibrate, the dialysate overlaying the protein solution and thus acting as a zero concentration reference. The time allowed to ensure equilibrium was 18 hours (Milthorpe, 1977) with penultimate and final photographs again being used to confirm that equilibrium had been attained.

6.2.3.2 **Measurement and analysis of interferograms**

Photographs of interferograms, a typical example of which is given in Figure 6.5, were measured using a Nikon Model 6C microcomparator fitted with a projector screen, photoelectric micrometer heads and a reversible counter (Nikon ER-M-25). The plates were aligned horizontally in the microcomparator using the central white fringe of the inner and outer reference fringes (see Figure 6.5). The positions of the meniscus and the solution-oil interface were then determined using as a reference the centre of the shadow cast by the reference wire in the counterbalance. These measurements were later converted into radial distances by dividing by the horizontal magnification factor (2.192 in this case) then adding 5.62 cm, the distance from the reference wire to the centre of rotation. The radial distance of the meniscus in the initial and final photographs was used to establish that no leakage had occurred during the experiments. To determine the fringe deviation down the cell the average of the central three white and two dark fringes was determined close to the meniscus and again at 200 μm intervals. The deviations from the horizontal were recorded as fractions of fringes by noting 1 fringe = 287 μm. The resultant plot of radial distance x *versus* fringe deviation $j(x)$ was corrected for cell deviations and extrapolated to the meniscus (x_m) and to the solution-oil interface (x_b) to give values for $j(x_m)$ and $j(x_b)$ respectively.

These values along with knowledge of the initial loading concentration in Rayleigh interference fringes, J^0, was then used to determine the meniscus fringe displacement, $J(x_m)$, in accordance with the following equation:

$$J(x_m) = J^0 - \int_{x_m^2}^{x_b^2} j(x)d(x^2)/(x_b^2 - x_m^2), \qquad (6.1)$$

Figure 6.5: A typical Rayleigh interference pattern obtained in a sedimentation equilibrium experimemt of the Chervenka (1970) meniscus depletion design. The direction of the gravitational field is from right to left. The various parts of the pattern are as follows:

(a) the outer reference fringes produced by the counter-balance,

(b) fluorocarbon FC-43 oil,

(c) fluorocarbon-solution interface,

(d) solution fringes,

(e) solution-air meniscus,

(f) air fringes,

(g) reference wire,

(h) inner reference fringes.

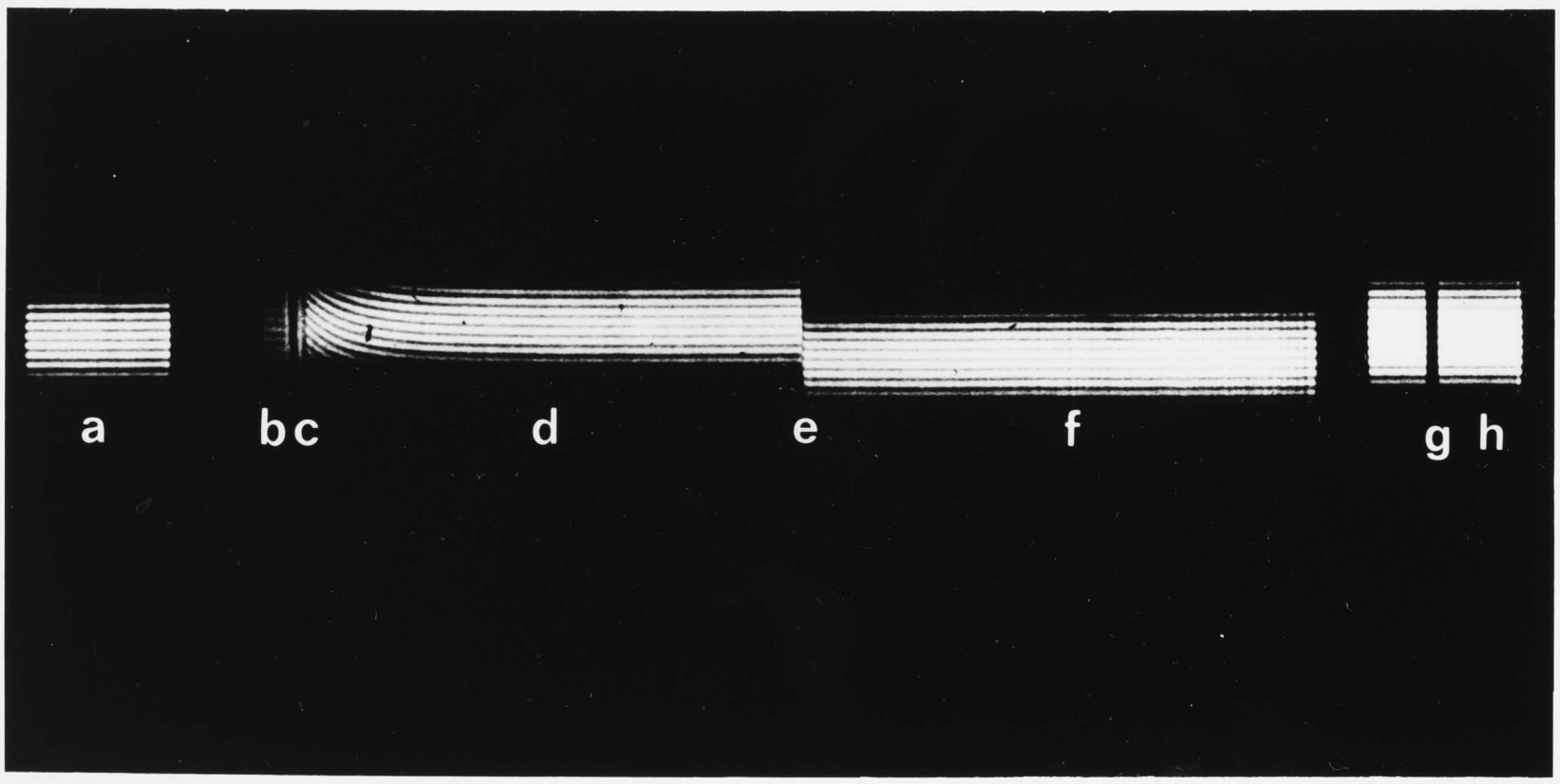
a
bc
d
e
f
g h

the integration being performed using a trapezoidal approximation.

In Chervenka (1970) meniscus depletion experiments application of this formula was not necessary as the effective concentration of protein at the meniscus is zero.

6.2.4 **Receptor Binding Studies**

6.2.4.1 **Receptor assay**

The assay procedure used to determine the amount of insulin binding activity during each stage of the purification process was a modification of the PEG-precipitation method of Cuatrecasas (1972). This method is based on the difference in solubility at 4 °C of insulin and its receptor in 10-12% PEG(6000), the insulin receptor along with any bound insulin forming a readily separable precipitate.

The assay procedure involved the incubation of a small aliquot ($\simeq$ 0.1 ml) of receptor preparation with 0.1 ng of A-14[^{125}I]-porcine insulin in a total volume 0.5 ml of assay buffer (50 mM Tris/HCl, 0.05% Triton X-100, 0.1% BSA, 0.1 mM PMSF, pH 7.4 at 35 °C). The receptor and buffer were placed in a 1.5 ml Eppendorf microfuge tube and preheated to 35 °C before the addition of the labelled insulin. The solution was rapidly mixed and placed in a thermostated orbital shaking water bath at 35 $\pm$ 1 °C. After 30 minutes the reaction was stopped and the bound insulin precipitated by the rapid sequential addition of 0.15 ml of ice cold 0.4% γ-globulin and 0.5 ml of ice cold 22% PEG(6000) followed by vortex mixing for 5 sec. The tubes were allowed to stand for 10 minutes at 4 °C before centrifuging at 11,000 xg for 5 minutes. The clear supernatant was discarded and the pellet resuspended in a further 0.5 ml of ice cold 22% PEG(6000) by vortex mixing. This washing step resulted in a significant drop in the level of non-specific binding. After recentrifuging at 11,000 xg for 5 minutes at 4 °C and again discarding the supernatant a heated scalpel was used to remove the base of the microfuge tube containing the protein pellet. The amount of ^{125}I, corresponding to the amount of bound insulin in the pellet, was then determined using an LKB 1271 RiaGamma Gamma counter.

6.2.4.2 Equilibrium binding response

The equilibrium binding response of insulin to its solubilized receptor was followed using a competitive binding assay. This was essentially a modification of the insulin binding assay described previously. The modification involved the addition of increasing amounts of unlabelled insulin to the incubation mixture along with the radioactively labelled insulin tracer. The experimental procedure used was as follows. Into a 1.5 ml Eppendorf microfuge tube was placed 0.35 ml of the appropriate buffer (50 mM Tris/HCl, 0.05% Triton X-100, 0.1% BSA, 0.1 mM PMSF pH 7.4 at 35 °C), containing either 10 mM $CaCl_2$ or 5 mM EDTA, depending on whether the experiment was to be conducted in the presence or absence of calcium ions, together with 0.1 ml of the appropriately diluted insulin receptor preparation. This mixture was preheated to 35 °C and then the binding reaction was started by the addition of 0.05 ml of a previously prepared mixed solution of native and labelled porcine insulins. These were prepared so that the addition of 0.05 ml of the mixture would result in a range of total insulin concentrations in the reaction mixture of between 0.05 and 10,000 ng/ml with either 0.05 or 0.10 ng/ml of this being radioactive tracer. Each tube was then incubated with shaking at 35 ± 1 °C in a thermostated orbital shaking water bath until an equilibrium had been established. This was generally taken as 60 minutes if calcium ions were present in the buffer and 90 minutes in the absence of calcium ions (see Chapter 5). After this period had elapsed the reaction was stopped and the bound insulin precipitated by the rapid addition of 0.15 ml of an ice cold solution of 0.4% γ-globulin and 0.5 ml of an ice cold solution of 22% PEG(6000). The amount of bound insulin was determined by the same centrifugation and counting procedure as that outlined in the preceding section in regard to the receptor assay. Four determinations at each total insulin concentration were conducted and the results averaged. The error in each result was taken as one standard deviation from the mean and was normally in the range of 5-10%.

In order to determine the amount of non-specific binding unlabelled insulin (100 μg/ml) was added to every fifth tube and the amount of bound tracer averaged for each set of binding results. The amount of non-specific binding was then calculated as a percentage of the free insulin tracer concentration at each point in a given set of results. No corrections were made to account for the effect of the self-association of insulin on the observed value for non-specific binding. To ensure that no component of the non-specific binding was due to the precipitation of free insulin a series of control experiments were conducted. These experiments confirmed that no free insulin was precipitated in the absence of receptor. For the purpose of formulating Scatchard plots the free tracer was taken to be the difference between the total tracer bound and the total tracer added, determined by counting triplicate 0.05 ml aliquots of the appropriate mixed insulin solution. The total amount of all forms of insulin specifically bound was then determined from the ratio of the bound and free tracer and the total amount of insulin in the solution.

6.2.4.3 **Binding time course**

The time course of the binding of insulin to the solubilized receptor was followed using again a modification of the binding assay procedure outlined previously. This involved the pre-equilibration at 35 °C of a solution consisting of 2-4 ml (60-120 mg protein) of concentrated receptor preparation and 25 ml of the appropriate binding study buffer (50 mM Tris/HCl, 0.1% BSA, 0.05% Triton X-100 0.1 mM PMSF, pH 7.4 at 35 °C), containing either 10 mM $CaCl_2$ or 5 mM EDTA, depending on whether the time course was to be conducted in the presence or absence of calcium ions. The binding reaction was commenced by the addition of A-14-[^{125}I]-porcine insulin (3-4 ng). The solution was rapidly mixed and a 0.5 ml zero time sample was taken. Further 0.5 ml samples were removed every minute for the first fifteen minutes, then approximately every two minutes thereafter. During the experiment the solution was maintained at 35 ± 1 °C in a thermostated orbital shaking water bath. Each sample that was removed from the incubation mixture was immediately added to a microfuge tube

containing 0.15 ml of an ice cold 0.4% γ-globulin solution. The insulin receptor, along with any bound insulin, was then precipitated by the addition of 0.5 ml of an ice cold 22% PEG(6000) solution followed by vortex mixing for five seconds. The capped tube was then snap frozen in liquid nitrogen before being stored frozen on dry ice. This freezing step was necessary to ensure consistent results as preliminary studies had shown that the amount of precipitate formed depended on the length of time the tubes were allowed to stand after the addition of the PEG. Freezing of the tubes allowed all samples to be assayed in batches under identical conditions after all the incubations had been completed. This was done by thawing the tubes for fifteen minutes at room temperature before using the same centrifugation, isolation and counting procedure as that described earlier in relation to the insulin binding assay, to determine the amount of insulin bound. No corrections were made for the effects of non-specific binding.

6.2.5 Computations

With the exception of the subroutines used for non-linear regression, all computer programmes used throughout the course of this work were written by this author. Programmes for the initial analysis of sedimentation equilibrium data were written in BASIC for use on a Digital PDP 11/34 computer. Programmes used for the iterative solutions of non-ideality equations and for the non-linear least-squares fitting procedures used to obtain values for insulin association constants in Chapters 4 and 5 were written in FORTRAN and executed on a Univac 1100/82 computer. The least-squares subroutine (LMM) used on the Univac is a part of International Mathematical and Statistical Libraries (IMSL Inc.) and was provided by the Australian National University computer centre.

ABSTRACT

This work has two interconnected themes. They are, the extension of binding theory relating to self-interacting ligand systems and, the elucidation of the role ligand self-association plays in the interaction of insulin with its membrane receptor. These two themes are interconnected in that theoretical developments have allowed the establishment of criteria against which models for the insulin insulin-receptor interaction could be tested.

The work commences in Chapter 2 with the consideration of the case of an indefinitely self-associating ligand interacting with a multivalent single state acceptor. The ligand is assumed to associate isodesmically, each polymeric species being monovalent toward the acceptor. Binding equations which describe the system are formulated in closed form and are used to investigate the system both mathematically and by way of numerical examples. Two striking features in relation to this system emerge. The first is that the system is non-saturable, a feature which may be diagnostic for some cases involving indefinitely self-interacting ligands. The second is that this system exclusively gives rise to binding curves which are convex to the r-axis when plotted in Scatchard format thus highlighting the need to consider ligand self-interaction when such systems are encountered experimentally.

In Chapter 3 the concept that self-interaction of the ligand may give rise to a bivalent species capable of crosslinking the acceptor molecules is introduced. A series of three models is then considered. In two, ligand self-interaction leads to the formation of receptor crosslinks whereas, for contrast, in the third, receptor crosslinks are formed through a single ligand bridge. For each case binding equations are formulated, again in closed form. The important point which emerges using these equations is that while the systems give rise to very different types of binding responses (convex, concave or com-

plex composites of these two forms) in each case a family of binding curves is predicted, the set arising from the dependence on the total concentration of acceptor in the system. This indicates that a study of the receptor concentration dependence of a system may be useful in elucidating the binding mechanism in cases where the possibility of receptor crosslinking exists.

The first step in elucidating the binding response in a system involving a self-interacting ligand is a detailed knowledge of the type of self-association pattern involved. In Chapter 4 sedimentation equilibrium studies are used to establish that a new pattern for the self-association of zinc-free insulin in solution is applicable over a wide range of conditions of pH, ionic strength and temperature. In this pattern, which is based on information from the existing literature on the X-ray crystal structure of insulin, the insulin monomer is viewed as having two distinct faces both capable of self-interaction. The analysis of the sedimentation equilibrium experiments presented in this chapter was facilitated by the formulation in closed form of an expression for the dependence of the weight-average molecular weight of the system on the total concentration of insulin in solution. Using this expression and others formulated by Nichol *et al.* (1984) it has been possible to obtain values for the two association constants which govern the system for each set of conditions studied, due allowance having been made for composition dependent non-ideality effects. Furthermore, by relating the pH, temperature and ionic strength dependence of the association constants with properties of various amino acid residues on the surface of the insulin monomer, it has also been possible to assign tentatively each constant to a particular reaction domain.

One important feature of this new pattern for the self-association of insulin is that bivalent polymeric species potentially capable of crosslinking the insulin receptor can arise. The possible implications of this for the binding response of insulin are addressed in Chapter 5. The chapter commences with a consideration of the distribution of polymeric insulin species in solution under conditions similar to those encountered *in vivo* and those relevant to *in vitro* insulin binding studies, proper regard being given to the complex nature of the solutions in which these binding studies are conducted. The

conclusion is drawn that over the range of total concentration used when obtaining binding data, especially in relation to *in vitro* studies, the insulin system may be approximated by a monomer-dimer equilibrium.

The chapter and the experimental aspects of this thesis conclude with a critical assessment of several models for the interaction between insulin and its membrane receptor. This work uses aspects of the binding theory developed in Chapter 3 in conjunction with binding curves obtained experimentally using insulin receptor purified from human placenta. From these studies it may be concluded that, while the self-association of insulin will contribute significantly to the overall form of the binding curve observed in the system, it is not the primary determining factor. The usefulness of the binding theory developed in Chapter 3 is also demonstrated, not only in regard to eliminating two possible mechanisms for the insulin system, but also in being able to reproduce the form of the insulin binding response. The implication emerges that there may well be a direct link between association of insulin receptors initiated by the binding of insulin and, at least in part, the convexity in the form of the binding response plotted in Scatchard format. This emphasizes the need to consider such effects in the analysis of other systems showing similar responses. Indeed, it is hoped that the binding equations developed in this work will add to the wider understanding of the behaviour of systems involving a self-interacting ligand.

BIBLIOGRAPHY

Adair, G.S. (1925). *J. Biol. Chem.* **63**, 529.

Adams, E.T. Jr., and Filmer, D.L. (1966). *Biochemistry* **5**, 2971.

Adams, E.T. Jr., and Fujita, H. (1963). In *Ultracentrifugal Analysis in Theory and Experiment*, Williams, J.W., Ed., Academic Press, New York, p.119.

Adams, E.T. Jr., Pekar, A.H., Soucek, D.A., Tang, L.H., Barlow, G., and Armstrong, J.L. (1969). *Biopolymers* **7**, 5.

Aiyer, R.A. (1983). *J. Biol. Chem.* **258**, 14992.

Alameda, G.K., Evelhoch, J.L., Sudmeier, J.L., and Birge, R.R. (1985). *Biochemistry* **24**, 1757.

Anzenbacker, P., and Kalous, V. (1975). *Biochim. Biophys. Acta* **386**, 603.

Baghurst, P.A., Nichol, L.W., and Winzor, D.J. (1978). *J. Theor. Biol.* **74**, 523.

Bajaj, S.P., Butkowski, R.J., and Mann, K.G. (1975). *J. Biol. Chem.* **250**, 2150.

Beaty, N.B., and Lane, M.D. (1983). *J. Biol. Chem.* **258**, 13043.

Blake, A., and Peacocke, A.R. (1968). *Biopolymers* **6**, 1225.

Blatt, W.F., Robinson, S.M., and Bixler, H.J. (1968). *Anal. Biochem.* **26**, 151.

Blundell, T.L., Dodson, G.G., Hodgkin, D.C., and Mercola, D.A. (1972). *Adv. Protein Chem.* **26**, 279.

Bonen, A., Hood, D.A., Tan, M.H., Sopper, M.M., and Begin-Heick, N. (1984). *Biochim. Biophys. Acta* **801**, 171.

Bosma, H.J., Voordouw, G., De Kok, A., and Veeger, C. (1980). *FEBS Lett.* **120**, 179.

Bradbury, J.H., Ramesh, V., and Dodson, G.G. (1981). *J. Mol. Biol.* **150**, 609.

Brinkworth, R.I., Masters, C.J., and Winzor, D.J. (1975). *Biochem. J.* **151**, 631.

Brown, J.C., and Rodkey, L.S. (1979). *J. Exp. Med.* **150**, 67.

Brown, N.C., and Reichard, P. (1969). *J. Mol. Biol.* **46**, 39.

Brown, H., Sanger, F., and Kitai, R. (1955). *Biochem. J.* **60**, 556.

Busse, W.D., and Carpenter, F.H. (1976). *Biochemistry* **15**, 1649.

Buxser, S., Puma, P., and Johnson, G.L. (1985). *J. Biol. Chem.* **260**, 1917.

Calvert, P.D., Nichol, L.W., and Sawyer, W.H. (1979). *J. Theor. Biol.* **80**, 233.

Capeau, J., Lascols, O., Flaig-Staedel, C., Blivet, M.J., Beck, J.P., and Picard, J. (1985). *Biochimie* **67**, 1133.

Casassa, E.F., and Eisenberg, H. (1964). *Adv. Protein Chem.* **19**, 287.

Chance, R.E., Root, M.A., and Galloway, J.A. (1976). *Acta Enodocrinologica Suppl.* **205**, 185.

Chervenka, C.H. (1970). *Anal. Biochem.* **34**, 24.

Chun, P.W., Kim, J.D., Lee, C.W., Shireman, R.B., and Cantarini, W.F. (1984). *J. Biol. Chem.* **259**, 2161.

Colowick, S.P., and Womack, F.C. (1969). *J. Biol. Chem.* **244**, 774.

Conn, P.M., Rogers, D.C., and McNeil, R. (1982). *Endocrinology* **111**, 335.

Conway, A., and Koshland, D.E. Jr. (1968). *Biochemistry* **7**, 4011.

Corin, R.E., and Donner, D.B. (1982). *J. Biol. Chem.* **257**, 104.

Cuatrecasas, P. (1972). *Proc. Natl. Acad. Sci. USA* **69**, 318.

Czech, M.P. (1984). *Recent Progress in Hormone Research* **40**, 347.

Czech, M.P., Massague, J., and Pilch, P.F. (1981). *Trends Biochem. Sci.* **6**, 222.

Davidson, M.B., and Venkatesan, N. (1982). *Metabolism* **31**, 1206.

Davis. B.J. (1964). *Ann. N.Y. Acad. Sci.* **121**, 404.

De Meyts, P. (1980). In *Hormones and Cell Regulation*, Dumont, J., and Nunez, J., Eds., Vol. 4. Elsevier/North-Holland Biomedical Press, Amsterdam, p.107.

De Meyts, P., Bianco, A.R., and Roth, J. (1976). *J. Biol. Chem.* **251**, 1877.

De Meyts, P., Roth, J., Neville, D.M. Jr., Gavin, J.R., and Lesniak, M.A. (1973). *Biochem. Biophys. Res. Comm.* **55**, 154.

Denton, R.M., Brownsey, R.W., and Belsham, G.J. (1981). *Diabetologia* **21**, 347.

Desai, K.S., Zinman, B., Steiner, G., and Hollenberg, C.H. (1978). *Can. J. Biochem.* **56**, 843.

Desbuquois, B. (1985). In *Polypeptide Hormone Receptors*, Posner, B.I., Ed. Marcel Dekker, Inc., New York, p.345.

Desbuquois, B., and Aurbach, G.D. (1971). *J. Clin. Endocr.* **33**, 732.

de Vries, C.P., and Van de Veen, E.A. (1985). *Biochimie* **67**, 1191.

Dodson, E.J., Dodson, G.G., Hubbard, R.E., and Reynolds, C.D. (1983). *Biopolymers* **22**, 281.

Dodson, E.J., Dodson, G.G., Lewitova, A., and Sabesan, M. (1978). *J. Mol. Biol.* **125**, 387.

Dombrose, F.A., Gitel, S.N., Zawalich, K., and Jackson, C.M. (1979). *J. Biol. Chem.* **254**, 5027.

Donner, D.B. (1980). *Proc. Natl. Acad. Sci. USA* **77**, 3176.

Dwight, H.B. (1961). *Tables of Integrals and Other Mathematical Data*, 4th ed., Macmillan Company Co. Inc., New York.

Eastham, R.D. (1978). *Biochemical Values in Clinical Medicine*, 6th ed. John Wright and Sons Ltd., Bristol.

Eckel, J., and Reinauer, H. (1984). *Diabetes* **33**, 214.

Edelhoch, H., Katchalski, E., Maybury, R.H., Hughes, W.L. Jr., and Edsall, J.T. (1953). *J. Am. Chem. Soc.* **75**, 5058.

Edsall, J.T. (1953). In *The Proteins*, 1st ed. Neurath, H., and Bailey, K., Eds. Academic Press, New York, Vol. IB, p.549.

Eisenberg, H., Josephs, R., and Reisler, E. (1976). *Adv. Protein Chem.* **30**, 101.

Fajans, S.S., and Floyd, J.C. Jr. (1972). In *Handbook of Physiology*, Geiger, S.R., Ed. American Physiological Society, Washington, D.C., Sect. 7, Vol. I, p.473.

Finn, F.M., Titus, G., Horstman, D., and Hofmann, K. (1984). *Proc. Natl. Acad. Sci. USA* **81**, 7328.

Flory, P.J. (1953). *Principles of Polymer Chemistry*, Cornell University Press, Ithaca, New York.

Frank, B.H., and Veros, A.J. (1968). *Biochem. Biophys. Res. Comm.* **32**, 155.

Fredericq, E. (1956). *Arch. Biochem. Biophys.* **65**, 218.

Frieden, C., and Colman, R.F. (1967). *J. Biol. Chem.* **242**, 1705.

Fujita, H. (1962). *Mathematical Theory of Sedimentation Analysis*, Academic Press, New York.

Fujita-Yamaguchi, Y. (1984). *J. Biol. Chem.* **259**, 1206.

Fujita-Yamaguchi, Y., Choi, S., Sakamoto, Y., and Itakura, K. (1983). *J. Biol. Chem.* **258**, 5045.

Gambhir, K.K., Archer, J.A., and Carter, L. (1977). *Clin. Chem.* **23**, 1590.

Gilbert, L.M., and Gilbert, G.A. (1973). *Methods in Enzymol.* **27**, 273.

Goldberg, R.J. (1952). *J. Am. Chem. Soc.* **74**, 5715.

Goldberg, R.J. (1953). *J. Am. Chem. Soc.* **75**, 3127.

Goldman, J., and Carpenter, F.H. (1974). *Biochemistry* **13**, 4566.

Greene, L.A., and Shooter, E.M. (1980). *Ann. Rev. Neurosci.* **3**, 353.

Grigorescu, F., White, M.F., and Kahn, C.R. (1983). *J. Biol. Chem.* **258**, 13708.

Hammes, G.G. (1981). In *Protein-Protein Interactions*, Frieden, C., and Nichol, L.W., Eds. John Wiley and Sons, New York, p.257.

Heffetz, D., and Zick, Y. (1986). *J. Biol. Chem.* **261**, 889.

Heidelberger, M., and Kendall, F.E. (1935). *J. Exp. Med.* **61**, 563.

Helmerhorst, E., and Stokes, G.B. (1983). *Biochemistry* **22**, 69.

Heyn, M.P., and Bretz, R. (1975). *Biophys. Chem.* **3**, 35.

Hinman, N.D., and Cann, J.R. (1976). *Molec. Pharmac.* **12**, 769.

Holladay, L.A., Ascoli, M., and Puett, D. (1977). *Biochim. Biophys. Acta* **494**, 245.

Houslay, M.D., and Heyworth, C.M. (1983). *Trends Biochem. Sci.* **8**, 449.

Howlett, G.J., Jeffrey, P.D., and Nichol, L.W. (1970). *J. Phys. Chem.* **74**, 3607.

Howlett, G.J., and Nichol, L.W. (1972). *J. Biol. Chem.* **247**, 5681.

Jackson, C.M., Peng, C.W., Brenckle, G.M., Jonas, A., and Stenflo, J. (1979). *J. Biol. Chem.* **254**, 5020.

Jacobs, S., and Cuatrecasas, P. (1983). *Ann. Rev. Pharmacol. Toxicol.* **23**, 461.

Jeffrey, P.D. (1981). In *Protein-Protein Interactions*, Frieden, C., and Nichol, L.W., Eds. John Wiley and Sons, New York, p.213.

Jeffrey, P.D. (1982). *Diabetologia* **23**, 381.

Jeffrey, P.D. (1984). *Biochemistry* **13**, 4441.

Jeffrey, P.D. (1985). *Biophys. Chem.* **21** 57.

Jeffrey, P.D., and Coates, J.H. (1966). *Biochemistry* **5**, 489.

Jeffrey, P.D., Milthorpe, B.K., and Nichol, L.W. (1976). *Biochemistry* **15**, 4660.

Jeffrey, P.D., Nichol, L.W., Turner, D.R., and Winzor, D.J. (1977). *J. Phys. Chem.* **81**, 776.

Kahn, C.R., Baird, K.L., Flier, J.S., Grunfeld, C., Harmon, J.T., Harrison, L.C., Karlsson, F.A., Kasuga, M., King, G.L., Lang, U.C., Podskalny, J.M., and Van Obberghen, E. (1981). *Recent Progress in Hormone Research* **37**, 477.

Kahn, C.R., Baird, K.L., Jarrett, D.B., and Flier, J.S. (1978). *Proc. Natl. Acad. Sci. USA* **75**, 4209.

Karnieli, E., Zarnowski, M.J., Hissin, P.J., Simpson, I.A., Salans, L.B., and Cushman, S.W. (1981). *J. Biol. Chem.* **256**, 4772.

Kauzmann, W. (1959). *Adv. Protein Chem.* **14**, 1.

Kim, H., Deonier, R.C., and Williams, J.W. (1977). *Chem. Rev.* **77**, 659.

King, A.C., and Cuatrecasas, P. (1981). *New Engl. J. Med.* **305**, 77.

Kirtley, M.E., and Koshland, D.E. Jr. (1967). *J. Biol. Chem.* **242**, 4192.

Klotz, I.M. (1946). *Arch. Biochem.* **9**, 109.

Klotz, I.M. (1953). In *The Proteins*, Neurath, H., and Bailey, Eds. Academic Press, New York, Vol. 1B, p.727.

Klotz, I.M., and Hunston, D.L. (1984). *J. Biol. Chem.* **259**, 10060.

Kohanski, R.A., and Lane, M.D. (1983). *J. Biol. Chem.* **258**, 7460.

Koshland, D.E. Jr., and Neet, K.E. (1968). *Annu. Rev. Biochem.* **37**, 359.

Koshland, D.E. Jr., Nemethy, G., and Filmer, D. (1966). *Biochemistry* **5**, 365.

Kurganov, B.I. (1984). *J. Theor. Biol.* **109**, 59.

Levitzki, A. (1978). 'Quantitative Aspects of Allosteric Mechanisms', in *Molecular Biology, Biochemistry and Biophysics*, Vol. 28. Springer-Verlag, Berlin-Heidelberg, p.1.

Levitzki, A., and Koshland, D.E. Jr. (1972). *Biochemistry* **11**, 247.

Lipkin, E.W., Teller, D.C., and de Haen, C. (1986a). *J. Biol. Chem.* **261**, 1694.

Lipkin, E.W., Teller, D.C., and de Haen, C. (1986b). *J. Biol. Chem.* **261**, 1702.

Lonnroth, P., DiGirolamo, M., and Smith, U. (1983). *Metabolism* **32**, 609.

Madar, D.A., Sarasua, M.M., Marsh, H.C., Pedersen, L.G., Gottschalk, K.E., Hiskey, R.G., and Koehler, K.A. (1982). *J. Biol. Chem.* **257**, 1836.

Marsh, J.W., Westley, J., and Steiner, D.F. (1984). *J. Biol. Chem.* **259**, 6641.

Milthorpe, B.K. (1977). *Sedimentation Equilibrium Studies on Associating Systems*, Ph.D. Thesis, Australian National University.

Milthorpe, B.K., Jeffrey, P.D., and Nichol, L.W. (1975). *Biophys. Chem.* **3**, 169.

Milthorpe, B.K., Nichol, L.W., and Jeffrey, P.D. (1977). *Biochim. Biophys. Acta* **495**, 195.

Minton, A.P. (1981). *Biopolymers* **20**, 2093.

Monod, J., Wyman, J., and Changeux, J.-P. (1965). *J. Mol. Biol.* **12**, 88.

Morgan, D.O., Ho, L., Korn, L.J., and Roth, R.A. (1986). *Proc. Natl. Acad. Sci. USA* **83**, 328.

McKenzie, H.A. (1969). In *Data for Biochemical Research*, Davison, R.M.C., Elliott, D.C., Elliott, W.H., and Jones, K.M., Eds. Oxford University Press, London, p.475.

McKenzie, G.H., and Sawyer, W.H. (1973). *J. Biol. Chem.* **248**, 549.

Nichol, L.W. (1980). In *The Regulation of Coagulation*, Mann, K.G., and Taylor, F.B., Eds. Elsevier/North-Holland, New York, p.43.

Nichol, L.W. (1981). In *Protein-Protein Interactions*, Frieden, C., and Nichol, L.W., Eds. John Wiley and Sons, New York, p.1.

Nichol, L.W., Jackson, W.J.H., and Winzor, D.J. (1967). *Biochemistry* **6**, 2449.

Nichol, L.W., and Ogston, A.G. (1965). *J. Phys. Chem.* **69**, 4365.

Nichol, L.W., and Ogston, A.G. (1981). *J. Phys. Chem.* **85**, 1173.

Nichol, L.W., Ogston, A.G., and Wills, P.R. (1981). *FEBS Lett.* **126**, 18.

Nichol, L.W., Owen, E.A., and Winzor, D.J. (1982). *J. Phys. Chem.* **86**, 5015.

Nichol, L.W., Sculley, M.J., Jeffrey, P.D., and Winzor, D.J. (1984). *J. Theor. Biol.* **109**, 285.

Nichol, L.W., Sculley, M.J., and Winzor, D.J. (1982). *J. Theor. Biol.* **96**, 723.

Nichol, L.W., Siezen, R.J., and Winzor, D.J. (1978). *Biophys. Chem.* **9**, 47.

Nichol, L.W., Siezen, R.J., and Winzor, D.J. (1979). *Biophys. Chem.* **10**, 17.

Nichol, L.W., Smith, G.D., and Ogston, A.G. (1969). *Biochim. Biophys. Acta* **184**, 1.

Nichol, L.W., Wills, P.R., and Winzor, D.J. (1979). *J. Theor. Biol.* **80**, 39.

Nichol, L.W., and Winzor, D.J. (1964). *J. Phys. Chem.* **68**, 2455.

Nichol, L.W., and Winzor, D.J. (1976a). *Biochemistry* **15**, 3015.

Nichol, L.W., and Winzor, D.J. (1976b). *J. Phys. Chem.* **80**, 1980.

Nichol, L.W., and Winzor, D.J. (1981). In *Protein-Protein Interactions*, Frieden, C., and Nichol, L.W., Eds. John Wiley and Sons, New York, p.337.

Ogston, A.G., and Winzor, D.J. (1975). *J. Phys. Chem.* **79**, 2496.

Palmiter, M.T., and Aladjem, F. (1963). *J. Theor. Biol.* **5**, 211.

Pang, D.T., and Shafer, J.A. (1983). *J. Biol. Chem.* **258**, 2514.

Pang, D.T., and Shafer, J.A. (1984). *J. Biol. Chem.* **259**, 8589.

Parker, F.S., and Bhaskar, K.R. (1968). *Biochemistry* **7**, 1286.

Peavy, D.E., Abram, J.D., Frank, B.H., and Duckworth, W.C. (1984). *Endocrinology* **114**, 1818.

Pekar, A.H., and Frank, B.H. (1972). *Biochemistry* **11**, 4013.

Peterson, S.W., Miller, A.L., Kelleher, R.S., and Murray, E.F. (1983). *J. Biol. Chem.* **258**, 9605.

Pollet, R.J., Standaert, M.L., and Haase, B.A. (1977). *J. Biol. Chem.* **252**, 5828.

Prendergast, F.G., and Mann, K.G. (1977). *J. Biol. Chem.* **252**, 840.

Pullen, R.A., Lindsay, D.G., Wood, S.P., Tickle, I.J., Blundell, T.L., Wollmer, A., Krail, G., Brandenburg, D., Zahn, H., Gliemann, J., and Gammeltoft, S. (1976). *Nature* **259**, 369.

Richards, E.G., Teller, D.C., and Schachman, H.K. (1968). *Biochemistry* **7**, 1054.

Ronnett, G.V., and Lane, M.D. (1981). *J. Biol. Chem.* **256**, 4704.

Ross, P.D., and Minton, A.P. (1977). *J. Mol. Biol.* **112**, 437.

Ryle, A.P., Sanger, F., Smith, L.F., and Kitai, R. (1955). *Biochem. J.* **60**, 541.

Salzman, A., Wan, C.F., and Rubin, C.S. (1984). *Biochemistry* **23**, 6555.

Scatchard, G. (1949). *Ann. N.Y. Acad. Sci.* **51**, 660.

Sculley, M.J., Nichol, L.W., and Winzor, D.J. (1981). *J. Theor. Biol.* **90**, 365.

Schlessinger, J., Shechter, Y., Willingham, M.C., and Pastan, I. (1978). *Proc. Natl. Acad. Sci. USA* **75**, 2659.

Singer, S.J. (1965). In *The Proteins*, 2nd ed. H. Neurath, Ed., Academic Press, New York, Vol. 3, p.269.

Smith, G.D., Swenson, D.C., Dodson, E.J., Dodson, G.G., and Reynolds, C.D. (1984). *Proc. Natl. Acad. Sci. USA* **81**, 7093.

Smith, R.M., and Jarett, L. (1983). *J. Cell. Physiol.* **115**, 199.

Steiner, R.F. (1952). *Arch. Biochem. Biophys.* **39**, 333.

Steiner, R.F. (1974). *J. Theor. Biol.* **45**, 93.

Storm, M.C., and Dunn, M.F. (1985). *Biochemistry* **24**, 1749.

Swann, J.C., and Hammes, G.G. (1969). *Biochemistry* **8**, 1.

Tanford, C., and Epstein, J. (1954). *J. Am. Chem. Soc.* **76**, 2163.

Tang, L.-H., Powell, D.R., Escott, B.M., and Adams, E.T. Jr. (1977). *Biophys. Chem.* **7**, 121.

Tellam, R.L., Sculley, M.J., Nichol, L.W., and Wills, P.R. (1983). *Biochem. J.* **213**, 651.

Tellam, R., Winzor, D.J., and Nichol, L.W. (1978). *Biochem. J.* **173**, 185.

Tung, M.S., and Steiner, R.F. (1974). *Eur. J. Biochem.* **44**, 49.

Van Holde, K.E., and Rossetti, G.P. (1967). *Biochemistry* **6**, 2189.

Van Obberghen, E., Ballotti, R., Gazzano, H., Fehlmann, M., Rossi, B., Gammeltoft, S., Debant, A., Le Marchand-Brustel, Y., and Kowalski, A. (1985). *Biochimie* **67**, 1119.

Williams, P.F., Caterson, I.D., and Turtle, J.R. (1984). *Biochim. Biophys. Acta* **797**, 27.

Wills, P.R., Nichol, L.W., and Siezen, R.J. (1980). *Biophys. Chem.* **11**, 71.

Winzor, D.J., Tellam, R., and Nichol, L.W. (1977). *Arch. Biochem. Biophys.* **178**, 327.

Wollmer, A., Straβburger, W., Hoenjet, E., Glattner, U., Fleischhauer, J., Mercola, D.A., de Graaf, R.A.G., Dodson, E.J., Dodson, G.G., Smith, D.G., Brandenburg, D., and Danho, W. (1980). In *Insulin: Chemistry, Structure and Function of Insulin and Related Hormones*, Brandenburg, D., and Wollmer, A., Eds. Walter de Gruyter, Berlin, p.27.

Wu, G.M. (1974). *Dissertation Abstracts* **35** (75), 7816.

Wyman, J. (1964). *Adv. Protein Chem.* **19**, 223.

Yphantis, D.A. (1964). *Biochemistry* **3**, 297.